Interactive comment on
“The Half-order Energy Balance Equation, Part 2:The inhomogeneous HEBE and 2D energy balance models”

Overall Notes on the revised manuscript:

In addition to making changing changes suggested by the referees, I also added a new section 2.3 that makes a direct comparison with the 1-D Budkyo-Sellers equation. This clarifies the similarities and differences. Appendix C was removed, developments elsewhere make it less pertinent.

Anonymous Referee #1

Received and published: 10 July 2020

General comments: I think this is a notable (two-part) paper. Its key message, that the heat flux at the earth’s surface is a derivative of order half of the temperature, and that this modifies the simplest EBMs in an important way is both significant in itself, and provides a foundation for the author’s concurrent work on fractional stochastic energy balance models.

Au: Thank you for the enthusiastic review!

I have only one gripe that needs attention. It relates to earlier work which needs to be more fully described and integrated into the manuscript. When this is done so it will actually reinforce the author’s message, I think.

Au: The Oldham references are quite useful, thanks! I respond in more detail below.

Specific comment: Earlier work on half-order derivatives in heat transfer

The list of references on fractional calculus seems to me to be comprehensive in general, but to be missing a key reference. Podlubny [1999] notes in his preface that:... from the viewpoint of applications in physics, chemistry and engineering it was undoubtedly the book written by K. B. Oldham and J. Spanier [i.e. "The Fractional Calculus", Academic Press, 1974; now in a Dover Edition] which played an outstanding role in the development of the subject which can be called applied fractional calculus. Moreover, it was the first book which was entirely devoted to a systematic presentation of the ideas, methods, and applications of the fractional calculus.

Referring back to this book suggests to me that to say, as the manuscript presently does, that“... half-order derivatives have occasionally [sic] been used in the context of the heat equation, (at least since [Babenko, 1986]) "substantially underestimates the extent to which half order derivatives have already been studied in the heat equation context. Oldham and Spanier devote their chapter 11 to applications of what they call the semi differential operator, i.e. the fractional derivative of half order, to diffusion problems including heat transfer.

The book built on their own papers, particularly *Oldham KB, Spanier J (1972) A general solution of the diffusion equation for semi infinite geometries, J Math Anal Appl 39:665–669* and *Oldham KB (1973) Diffusive transport to planar, cylindrical and spher-ical electrodes, J Electroanal Chem Interfacial Electrochem, 41:351–358*. They give the diffusion equation as:

$$\frac{\partial}{\partial t}F(\xi,\eta,\zeta,t) = \kappa\nabla^2 F(\xi,\eta,\zeta,t) \tag{1}$$

and then note that in three special, semi-infinite, cases this can be simplified so that Laplacian depends only on the radial co-ordinate r and t. In the planar case they give:

$$\frac{\partial}{\partial t}F(r,t) - \kappa\frac{\partial^2}{\partial r^2}F(r,t) = 0 \qquad (2)$$

They take the system is initially in equilibrium F(r,t) =F_0, for t <0,r≥0. An unspecified perturbation occurs at t= 0, and for times of interest t <0 it does not affect regions remote from the r= 0 boundary. Hence F(r,t) =F_0, for t≤τ,r=∞, and in the case of planar geometry they derive the solution:

$$\frac{\partial}{\partial r}F(r,t) = -\frac{1}{\sqrt{\kappa}}\frac{\partial^{1/2}}{\partial t^{1/2}}F(r,t) + \frac{F_0}{\sqrt{\pi\kappa t}} \qquad (3)$$

They then go on to consider the problem of 1D heat conduction in a semi-infinite plane, and so look at the heat equation in the form:

$$\frac{\partial}{\partial t}T(r,t) - \frac{K}{\rho\sigma}\frac{\partial^2}{\partial r^2}T(r,t) = 0 \qquad (4)$$

with appropriate boundary conditions of T(r,0) = 0 and T(∞,t) = 0.The heat flux sought is

$$J(t) \equiv -K\frac{\partial}{\partial r}T(0,t) \qquad (5)$$

which they get from their earlier solution for ∂F(r,t)/∂r by putting T for F,K/ρσ for κ,and using

$$J(T) = -K\frac{\partial}{\partial r}T(0,t) = \sqrt{K\rho\sigma}\frac{\partial^{1/2}}{\partial t^{1/2}}T(0,t) \qquad (6)$$

Because this result, Oldham and Spanier’s equation 11.2.10 is closely related to equation 43 in part I of the present ms, I think that it should be explained clearly whether i) the present paper is effectively an illustration of Oldham and Spanier's result in the EBM context, or ii) whether it offers a derivation in a domain to which Oldham and Spanier's result did not apply. Either situation will be important and publishable but readers need to know which applies. Interestingly, Oldham and Spanier noted that the equation had been obtained by Meyerin 1960 in a Canadian NRC technical report ("A heat-flux-meter for use with thin film surface thermometers"), but rather than being written as a half order derivative it was then given in the alternative integral form:

$$J(T) = \sqrt{\frac{K\rho\sigma}{4\pi}}[\frac{2T(0,t)}{\sqrt{t}} + \int_0^t \frac{T(0,t) - T(0,\tau)}{\sqrt{t-\tau}} d\tau] \tag{7}$$

without explicitly using fractional calculus. It was thus known in the heat transfer context even before the first EBMs were derived, in a sense reinforcing the present author's point.

Au: There are several important differences w.r.t. to Oldham's results.

a) Oldham considers only a single spatial degree of freedom r corresponding to either the "zero-dimensional" model (eq. 22 part 1) or cylindrical or spherical geometries that we do not consider. He nowhere considers fractional space-time operators as in part 2. I.e. he neither treats homogeneous operators but with inhomogeneous boundary conditions, nor does Oldham treat inhomogeneous media (inhomogeneous transport operators). In other words essentially all of part 2 (eq. 3 and later) is outside his scope.

b) Our boundary radiative-conductive boundary conditions are special cases of "Robin" boundary conditions i.e. they involve a linear combination of the field and it's normal gradient over a surface. Although Robin boundary conditions are occasionally used in insulating boundary condition problems in convective diffusive equations, they are not identical to the radiative-conductive conditions used here. Oldham mentions Cauchy, Neumann and Dirichlet *boundary conditions and says that "any other type" could be used. In other words he realized that his formalism was more general than the applications he developped, but did not pursue these. I will add this information in the revised ms.*

c). Although it is not essential, Oldham's application of the method was to use more or less standard boundary conditions (Dirichlet) and then deduce the heat flux across surfaces from this. As far as I can tell, since then, this is almost invariably the way the method has been applied.

d) A final more minor difference is that we also treated the Weyl derivative and used the corresponding Fourier techniques.

We added references to these difference in the new ms.

Anonymous Referee #2

Received and published: 13 July 2020

This second part reviewed here extends the approach of Part 1 to higher spatial dimension and inhomogeneous thermal models of the earth's response to radiative forcing.There is an appropriate summary of Part 1 that puts the new contribution into context. The full model considered here includes varying horizontal and vertical thermal diffusivities, thermal capacities, sensitivities and spatio-temporal forcing. By a heuristic method of Babenko, the author expands the inhomogeneous operator to give 2D energy balance equations that will be useful for studying spatio-temporal responses to forcing. The manuscript includes a number of appendices that examine horizontal structures, cross-correlations, space-time factorization of quantities such as autocorrelation and that extends the results from flat space to the sphere. The analysis seems to be carefully done, and care is taken to distinguish cases where there may not be a rigorous justification.

Au: I thank the referee for the very positive review!

I would be interested to see a bit more discussion of the "bottom boundary condition" T=0 at z=-infinity. I think it would also be useful to include some discussion of how atmosphere/ocean convection is/is not represented in the model.

Au: The role of the bottom boundary condition was addressed in part I where (just after eq. 29) it is shown that the influence of the bottom BC decays exponentially quickly with depth so that below a few diffusion depths it is essentially irrelevant. In oceans this would likely imply depths of hundreds of meters. In part I I added some new material clarifying the nature of the surface.

The Half-order Energy Balance Equation, Part 2: The inhomogeneous HEBE and 2D energy balance models

Shaun Lovejoy

Physics dept., McGill University, Montreal, Que. H3A 2T8, Canada

Correspondence: Shaun Lovejoy (lovejoy@physics.mcgill.ca)

Abstract: In part I, we considered the zero-dimensional heat equation showing quite generally that conductive – radiative surface boundary conditions lead to half-ordered derivative relationships between surface heat fluxes and temperatures: the Half-ordered Energy balance Equation (HEBE). The real Earth – even when averaged in time over the weather scales (up to ≈ 10 days) – is highly heterogeneous, in this part II, we thus extend our treatment to the horizontal direction. We first consider a homogeneous Earth but with spatially varying forcing, both on a plane and also on the sphere: we compare our new equations with the canonical 1-D Budyko-Sellers equations. Using Laplace and Fourier techniques, we derive the Generalized HEBE (the GHEBE) based on half-ordered space-time operators. We analytically solve the homogeneous GHEBE, and show how these operators can be given precise interpretations.

We then consider the full inhomogeneous problem with horizontally varying diffusivities, thermal capacities, climate sensitivities and forcings. For this we use Babenko's operator method which generalizes Laplace and Fourier methods. By expanding the inhomogeneous space-time operator at both high and low frequencies, we derive 2-D energy balance equations that can be used for macroweather forecasting, climate projections and for studying the approach to new (~~thermodynamic~~ equilibrium) climate states when the forcings are all increased and held constant.

1 Introduction

In part I, we showed that when the surface of a body exchanges heat both conductively and radiatively, that its flux depends on the half order derivative of the surface temperature. This implies that energy stored in the subsurface effectively has a huge power law memory. This contrasts with the usual phenomenological assumption used notably in box models (including zero dimensional global energy balance models) that the order of derivative is an integer (one) and that on the contrary, the memory is only exponential (short). The result followed directly by assuming that the continuum mechanics heat equation was obeyed and the depth of the media was of the order of a few diffusion depths~~,~~ ; for the Earth, perhaps several hundred meters. The basic result was a classical application of the heat equation barely going beyond results that [*Brunt*, 1932] already found "in any textbook".

A consequence was that although Newton's law of cooling is obeyed, that the temperature obeyed the half-order energy balance equation (HEBE) rather than the phenomenological first order Energy balance Equation (EBE). When applied to the Earth, the HEBE and its implied long memory explains the success of both climate projections through to 2100 [*Hebert*, 2017], [*Lovejoy et al.*, 2017], [*Hébert et al.*, 2020] and macroweather (monthly, seasonal) temperature forecasts [*Lovejoy et al.*, 2015], [*Del Rio Amador and Lovejoy*, 2019], [*Del Rio Amador and Lovejoy*, 2020a; *Del Rio Amador and Lovejoy*, 2020b]. We also considered the responses to periodic forcings showing that surface heat fluxes and temperatures are related by a complex thermal impedance ($Z(\omega)$, ω is the frequency). In the Earth system, $Z(\omega) = s\cancel{\lambda}(\omega)$ where $s\cancel{\lambda}(\omega)$ is the complex climate sensitivity that we estimated from a simple semi-empirical model.

Formatted: Font: Italic

Although in part 1 we discussed the classical 1-D application of the heat equation to the Earth's latitudinal energy balance (Budyko-Sellers models) - especially their ad hoc treatment of the surface boundary condition – we restricted the discussion to zero horizontal dimensions. In this part II, we first (section 2) extend the part I treatment to ~~horizontally~~ systems with homogeneous properties but with inhomogeneous forcings, first in the horizontal plane (section 2.1, 2.2), then - following Budyko-Sellers - latitudinally varying on the sphere (section 2.3). ~~systems but with inhomogeneous forcings, we then consider the more realistic case of horizontally inhomogeneous media.~~ The homogeneous case is quite classical and can be treated with standard Laplace and Fourier techniques, it leads to the (horizontally) Generalized HEBE: the GHEBE. Although the GHEBE has a more complex (space-time) fractional derivative operator that is unlike anything we know of in the literature~~,~~ - like the HEBE, it can nevertheless be given precise meaning via its Green's function.

In section 3, we derive the inhomogeneous GHEBE and HEBE needed for applications. This is done by using of Babenko's method [*Babenko*, 1986] which is essentially a generalization of ~~the~~ Laplace and Fourier transform techniques. The challenge with Babenko's method is to interpret the inhomogeneous space-time fractional operators. Following Babenko, we do this using both high and low frequency expansions corresponding respectively to processes dominated by storage and by horizontal heat transport. The long time limit describes the new energy balance climate state that results when the forcing is increased everywhere and held fixed: for the model this corresponds to equilibrium. We also include several appendices focused on empirical parameter estimates (appendix A), the implications for two point and space-time temperature statistics (when the system is stochastically forced, internal variability, appendix~~ces~~ B~~, C~~), and finally (~~appendix D~~appendix C), the changes needed to account for the Earth's spherical geometry, including the definition of fractional operators on the sphere.

2. The two-dimensional homogeneous heat equation

2.1 The homogeneous GHEBE

In part I we recalled the heat equation for the time-varying temperature anomalies (T) with diffusive and (horizontal) effective advective velocity ($\underline{v}$):

$$\left(\frac{\partial}{\partial t}-\kappa_v\frac{\partial^2}{\partial z^2}\right)T=-\underline{v}\cdot\nabla_h T+\kappa_h\nabla_h^2 T \tag{1}$$

(This is written in the still general form of eq. 19, part I). κ_h, κ_v are horizontal and vertical thermal diffusivities, z the vertical coordinate (pointing upwards, the Earth is $z\leq 0$), t the time, $\underline{x}=(x,y)$ the horizontal coordinates, $\nabla_h=\hat{x}\partial/\partial x+\hat{y}\partial/\partial y$ (the circonflexes indicate unit vectors). These equations must now be solved using the conductive-radiative surface boundary condition:

$$\left.\left(\frac{T(\underline{x},z,t)}{s}+\rho c\kappa_v\frac{\partial T(\underline{x},z,t)}{\partial z}\right)\right|_{z=0}=F(\underline{x},t) \tag{2}$$

ρ, c are the fluid densities and specific heats, s ~~λ~~ is the climate sensitivity and F is the anomaly forcing. The initial conditions are $T = 0$ at $z = -\infty$ (all t), and $T\left(\underline{x}, z, t = 0\right) = 0$ (Riemann-Liouville) or below, $T\left(\underline{x}, z, t = -\infty\right) = 0$ (Weyl).

Formatted: Font: Italic

In part I, we nondimensionalized the zero-dimensional homogeneous operators by nondimensionalizing time by the relaxation time: $t \to t/\tau$ (with $\tau = \kappa_v \left(\rho c s\right)^2$) and nondimensionalizing the vertical distance by the vertical diffusion depth: $z \to z/l_v$, with $l_v = \left(\tau \kappa_v\right)^{1/2}$. Considering now the full equation with advective and diffusive transport, we nondimensionalize the horizontal coordinates by the horizontal diffusion length: $\underline{x} \to \underline{x}/l_h$, (with $l_h = \left(\tau \kappa_h\right)^{1/2}$) and use the nondimensional advection velocity $\underline{\alpha} = \frac{\underline{v}}{V}$ (with speed $V = \frac{l_h}{\tau}$). If we now take s~~λ~~ = 1 (equivalent to using dimensions of temperature for the forcing F), we obtain:

Formatted: Font: Italic

$$\left(\frac{\partial^2}{\partial z^2} - \left(\frac{\partial}{\partial t} + \left(-\nabla_h^2\right) - \underline{\alpha} \cdot \nabla_h\right)\right) T = 0$$

$$\left.\frac{\partial T}{\partial z}\right|_{z=0} + T\left(t, \underline{x}; 0\right) = F\left(t, \underline{x}\right) \qquad (3)$$

For the heat equation and the conductive-radiative surface boundary condition respectively. For initial conditions such that $T = 0$ for $t \leq 0$, as in part I, we take Laplace transforms in time, but we now take Fourier transforms in the horizontal:

$$\left(\frac{\partial^2}{\partial z^2} - \left(\frac{\partial}{\partial t} + \left(-\nabla_h^2\right) - \underline{\alpha} \cdot \nabla_h\right)\right) T = 0 \overset{L.T.(t), F.T.(\underline{x})}{\leftrightarrow} \left(\frac{d^2}{dz^2} - \left(p + k^2 - i\underline{\alpha} \cdot \underline{k}\right)\right) \hat{T} = 0 \qquad (4)$$

Where "F.T." is the Fourier transform in horizontal space, $\underline{k}$ for the conjugate of $\underline{x}$, $k = \left|\underline{k}\right|$ (the vector modulus) with conjugate variable $r = \left|\underline{x}\right|$ (as usual, $\nabla_h \overset{F.T.}{\leftrightarrow} i\underline{k}$). Fourier transforms in space are convenient for either infinite horizontal media, or media with periodic horizontal boundary conditions. In ~~appendix D~~appendix C, we consider the changes needed to account for spherical geometry.

When $F\left(t, \underline{x}\right) = \delta\left(t\right)\delta\left(\underline{x}\right)$, the solution $T\left(t, \underline{x}\right) \to G_\delta\left(t, \underline{x}\right)$ and $\hat{T}\left(p, \underline{k}\right) \to \hat{G}_\delta\left(p, \underline{k}\right)$ where G_δ is the impulse (Dirac) response Green's function, part I, eq. 30. From eq. 4, we see that this is the same as the zero dimensional equation (eq. 24, part I) but with $p \to p + k^2 - i\underline{\alpha} \cdot \underline{k}$ i.e. for the corresponding Green's function:

$$\widehat{G_\delta}\left(p,k;z\right)=\widehat{G_\delta}\left(p+k^2-i\underline{\alpha}\cdot\underline{k};z\right) \tag{5}$$

A note on notation: the first argument is time, with the vertical separated by a semi-colon. When there is a horizontal coordinate it comes after time, before the semicolon. With this notation, the right hand side of eq. 5 is the L.T. of the zero-dimensional (time-depth) Green's function $G_\delta\left(t;z\right)$, the left hand side is the Laplace (time) and Fourier transform (horizontal, space) transform.

We can now use the basic Laplace shift property:

$$e^{\left(-k^2+i\underline{\alpha}\cdot\underline{k}\right)t}G_\delta\left(t;z\right)\overset{L.T.(t)}{\leftrightarrow}\widehat{G_\delta}\left(p+k^2-i\underline{\alpha}\cdot\underline{k};z\right) \tag{6}$$

To conclude that:

$$\hat{G}_\delta\left(t,\underline{k};z\right)=e^{\left(-k^2+i\underline{\alpha}\cdot\underline{k}\right)t}G_\delta\left(t;z\right) \tag{7}$$

Decomposing this into a circularly symmetric diffusion part $\widehat{G}_{\delta,dif}\left(t,k;z\right)$ and a factor $e^{i\underline{k}\cdot\underline{\alpha}t}$ that shifts phases, we obtain:

$$\hat{G}_\delta\left(t,\underline{k};z\right)=e^{i\underline{k}\cdot\underline{\alpha}t}\widehat{G}_{\delta,dif}\left(t,k;z\right);\qquad \widehat{G}_{\delta,dif}\left(t,k;z\right)=e^{-k^2t}G_\delta\left(t;z\right) \tag{8}$$

By circular symmetry of $\widehat{G}_{\delta,dif}\left(t,k;z\right)$, its inverse (2-D) Fourier transform reduces to an inverse Hankel transform ("H.T.").

Using:

$$\frac{e^{-r^2/(4t)}}{2t}\overset{H.T.}{\leftrightarrow}e^{-k^2t} \tag{9}$$

We therefore obtain for the diffusive part of the surface impulse response (i.e. the response with source spatial forcing $\delta\left(\underline{x}\right)=\delta\left(r\right)/\left(2\pi r\right)$):

$$G_{\delta,dif}\left(t,r;z\right)=\frac{e^{-r^2/(4t)}}{2t}G_\delta\left(t;z\right) \tag{10}$$

Where $G_\delta\left(t;z\right)$ is the zero-dimensional impulse response. If needed, its integral representation is given in eq. ~~30~~34, part I. The last step is to take into account the advective term associated with the phase shift $\underline{k}\cdot\underline{\alpha}t$. For this final step, we use the Fourier shift theorem to obtain:

$$G_\delta\left(t,\underline{x};z\right)=G_{\delta,dif}\left(t,\left|\underline{x}-\underline{\alpha}t\right|;z\right)=\frac{e^{-\left|\underline{x}-\underline{\alpha}t\right|^2/(4t)}}{2t}G_\delta\left(t;z\right) \tag{11}$$

This is the general surface result for the diffusive-advective transport part of the spatially homogeneous case. As expected, the advective transport simply displaces the ~~center~~ centre of the impulse response with nondimensional velocity $\underline{\alpha}$. As usual, the solutions for arbitrary forcing $F(t,\underline{x})$ can be obtained by convolution.

For the surface we obtain the simpler expressions:

$$G_{\delta,dif}\left(t,r;0\right)=\frac{e^{-r^2/(4t)}}{2t}\left(\frac{1}{\sqrt{\pi t}}-e^t erfc\sqrt{t}\right)$$

$$G_{\Theta,dif}\left(t,r;0\right)=\int_0^t G_{\delta,dif}\left(t,r;0\right)dt=\frac{1}{r}erfc\left(\frac{r}{2\sqrt{t}}\right)-\int_0^t\frac{e^{-\frac{r^2}{4s}+s}}{2s}erfc\left(s^{1/2}\right)ds \tag{12}$$

(see eq. ~~31~~35, part I). From these, the general surface results including advection are obtained with $r\rightarrow\left|\underline{x}-\underline{\alpha}t\right|$, i.e. $G_\delta\left(t,\underline{x};0\right)=G_{\delta,dif}\left(t,\left|\underline{x}-\underline{\alpha}t\right|;0\right)$.

Since the advection term has this simple consequence, below we take $\underline{\alpha}$ = 0, considering only diffusive transport, advection can easily be included if needed (i.e. below, we take $G_\delta\left(t,r;0\right)=G_{\delta,dif}\left(t,r;0\right)$).

To better understand the impulse response, fig. 1 shows this surface $G_\delta\left(t,r;0\right)$ for various radial distances r and fig. 2 shows the corresponding time dependence of the time integral of G_δ; the unit step response G_Θ for various distances r, illustrating the power law approach to ~~thermodynamic~~ equilibrium at large t (discussed in section 2.2). The corresponding long time, short distance expansions are:

$$\begin{aligned}G_\delta\left(t,r;0\right)&\approx\frac{t^{-5/2}}{4\sqrt{\pi}}-\frac{\left(6+r^2\right)}{16\sqrt{\pi}}t^{-7/2}+O\left(t^{-9/2}\right)\\ G_\Theta\left(t,r;0\right)&\approx G_{therm,\delta}\left(r;0\right)-\frac{t^{-3/2}}{6\sqrt{\pi}}+\frac{\left(6+r^2\right)}{40\sqrt{\pi}}t^{-5/2}+O\left(t^{-7/2}\right)\end{aligned};\qquad\begin{aligned}t&>>1\\ r&<<1\end{aligned} \tag{13}$$

Where $G_{therm,\delta}(r,0)$ is the Green's function for the (spatial Dirac) "hotspot" ~~thermodynamic~~ equilibrium response discussed below (eq. 20). Note that the leading term in $G_\delta(t,r;0)$ is independent of *r*, and the leading term in the approach to ~~thermodynamic~~ equilibrium $G_\Theta(t,r;0)$ is also independent of *r*.

Just as we derived the zero-dimensional HEBE by showing that it had the same Green's function as the $z = 0$ transport equation Green's function, we can likewise derive the homogeneous Generalized Half-Order Energy Balance Equation (GHEBE) which is the space-time surface equation whose Green's function is given in eq. 12. Following the derivation of the HEBE, in part I eq. 29, and replacing $p \to p + k^2 - i\underline{\alpha}\cdot\underline{k}$ we obtain:

$$\hat{G}_\delta(p,\underline{k};z) = \frac{e^{\sqrt{p+k^2-i\underline{\alpha}\cdot\underline{k}}\,z}}{\sqrt{p+k^2-i\underline{\alpha}\cdot\underline{k}}+1} \tag{14}$$

Hence, for $z = 0$:

$$\left[\left(\frac{\partial}{\partial t}+\left(-\nabla_h^2\right)-i\underline{\alpha}\cdot\nabla_h\right)^{1/2}+1\right]G_\delta(t,\underline{x};0)=\delta(t)\delta(\underline{x}) \overset{(L.T.(t),F.T.(\underline{x}))}{\longleftrightarrow} \left(\sqrt{p+k^2-i\underline{\alpha}\cdot\underline{k}}+1\right)\hat{G}_\delta(p,\underline{k};0)=1 \tag{15}$$

The left hand equation is the homogeneous GHEBE whose Green's function is given by eq. 12. We have therefore found a surprisingly simple explicit formula for the (inverse) half-order space-time GHEBE operator:

$$\left[\left(\frac{\partial}{\partial t}+\left(-\nabla_h^2\right)-i\underline{\alpha}\cdot\nabla_h\right)^{1/2}+1\right]^{-1}=G_\delta(t,\underline{x};0)* \tag{16}$$

where "$*$" indicates convolution. This allows us to give a precise interpretation of the half-order operator. Therefore the dimensional, homogeneous, GHEBE and its full solution are:

$$\left(\tau\frac{\partial}{\partial t}+\left(-l_h^2\nabla_h^2\right)-il_h\underline{\alpha}\cdot\nabla_h\right)^{1/2}T_s(t,\underline{x})+T_s(t,\underline{x})=sF(t,\underline{x})$$

$$\begin{aligned} T_s(t,\underline{x}) &= s\int_{surf}\int_0^t G_\delta\left(\frac{t-t'}{\tau},\frac{\left|\underline{x}-\underline{x}'\right|}{l_h};0\right)F(t',\underline{x}')\frac{dt'}{\tau}\frac{d\underline{x}'}{l_h^2} \\ &= \frac{s}{l_h^2}\int_{surf}\int_0^t \frac{e^{-\tau\left|\underline{x}-\underline{x}'-l_h\underline{\alpha}(t-t')/\tau\right|^2/\left(4l_h^2(t-t')\right)}}{2(t-t')}\left(\sqrt{\frac{\tau}{\pi(t-t')}}-e^{(t-t')/\tau}erfc\sqrt{\frac{(t-t')}{\tau}}\right)F(t',\underline{x}')dt'd\underline{x}' \end{aligned} \tag{17}$$

Field Code Changed

(“surf” is the surface over which the forcing acts, the bottom line uses the explicit eq. 12 for G_δ).

The above shows that even with the purely classical integer-ordered Budyko-Sellers type heat equation, that surface temperatures already obey long memory, half order equations. However, it is not certain that the classical heat equation is in fact the most appropriate model. Straightforward generalizations to fractional heat equations - where $\tau \frac{\partial T}{\partial t} \to \tau^{2H}\,{}_{\infty}D_t^{2H} T$ lead directly to fractional energy balance equations for surface temperatures, we investigate fractional heat equations elsewhere. Physically, this generalization from the classical fractional value H = 1/2 could be a consequence of turbulent diffusive transport which since at least Richardson been known to have anomalous diffusion.

2.2 Energy balance, ~~Thermodynamic~~ equilibrium

If $F(t,x)$ = 0 then there is a radiative energy balance at time t, point x, but the temperature may be changing. However, i~~I~~f $F(t,x)$ = 0 for a long enough time, and for all x ~~$F(t)$ = 0~~, then the time derivatives ($\frac{\partial}{\partial t}=0$) vanish and Earth is in a steady energy balance (“climate”) state, $T_{clim}(x)$, so that the temperature anomaly $T(t,x)$ = 0. Now consider a step function increase $F(t,\underline{x})=\Theta(t)F_0(\underline{x})$. Then as $t\to\infty$, the time derivatives will vanish and a new (steady) climate state (with temperature $T_0(\underline{x})$) will be reached in which the horizontal transport and anomalous black body emission balance the new forcing: $\left(\left(-\nabla_h^2\right)^{1/2}+1\right)T_0(\underline{x})=F_0(\underline{x})$. The new state is steady in time and is in energy balance with outer space and its local surroundings, but it is not strictly correct to describe $T_0(\underline{x})$ as one of thermal equilibrium. This is because thermal equilibrium would imply that the temperature everywhere is constant (thermodynamic equilibrium is an even more stringent condition). Nevertheless the term “radiative equilibrium” is commonly used in the context of planetary energy balance, so we will use the terms energy balance and equilibrium synonymously.

Let us now investigate the equilibrium state. Since~~, then the system is at equilibrium and will stay there. However, if F is a step function in time, then as $t\to\infty$, a new equilibrium will be established. At equilibrium,~~ d/dt = 0, ~~so that~~ the conjugate variable p = 0, ~~. W~~with this and $\underline{\alpha}$ = 0 in eq. 15, we obtain the equation for the (spatial) surface impulse response $G_{eq,\delta}(r;0)$ for ~~thermodynamic~~ equilibrium (subscript “~~therm~~eq”):

$$\left(\left(-\nabla_h^2\right)^{1/2}+1\right)G_{eq,\delta}=\delta(\underline{x})\overset{F.T.}{\leftrightarrow}(k+1)\hat{G}_{eq,\delta}=1 \qquad (18)$$

Field Code Changed

Formatted: Font: Italic

Formatted: Font: Italic

Formatted: Font: Italic, Underline

Formatted: Font: Italic

Formatted: Font: Italic, Underline

Formatted: Font: Italic, Underline

Formatted: Font: Italic

Formatted: Font: Italic, Subscript

Formatted: Font: Italic, Underline

Formatted: Font: Italic

Formatted: Font: Italic

Formatted: Font: Italic, Underline

i.e. the same as eq. 4 but with $p = 0$ (and $\underline{\alpha} = 0$) hence:

$$\hat{G}_{eq,\delta}(k;z) = \frac{e^{kz}}{1+k} \tag{19}$$

The equilibrium surface temperature (spatial) impulse (Dirac "hotspot") Green's function is therefore:

$$G_{eq,\delta}(r,0) = \frac{1}{r} + \frac{\pi}{2}\left(Y_0(r) - H_0(r)\right) \overset{(H.T.)}{\leftrightarrow} \hat{G}_{eq,\delta}(k;0) = \frac{1}{1+k} \tag{20}$$

Where H_0 is the zeroth order Struve function and Y_0 is the zeroth order Bessel function of the second kind. For large r, we have the expansions:

$$G_{eq,\delta}(r;0) \approx \frac{1}{r^3} - \frac{9}{r^5} + O\left(r^{-7}\right); \quad r >> 0 \tag{21}$$

$$G_{eq,\delta}(r;0) \approx \frac{1}{r} + \log r + \gamma_E - \log 2 - r + \frac{r^2}{4}\left(1 + \log 2 - \gamma_E\right) - \frac{r^2}{4}\log r + \ldots; \quad r \approx 0$$

The $1/r^3$ asymptotic decay is fast and implies that spatial hotspots remain fairly localized; indeed, it is easy to show that if instead we had a Dirac surface heat flux source driving the system (i.e. with surface BC $\left.\frac{\partial T}{\partial z}\right|_{z=0} = \delta(\underline{x})$ i.e. without radiation) that the decay would be the much faster ($1/r$). Forcing inhomogeneities thus remain much more localized than would otherwise be the case.

To study the convergence to ~~thermodynamic~~ equilibrium, consider a simple model of a surface "hot spot" where the forcing is confined to a unit circle and turned on and held at a constant unit temperature at $t = 0$. This is the spatial equivalent of a step forcing in space, we combine it with a step (Heaviside) in time:

$$F(t,r) = \Theta(t)\Pi_1(r); \quad \Pi_1(r) = \begin{matrix} 1 & r \le 1 \\ 0 & r > 1 \end{matrix} \tag{22}$$

$\Pi_1(r)$ is the corresponding indicator function. We now use the transform pair $\Pi_1(r) \overset{H.T.}{\leftrightarrow} \frac{J_1(k)}{k}$ to perform the convolution:

$$T_s(t,r) = G_\Theta(t,r;0) * \Theta(t)\Pi_1(r) \overset{H.T.}{\leftrightarrow} \frac{J_1(k)}{k}\hat{G}_\Theta(t,k;0) \qquad (23)$$

(J_1 is the first order Bessel function of first kind). Taking the limit $t \to \infty$ we obtain the ~~thermodynamic~~ equilibrium temperature distribution. Alternatively we could find it directly by from eq. 19:

$$T_{eq,s}(r) = T_s(\infty,r) \overset{H.T.}{\leftrightarrow} \frac{J_1(k)}{k(1+k)} \qquad (24)$$

Fig. 4 shows the cross section as a function of the distance from the circle's center at various times (the inverse Hankel transforms were done numerically). We note that the temperature rises very quickly at first, then slowly reaches equilibrium (thick). The figure also shows (dashed) the ~~thermodynamic~~ equilibrium when the forcing is purely due to unit conductive heating over the unit circle. The difference between the dashed and the thick ~~thermodynamic~~ equilibrium curves are purely due to the radiative loses in the latter. (Note that in the zero-dimensional case (part I), using pure heating forcing boundary conditions leads to diverging temperatures, there is no ~~thermodynamic~~ equilibrium. This explains why Brunt instead used temperature forcing boundary conditions. Here, in two horizontal dimensions, boundary conditions that impose a fixed temperature over the circle are problematic since they imply infinite horizontal temperature gradients and infinite horizontal heat fluxes).

Figs. 5, 6 shows the same evolution but with temperature as a function of time for various distances (fig. 5) and as contours in space-time (fig. 6). We see that equilibrium is largely established in the first two relaxation times (here τ = 1) and most of the perturbation is confined to two horizontal diffusion distances (here, $l_h = 1$).

2.3 Comparison of the HEBE with the standard 1-D Budyko - Sellers model on a sphere

Formatted: Font: Bold
Formatted: Heading 2 Char
Formatted: Heading 2 Char
Formatted: Heading 2 Char

It is helpful to clearly understand the similarities and differences between the HEBE and the usual 1-D (latitudinal) B-S approach (see the comprehensive monograph [*North and Kim*, 2017], and see [*Zhuang et al.*, 2017], [*Ziegler and Rehfeld*, 2020] for recent applications, development). Since the latter model is on a sphere but with only latitudinal dependence, we write the horizontal transport term $\nabla_h \cdot D_{B-S} \nabla_h$ using gradient and divergence operators: $\nabla_h \cdot = -\frac{1}{R}\frac{d}{d\mu}\sqrt{1-\mu^2};\quad \nabla_h = -\frac{\sqrt{1-\mu^2}}{R}\frac{d}{d\mu}$ with θ = colatitude and μ = cos θ. In standard notation [*North and Kim*, 2017]) the B-S equation is thus written:

Field Code Changed
Formatted: Font: Cambria

$$C\frac{\partial T}{\partial t}-\frac{\partial}{\partial\mu}\left(D_{B-S}(\mu)\left(1-\mu^2\right)\frac{\partial}{\partial\mu}T\right)+B(\mu)T+A(\mu)=Q_0H(\mu);\quad H(\mu)=S(\mu)a(\mu) \qquad (25)$$

Where C is the specific heat per area, D_{B-S} the thermal conductivity per radian of arc, B is the climate feedback parameter, the inverse of climate sensitivity ($B=1/s$), Q_0, the solar constant, H the heat function, S is the insolation distribution function, a is the co-albedo and A is the constant term from the linearization of the black-body emission. If we measure temperatures with respect to the mean (reference) Earth temperature so that the A term balances the mean forcing), then the B-S equation with dimensionless operators can be written:

$$\left(\tau\frac{\partial}{\partial t}-s\frac{\partial}{\partial\mu}D_{B-S}(\mu)\left(1-\mu^2\right)\frac{\partial}{\partial\mu}\right)T+T=sF \qquad (26)$$

(the product sD_{B-S} is dimensionless, $\tau=C/B$) where F is the anomaly with respect to the global average.

In part I section 3.1.1, we expressed the horizontal transport operator in terms of the transport coefficient D_F that allows us to write the HEBE in the form:

$$\left(\tau\frac{\partial}{\partial t}+\zeta\right)^{1/2}T+T=sF;\quad \zeta=-sR\nabla_h\cdot D_F\nabla_h;\quad D_F(\underline{x})=\frac{l_h(\underline{x})}{Rs(\underline{x})}=\kappa_h\frac{\beta\rho c}{R} \qquad (27)$$

where $\beta=\left(\kappa_v/\kappa_h\right)^{1/2}$. Using $\zeta=-s\frac{d}{d\mu}D_F(\mu)\left(1-\mu^2\right)\frac{d}{d\mu}$ for the transport operator, we obtain the 1-D HEBE on the sphere:

$$\left(\tau\frac{\partial}{\partial t}-s\frac{\partial}{\partial\mu}D_F(\mu)\left(1-\mu^2\right)\frac{\partial}{\partial\mu}\right)^{1/2}T+T=sF \qquad (28)$$

In the case of constant thermal diffusion coefficients we may solve both equations using Legendre polynomials $P_n(\mu)$ that are eigenfunctions of the Laplacian: $\left(-\frac{\partial}{\partial\mu}\left(1-\mu^2\right)\frac{\partial}{\partial\mu}\right)P_n(\mu)=n(n+1)P_n(\mu)$ (with boundary conditions at the poles being zero horizontal heat flux, see also appendix C for more general results on the sphere). Expanding the temperature and forcing in terms of the Legendre polynomials and taking Laplace transforms of the coefficients in time, we obtain:

Formatted: Equation

Field Code Changed

Formatted: Equation

Field Code Changed

Formatted: Font: Italic

Formatted: Font: Italic

Formatted: Equation

Field Code Changed

Field Code Changed

Formatted: Equation

Formatted: Font: Italic

Formatted: Font: Italic, Subscript

Formatted: Font: Symbol

Field Code Changed

$$T(t,\mu)=\sum_{n=0}^{\infty}T_n(t)P_n(\mu)\overset{L.T.}{\leftrightarrow}\widehat{T}(p,\mu)=\sum_{n=0}^{\infty}\widehat{T}_n(p)P_n(\mu)$$

$$F(t,\mu)=\sum_{n=0}^{\infty}F_n(t)P_n(\mu)\overset{L.T.}{\leftrightarrow}\widehat{F}(p,\mu)=\sum_{n=0}^{\infty}\widehat{F}_n(p)P_n(\mu) \qquad (29)$$

We then obtain equations for the Laplace transform of the n^{th} Legendre coefficients:

$$\begin{gathered}\left(\tau p+\xi_{B-S,n}\right)\widehat{T}_n+\widehat{T}_n=s\widehat{F}_n;\quad \xi_{B-S,n}=sD_{B-S}n(n+1)\\ \left(\tau p+\xi_{F,n}\right)^{1/2}\widehat{T}_n+\widehat{T}_n=s\widehat{F}_n;\quad \xi_{F,n}=sD_F n(n+1)\end{gathered} \qquad (30)$$

So that:

$$\widehat{T}_n(p)=s\widehat{G}_\delta^{(n)}(p)\widehat{F}_n(p);\qquad \begin{gathered}\widehat{G}_{\delta,B-S}^{(n)}(p)=\widehat{G}_{\delta,1}\left(\tau p+\xi_{B-S,n}\right);\\ \widehat{G}_{\delta,F}^{(n)}(p)=\widehat{G}_{\delta,1/2}\left(\tau p+\xi_{F,n}\right);\end{gathered}\qquad \widehat{G}_{\delta,H}(p)=\frac{1}{1+p^H} \qquad (31)$$

In real space:

$$\begin{gathered}\tau^{-1}e^{-\xi_{B-S,n}t/\tau}G_{0,B-S}^{(n)}(t/\tau)\overset{L.T.}{\leftrightarrow}\widehat{G}_{0,1}^{(n)}\left(p\tau+\xi_{B-S,n}\right)\\ \tau^{-1}e^{-\xi_{1/2,n}t/\tau}G_{0,F}^{(n)}(t/\tau)\overset{L.T.}{\leftrightarrow}\widehat{G}_{0,1/2}^{(n)}\left(p\tau+\xi_{F,n}\right)\end{gathered} \qquad (32)$$

(note that the generalization to the FEBE is obtained by the replacement $\tau p\to(\tau p)^{2H}$ so that $\widehat{G}_{\delta,H}^{(n)}(p)=1/\left(1+\left((\tau p)^{2H}+\xi_{F,n}\right)^{1/2}\right)$ whereas $\widehat{G}_{\delta,B-S}^{(n)}(p)=1/\left(1+\tau p+\xi_{B-S,n}\right)$ so that $\widehat{G}_{\delta,B-S}^{(n)}$ is *not* a special case of the FEBE). Using:

$$e^{-t} \overset{L.T.}{\leftrightarrow} \frac{1}{1+p}$$

$$\sqrt{\frac{1}{\pi t}} - e^{t/\tau} erfc\sqrt{t} \overset{L.T.}{\leftrightarrow} \frac{1}{1+p^{1/2}} \qquad (33)$$

(eq. 35, part I), combining this with eq. 32, we obtain for the impulse responses:

$$G^{(n)}_{\delta,B-S}(t) = \tau^{-1} e^{-(1+\xi_{B-S,n})t/\tau}$$

$$G^{(n)}_{\delta,F}(t) = \tau^{-1} e^{-\xi_{F,n} t/\tau}\left(\sqrt{\frac{\tau}{\pi t}} - e^{t/\tau} erfc\sqrt{\frac{t}{\tau}}\right) \qquad (34)$$

Integrating these with respect to t, we obtain the step responses:

$$G^{(n)}_{\Theta,B-S}(t) = \frac{1}{\xi_{B-S,n}+1}\left(1-e^{-(\xi_{B-S,n}+1)t/\tau}\right)$$

$$G^{(n)}_{\Theta,F}(t) = \frac{\sqrt{\xi_{F,n}}\, erf\sqrt{\xi_{F,n}\frac{t}{\tau}} - 1 + e^{-t(\xi_{F,n}-1)/\tau} erfc\sqrt{\frac{t}{\tau}}}{\xi_{F,n}-1} \qquad (35)$$

The long time limit represents Earth energy balance (equilibrium):

$$G^{(n)}_{eq,B-S} = G^{(n)}_{\Theta,1}(\infty) = \frac{1}{1+\xi_{B-S,n}} = \frac{1}{1+sD_{B-S}n(n+1)}$$

$$G^{(n)}_{eq,F} = G^{(n)}_{\Theta,F}(\infty) = \frac{1}{1+\sqrt{\xi_{F,n}}} = \frac{1}{1+\sqrt{sD_F n(n+1)}} \quad ; \quad \xi \geq 0 \qquad (36)$$

If $\xi<0$, then there is an unphysical divergence so that sD_F must be >0. Since $P_n(\mu)$ has n zeroes, n plays the role of wavenumber, it specifies structures of horizontal size ≈ $\pi R/n$. Therefore we see that the B-S model (where G falls off as n^{-2}) will yield a much smoother equilibrium temperature than the HEBE where it falls off as n^{-1}. Note that when generalized from the HEBE to the FEBE (with $p \rightarrow p^{2H}$), this equilibrium result is unchanged.

For the HEBE, the short and long time behaviours are:

Formatted: Equation

Formatted: Equation

Formatted: Font: Italic

Formatted: Equation

Field Code Changed

Formatted: Equation

Field Code Changed

Formatted: Font: Symbol

Formatted: Font: Italic

Formatted: Font: Italic

Formatted: Font: Italic, Subscript

Formatted: Font: Symbol

Formatted: Font: Italic

Formatted: Font: Italic

Formatted: Font: Symbol

Formatted: Font: Italic

Formatted: Font: Italic

Formatted: Font: Italic

Formatted: Font: Italic

Formatted: Superscript

Formatted: Font: Italic

Formatted: Superscript

Formatted: Font: Italic

Formatted: Font: Italic

Formatted: Superscript

Formatted: Font: Italic, Superscript

$$G_{\Theta,F}^{(n)}(t) = \frac{2t^{1/2}}{\sqrt{\pi\tau}} - \frac{t}{\tau} - \frac{2(\xi_{F,n}-2)}{3\sqrt{\pi}}\left(\frac{t}{\tau}\right)^{3/2} + \frac{1}{2}(\xi_{F,n}-1)\left(\frac{t}{\tau}\right)^{2} + \ldots; \qquad t << \tau; \quad n \ge 0$$

$$G_{\Theta,F}^{(0)}(t) = 1 - \frac{1}{\sqrt{\pi t}} + \frac{1}{2t\sqrt{\pi t}} - \ldots; \quad t >> \tau; \quad n = 0 \qquad (37)$$

$$G_{\Theta,F}^{(n)}(t) = \frac{1}{1+\sqrt{\xi_{F,n}}} - \frac{e^{-\xi_{F,n}t/\tau}}{2\sqrt{\pi}\xi_{F,n}}\left(\frac{t}{\tau}\right)^{-3/2}\left(1 - \frac{3}{2}\left(\frac{1+\xi_{F,n}}{\xi_{F,n}t/\tau}\right) + \ldots\right); \qquad t >> \tau; \quad n \ge 1$$

The asymptotic response for $G_{\Theta,F}^{(n)}(t)$ is interesting because it tells us how quickly equilibrium is reached. When $n = 0$ we have $P_0(\mu) = 1$, so that this component corresponds to the mean. Since $\xi_{F,0} = 0$ we see that it is identical to the zero-dimensional result in part I: equilibrium is approach in a power law fashion ($t^{-1/2}$ for large t), whereas for $n = 0$, the B-S model approach to equilibrium is exponential. However for $n \ge 1$, HEBE power law terms are exponentially damped, with exponential decay time: $\tau_{F,n} = \tau / \xi_{F,n}$ whereas the B-S model is exponentially damped for all n with $\tau_{B-S,n} = \tau / (1+\xi_{B-S,n})$.

In order to make a more detailed comparison between the models, we can follow [*North and Kim*, 2017] who consider a model with constant D_{S-B} and that is north-south symmetric so that the odd numbered polynomials vanish. They empirically give the climate equilibrium values for n = 0, 2, 4; the (constant) $n = 0$ term is used to obtain the mean temperature 288K. Other pertinent empirical data are $s = 1/B = 0.50$ KW^{-1}m^2, $F_2 = -180.7$ W/m^2, $F_4 = 20.8$K, $T_2 = -30$K, $T_4 = -4$K. From eq. 36 for the equilibrium temperature Green's function, we obtain: $T_{eq,n} = sG_{eq,B-S}^{(n)}F_n$. The $n = 2$ relationship is use to estimate $D_{B-S} = \frac{1}{6s}\left(\frac{sF_2}{T_2} - 1\right) = 0.67$ Wm^{-2}K^{-1}, with this estimate, we obtain $T_4 = F_4 / (1+\xi_{B-S,n}) = F_4 / (1+20D_{B-S}s) \approx$ 1.35K which is not far from the empirical estimate $T_4 = -4$K ([*North and Kim*, 2017]), it also yields the dimensionless quantity $sD_{B-S} = 0.33$. If we follow the same procedure for the HEBE, we estimate $D_F = \frac{1}{6s}\left(\frac{sF_2}{T_2} - 1\right)^2$, comparing this with the B-S relation, we find: $sD_F = 6(sD_{S-B})^2$ the dimensionless $sD_F = 0.67$, and $D_F = 1.33$ Wm^{-2}K^{-1}, $T_4 = 2.23$K (again not far from the data). We note that the ratio $D_F / D_{B-S} \approx 2$ so that the estimates are close.

We can use this information to estimate l_h in the HEBE. From the definition of D_{B-S} as a thermal conduction coefficient per radian we obtain $D_{B-S} = K/R$ so that $\kappa_h = K/\rho c = RD_{B-S}/\rho c \approx 1m^2/s$. To find the transport length, we can use $l_h = \beta\kappa_h \rho c s$, $\beta = \left(\frac{\kappa_v}{\kappa_h}\right)^{1/2}$, to obtain:

$$\frac{l_h}{R} = \beta s D_{B-S} \qquad (38)$$

Alternatively, we can estimate l_h from the global scale D_H:

$$\frac{l_h}{R} = s D_F \qquad (39)$$

We see that these l_h estimates differ by a factor of $\beta D_{B-S}/D_F \approx \beta/2$. Since typical numerical models with resolutions of hundreds of kilometers use $\kappa_v \approx 10^{-4}$ m^2/s, and $\kappa_h \approx 1m^2/s$, at least at these scales $\beta \approx 10^{-2}$ so that the difference in the estimates may be large. For example since $sD_{B-S} \approx 0.33$, we find that the former yields $l_h \approx 20$km, while the latter yields, $l_h \approx 4000$ km. One way to reconcile the difference is to assume that β - that characterizes the horizontal-vertical effective diffusivity ratio - has a systematic scale dependence due to a difference in the scaling properties of κ_h and κ_v so that at global scales $\beta \approx 1$ (this may arise as a consequence of the scaling anisotropic horizontal structure of the atmosphere at weather scales, notably of the horizontal wind field, the 23/9D model, [*Schertzer and Lovejoy*, 1985]).

A different (possibly additional) way of reconciling the estimates is to consider the potentially large (multifractal) intermittency of the diffusivities that introduces s strong scale effect. For example, θ [*Havlin and Ben-Avraham*, 1987], [*Weissman*, 1988], [*Lovejoy et al.*, 1998]) show that in 1-D, the large scale effective thermal resistance ρ_T – the inverse diffusivity - is the average of the small scale resistances. If we denote the spatial averages over a scale L by a subscript, and assume that the resistivity is scaling (scale invariant) up to planetary scales (denote this by R), then it will generally follow the following multifractal statistics:

$$\left\langle \rho_{T,L}^q \right\rangle = \left(\frac{R}{L}\right)^{K_\rho(q)} \left\langle \rho_{T,R}^q \right\rangle \qquad (40)$$

Where the angle brackets denote statistical averages and $K_\rho(q)$ is the moment scaling function that characterizes the scaling of the q^{th} order statistical moment order of the thermal resistance.

The thermal resistance is proportional to the inverse thermal diffusivity, therefore the effective HEBE diffusive transport coefficient at scale L satisfies:

Formatted: Indent: First line: 1 cm
Formatted ... [1]
Field Code Changed
Field Code Changed
Field Code Changed
Formatted: Equation
Field Code Changed
Formatted ... [2]
Formatted: Equation
Field Code Changed
Formatted ... [3]
Formatted ... [4]
Formatted: Equation
Field Code Changed
Formatted ... [5]
Formatted: Font: Italic

$$D_{F,L} \propto \kappa_{h,L} \propto \left(\rho_T^-\right)_L^{-1} \approx \left(\frac{R}{L}\right)^{-K_\rho(-1)} D_{F,R} \quad (41)$$

Finally, using $l_{h,L} \propto D_{F,L}$ we obtain:

$$l_{h,L} \propto \left(\frac{L}{R}\right)^{K_\rho(-1)} l_{h,R} \quad (42)$$

Which relates the transport length at small scales *L* and planetary scales *R*. Depending on $K_\rho(-1)$, the ratio $l_{h,L}/l_{h,R}$ can be quite small. For example, if the thermal resistivity statistics are taken as log-normal, then: $K_\rho(q) = C_1 q(q-1)$ so that $K_\rho(-1) = 2C_1$ so that $l_{h,L} \propto (L/R)^{2C_1} l_{h,R}$. As discussed in appendix A, $C_1 \approx 0.16$ for the temperature in space (see also [*Lovejoy*, 2018]). Using this value as a guide, we find $l_{h,L} \propto (L/R)^{0.32} l_{h,R}$ so that depending on the small scale resolution *L*, we can easily explain a factor of 10 or more increase in the effective transport length at large scales. Clearly the scale dependence of κ_h, κ_v is an important topic for future FEBE research.

3. The inhomogeneous heat equation

3.1 Babenko's method

The homogeneous heat equation in a semi-infinite domain is a classical problem and conductive - radiative surface boundary conditions naturally lead to fractional order operators, the HEBE and GHEBE. Although we have seen that fractional operators appear quite naturally, their advantages are much more compelling for the more realistic inhomogeneous equations relevant for the Earth. We ~~will~~ therefore ~~now~~ proceed to derive the inhomogeneous HEBE and GHEBE using Babenko's method. The more usual application is to find the surface heat flux given a solution to the conduction equation (see for example [*Magin et al.*, 2004], [*Chenkuan and Clarkson*, 2018]), the following application appears to be original.

In the inhomogeneous case with $\tau = \tau(\underline{x})$, $l_h = l_h(\underline{x})$, $l_v = l_v(\underline{x})$, $\underline{\alpha} = \underline{\alpha}(\underline{x})$, there is no unique nondimensionalization. Therefore, we express the inhomogeneous anomaly heat equation with nondimensional operators as:

$$\left(\tau\frac{\partial}{\partial t}+l_h\zeta-\left(l_v\frac{\partial}{\partial z}\right)^2\right)T=0;\qquad \zeta=\left(\underline{\alpha}\cdot\nabla_h+l_h\left(-\nabla_h^2\right)\right)$$ (43~~25~~)

Field Code Changed

Where we have used $\kappa_v\left(\underline{x}\right)=l_v^2\frac{\partial^2}{\partial z^2}=\left(l_v\frac{\partial}{\partial z}\right)^2$ and ζ is a time independent horizontal transport operator allowing for both advective and diffusive transport. Under the fairly general conditions, when ζ operates on the temperature field, it is proportional to the nondimensional divergence of the horizontal heat flux (discussed in part I, see eq. 4). Since the forcing is via the surface boundary condition rather than by an inhomogeneous term, eq. ~~25~~ 43 is mathematically homogeneous.

The first step in Babenko's method (see e.g. [*Podlubny*, 1999], [*Magin et al.*, 2004]), is to factor the differential operator:

$$\left(\Lambda+l_v\frac{\partial}{\partial z}\right)\left(\Lambda-l_v\frac{\partial}{\partial z}\right)T=0;\quad \Lambda=\left(\tau\frac{\partial}{\partial t}+l_h\zeta\right)^{1/2}$$ (44~~26~~)

Field Code Changed

As usual, the general solution of a homogeneous equation is a linear combination of elementary solutions A_+ and A_-:

$$\left(\Lambda+l_v\frac{\partial}{\partial z}\right)A_+\left(t,\underline{x};z\right)=0;\quad \left(\Lambda-l_v\frac{\partial}{\partial z}\right)A_-\left(t,\underline{x};z\right)=0$$ (45~~27~~)

The A_+ solution leads to solutions that diverge at $z=-\infty$ whereas A_- leads to the required physical solutions with $T\left(-\infty\right)=0$, ([*Podlubny*, 1999]). Therefore we are interested in solutions to:

$$\left(\Lambda-l_v\frac{\partial}{\partial z}\right)T\left(t,\underline{x};z\right)=0$$ (46~~28~~)

putting $z=0$ and *using* $Q_z=-\left(l_v/s\right)\partial T/\partial z$ (part I, eq. 22)~~6~~, we obtain:

Formatted: Font: Italic

Formatted: Font: Not Italic

Formatted: Font: Not Italic

$$\left(\tau\frac{\partial}{\partial t}+l_h\zeta\right)^{1/2}T_s=l_v\left.\frac{\partial T}{\partial z}\right|_{z=0}=sQ_s;\qquad \begin{array}{l}T_s\left(t,\underline{x}\right)=T\left(t,\underline{x};0\right)\\ Q_s\left(t,\underline{x}\right)=-\left(\underline{Q}_d\left(t,\underline{x};0\right)\right)_z\end{array}$$ (47~~29~~)

Field Code Changed

where $T_s(t,\underline{x})$ is the surface temperature anomaly and Q_s is the heat flux into the surface (the negative of $Q_{s,d,z}$ which is the z component of the surface conductive (sensible) heat flux). Before interpreting the half order operator on the left, we can

Field Code Changed

already give this equation a physical interpretation. When Q_s >0, sensible heat is forced into the Earth, some of it is stored in the subsurface (the $\tau\frac{\partial}{\partial t}$ term, the same horizontal position $\underline{x}$ but stored by heating up the subsurface, z<0), and some of the heat (the $l_h\zeta$ term), is transported horizontally to neighbouring regions (and conversely when Q_s <0). We can also understand the basic difference between the A_+ and A_- solutions: whereas the physically relevant A_- solution correspond to energy storage and horizontal transport in the region z<0, the A_+ solutions correspond to the region z>0 assumed to be devoid of conducting material.

The final step is to use the fact that the conductive heat flux Q_s is equal to the radiative imbalance (part I, fig. 1):

$$Q_s = R_\uparrow - R_\downarrow = \frac{T_s}{s} - F$$

(48~~30~~)

Combining the equations 29, 30 we obtain the inhomogeneous Generalized Half-order Energy Balance Equation (GHEBE):

$$\left(\tau(\underline{x})\frac{\partial}{\partial t} + l_h(\underline{x})\zeta(\underline{x})\right)^{1/2} T_s(t,\underline{x}) + T_s(t,\underline{x}) = s(\underline{x})F(t,\underline{x})$$

(49~~31~~)

If needed, the internal field $T(t,\underline{x};z)$, can be found by solving eq. ~~31~~ 49 for $T_s(t,\underline{x})$ which is the z = 0 boundary condition for the full eq. ~~25~~43. We see that eq. ~~31~~ 49 reduces to the homogeneous GHEBE (eq. 17) when τ, l_h, s~~λ~~, $\underline{\alpha}$ are constant. By comparing this derivation with that of the homogeneous GHEBE via the classical Laplace-Fourier transform method (section 2.1), it is clear that Babenko's method is very similar, but is more general. Whereas in the homogeneous equation, where the transforms reduce the derivative operations to algebra, the difficulty with Babenko's method is to find proper interpretations of the fractional operators. However, in the above, we assumed that τ was only a function of position, so that Laplace (or Fourier) transform methods still apply in the time domain, in the next section we discuss the more challenging interpretation of the fractional inhomogeneous spatial operators.

3.2 The zeroth order high frequency GHEBE: the HEBE

Before discussing the inhomogeneous GHEBE, consider the case where the horizontal term $l_h\zeta$ is small compared to $\tau\frac{\partial}{\partial t}$; below we argue that this is a good approximation for scales up to years and decades and greater than tens of kilometers (table 1, appendix A). Recall that the this horizontal transport term is in fact proportional to the divergence of the horizontal heat flux so that it may be small even when heat fluxes are significant [*Trenberth et al.*, 2009]. Alternatively, in globally averaged

Field Code Changed

Field Code Changed

Field Code Changed

Formatted: Font: Italic

models, there are no horizontal inhomogeneities so that ζ = 0. In these cases $\Lambda=\tau\left(\underline{x}\right)^{1/2}\frac{\partial^{1/2}}{\partial t^{1/2}}$; and we obtain the inhomogeneous HEBE as a special case of the inhomogeneous FEBE:

$$\tau\left(\underline{x}\right)^{H}\,{}_{-\infty}D_t^H T_s\left(t,\underline{x}\right)+T_s\left(t,\underline{x}\right)=s\left(\underline{x}\right)F\left(t,\underline{x}\right);\qquad H=1/2$$ (50~~32~~)

We have written it with a general H since as in part I, an inhomogeneous version of the EBE may be obtained with H = 1. We have also used the Weyl derivative (i.e. from $t=-\infty$) since this accommodated periodic or statistically stationary forcing as well as forcing starting at t = 0 (I this case we simply consider F = 0 for $t\leq 0$). Eq. ~~32~~ 50 shows that the HEBE only depends on the local climate sensitivity and the local relaxation time. We'll see below that explicit dependence on the horizontal transport (ν, κ_h) and specific heat per volume ρc is only important at scales somewhat smaller than the transport length scale (or alternatively at extremely long time scales, section 3.~~5~~6). Before solving the HEBE, it is instructive to introduce the notation $T_\infty\left(t,\underline{x}\right)=s\left(\underline{x}\right)F\left(t,\underline{x}\right)$. T_∞ is the equilibrium temperature that would be reached at time t, if at each location $\underline{x}$, F was suddenly stopped and fixed at that value. With this notation, we may integrate both sides of eq. ~~32~~ 50 by order H, and multiply by τ^{-H} to obtain:

$$T_s\left(t,\underline{x}\right)=\frac{1}{\Gamma\left(H\right)}\int_{-\infty}^{t}\left(\frac{t-u}{\tau\left(\underline{x}\right)}\right)^{H-1}\left(T_\infty\left(u,\underline{x}\right)-T_s\left(u,\underline{x}\right)\right)\frac{du}{\tau\left(\underline{x}\right)};\quad 0<H<1$$ (51~~33~~)

Field Code Changed

Written in this form, it is obvious that the temperature is constantly relaxing in a power law manner to T_∞ (although if F ~~and~~ is time dependent, equilibrium will in general never in fact be established). In the usual EBM special case (H = 1), the power law must be replaced by an exponential, the HEBE is obtained with H = 1/2. Since $T_\infty = sF$, ~~physically~~ the deviation from T_∞ - the term $\tau^{H}\,{}_{-\infty}D_t^H T_s$ (eq. ~~32~~50) - physically corresponds to the energy imbalance, as before, it is a power law, long memory energy storage term.

Field Code Changed

Field Code Changed

Field Code Changed

The FEBE is a linear differential equation that can be solved using Green's functions [*Miller and Ross*, 1993], [*Podlubny*, 1999]. The solution is:

$$T_s\left(\underline{x},t\right)=\frac{s\left(\underline{x}\right)}{\tau\left(\underline{x}\right)}\int_{-\infty}^{t}G_{\delta,H}\left(\frac{t-u}{\tau\left(\underline{x}\right)}\right)F\left(\underline{x},u\right)du$$ (52~~34~~)

where ~~G_0~~ $G_{\delta,H}$ is the H order Mittag-Leffler impulse response Green's function ([*Lovejoy*, 2019a]). In general, $G_{\delta\cancel{0},H}$ is only expressible in terms of infinite series, exceptions are the $H = 1$ EBE ($G_{\delta\cancel{0},1} = e^{-t}$); and the $H = ½$ HEBE (eq. 33~~with in the notation above~~ $G_{0,1/2}(t)=G_\delta(t;0)=\frac{1}{\sqrt{\pi t}}-e^t erfc\sqrt{t}$ ~~(eq. 31, part I~~).

The corresponding step response $G_{\Theta,1/2}$ = ~~$G_{1,1/2}$ = G_Θ~~ is the integral of ~~$G_{0,1/2}$~~ $G_{\delta,1/2}$ (respectively $G_{1,1/2}$, $G_{0,1/2}$ in the notation of eq. ~~32~~36, part I~~)~~), it describes relaxation to ~~thermodynamic~~ equilibrium when F is a step function; similarly, the ramp (linear forcing) response $G_{2,1/2}$ (eq. ~~32~~36, part I), is the integral of the step response.

3.3 Some features of stochastic forcing

The FEBE and the HEBE are examples of fractional relaxation equations; these have primarily been discussed in the context of deterministic forcings that start at $t = 0$. The corresponding stochastic fractional relaxation processes (in physics, "fractional Langevin equations", (FLE) see the references in [*Lovejoy*, 2019a]) - here corresponds to stochastic internal forcing. The FLE ~~have~~ has received little attention, although [*Kobelev and Romanov*, 2000], [*West et al.*, 2003] discuss the corresponding nonstationary random walks. The statistically stationary stochastic case that results when Weyl rather than Riemann-Liouville fractional derivatives are used is treated in [*Lovejoy*, 2019a], including the HEBE autocorrelation function and prediction problem (and its limits) when F is a Gaussian white noise.

To understand the noise driven HEBE, it is helpful to Fourier analyze it using $\left({}_{-\infty}D_t^H\right)\xrightarrow{Fourier}\left(i\omega\right)^H$ [*Lovejoy*, 2019a], section 3.3 part I~~and appendix C~~. At high frequencies, the derivative (energy storage) term dominates so that the temperature is a fractional integral (order H) of the forcing. At low frequencies, the derivative term can be neglected so that $T \approx s$~~λ~~F implying that the equilibrium temperature follows the forcing and that s~~λ~~ is indeed the usual climate sensitivity. Alternatively, in real space, if $F(t)$ is a unit step function $\Theta(t)$ and s ~~λ~~ = 1, then for $H \neq 1$ the long time relaxation to the equilibrium temperature response~~,~~ is a power law: $G_{\Theta,H}(t)\approx 1-t^{-H}$ (part I eq. 33). Similarly, for small t, for $H < 1$, the impulse response is singular $G_{\delta,H}(t)\approx t^{H-1}$ (part I eq. 33). Due to this singularity, when $F(t)$ is a Gaussian white noise, at high frequencies, T will be a fractional Gaussian noise (fGn) with exponent $H_{fGn} = H - ½$; averages over time Δt will behave as $\left\langle T_{\Delta t}^2\right\rangle^{1/2}\propto \Delta t^{H_{fGn}}$. When $H \leq 1/2$ ($H_{fGn} \leq 0$) and the resolution is increased ($\Delta t \rightarrow 0$), this implies strong resolution dependencies (mathematically, small scale divergences) ~~when the resolution is increased ($\Delta t \rightarrow 0$)~~ and so it is important in data analysis, including the estimation of the temperature of the Earth [*Lovejoy*, 2017]. When forced by a white noise, the HEBE is exactly at the critical value $H_{fGn} = 0$ corresponding to a "1/f" noise (~~note that the Earth's internal variability forcing is not necessarily a white noise, it might have a different scaling behaviour~~research in progress indicates that it is at least close

Formatted: Font: Symbol

Formatted: Font: Italic

Formatted: Font: Italic

to a white noise). A particularly relevant aspect is that the correlation function and spectrum change very slowly from high to low frequencies [*Lovejoy*, 2019a]. With data over a limited ranges of scales – e.g. months to decades – then, depending on the relaxation time τ, the HEBE could mimic the FEBE with any H in the range $0< H \leq ½$ (hence $-1/2\leq H_{fGn} \leq 0$). It can therefore potentially account for the geographical variations in H reported in [*Lovejoy et al.*, 2017] as being spurious consequences of geographical variations in $\tau(\underline{x})$.

At global scales, the high and low frequency HEBE behaviours are close to observations. For example, the global value $H = 0.5\pm0.2$ was found for the long time behaviour needed to project the earth's temperature to 2100 [*Hebert*, 2017], [*Hébert et al.*, 2020], and [*Procyk et al.*, 2020] also using centennial scale global temperature estimates but using the FEBE directly, found the less uncertain $H = 0.38\pm0.05$; and using data at monthly and seasonal scales [*Del Rio Amador and Lovejoy*, 2019] found the value $H = 0.42\pm0.03$ and used it~~for the internal macroweather variability needed to make monthly and seasonal forecasts [*Del Rio Amador and Lovejoy*, 2019] (note that this was inferred by make the usual assumption that the internal forcing *F* is a Gaussian white noise, and this may not be the case~~). Appendix B discusses the spatial cross correlation matrix implied by the HEBE that is needed for example in calculating Empirical Orthogonal Functions (EOFs, or for the space-time macroweather model developped in [*Del Rio Amador and Lovejoy*, 2020b]).

~~*We could also mention that if F is spatially statistically homogeneous and independent of the parameters λ, τ, then not only will the macroweather temperature fluctuations be well reproduced, but also, up to the relaxation time, the temperature may easily respect a space-time symmetry called space-time statistical factorization, ("STSF"; e.g.*~~ $R_{space-time}(\Delta\underline{x},\Delta t)=R_{space}(\Delta\underline{x})R_{time}(\Delta t)$ ~~*where R represents the autocorrelation function), see appendix C. Empirically, the STSF is at least approximately obeyed by space-time temperature and precipitation fluctuations ([Lovejoy and de Lima, 2015]), and if respected, the STSF has important implications for macroweather temperature forecasting.*~~

Although the HEBE was derived for anomalies, these were not defined as small perturbations but rather as time-varying components of the full solution of the temperature (energy) equation with the time independent part corresponding to the climate state. The only point at which T was assumed to be small was with respect to the absolute local climate temperature about which the black body radiation was linearized, a fairly weak restriction on T. We could also mention that by allowing the albedo or other parameters to change in time, the HEBE could easily be extended to the study of past or future climates where it would broaden the spectrum potentially improving the modeling of glacial cycles.

An important feature of fractional differential operators is that they imply long memories, this is the source of the skill in macroweather forecasts ([*Lovejoy et al.*, 2015], [*Del Rio Amador and Lovejoy*, 2019]). The fractional term with the long memory corresponds to the energy storage process. In contrast, [*Lionel et al.*, 2014] introduced a class of ad hoc Energy Balance Models with Memory (EBMM) whose (nonfractional) time derivative depends on integrals over the past state of the system.

Formatted: Font: Italic

Formatted: Font: Italic

Formatted: Normal

3.4 The first order in space GHEBE

The HEBE is the GHEBE limit where horizontal transport effects are dominated by temporal relaxation processes and are ignored. Although this spatial scale depends on the time scale, appendix A estimates that at monthly time scales, this spatial scale is ~~of the order of~~less ≈10 km and even at centennial scales it may only be only 100km or so. For these small spatial scales, we follow [*Babenko*, 1986], [*Kulish and Lage*, 2000], [*Magin et al.*, 2004], and expand the square root operator using the binomial expansion:

$$\Lambda = \tau^{1/2}\sqrt{\frac{\partial}{\partial t}+V\zeta} \approx \left(\tau\frac{\partial}{\partial t}\right)^{1/2}\left(1+\frac{1}{2}\left(\frac{\partial}{\partial t}\right)^{-1}V\zeta-\frac{1}{8}\left(\frac{\partial}{\partial t}\right)^{-2}\left(V\zeta\right)^{2}+\ldots\right)$$

$$V=\frac{l_h}{\tau}=\left(\frac{\kappa_h}{\kappa_v}\right)\frac{1}{\rho cs} \qquad (53~~35~~)$$

(for the expansion to be strictly valid, τ must be a constant in time and in space; we have already assumed that $V\zeta$ is independent of time). As usual with Babenko's method, a rigorous mathematical justification is not available ([*Podlubny*, 1999]), although recall that τ, and l_h are only functions of position so that for the temporal operator, Laplace and Fourier transforms techniques still work.

Formatted: Font: Symbol

Considering the spatial part of the fractional operator, we see that it is weighted by the effective heat transport velocity V; as shown below, it plays the role of a small parameter (table 1, appendix A estimate it as ≈10^{-4}m/s). Therefore, dropping the subscript "*s*" here and below, the GHEBE is:

$$\begin{aligned}&\tau^{1/2}\left(\frac{\partial}{\partial t}+V\zeta\right)^{1/2}T+T=\\&\tau^{1/2}\,{}_{-\infty}D_t^{1/2}T+T+\frac{1}{2}V\tau^{1/2}\left({}_{-\infty}D_t^{-1/2}\zeta\right)T-\frac{1}{8}V^2\tau^{1/2}\left({}_{-\infty}D_t^{-3/2}\zeta^2\right)T+\ldots=sF\end{aligned} \qquad (54~~36~~)$$

with the Weyl fractional derivatives (these are partial fractional derivatives).

Keeping only the spatial terms leading in the small parameter V, we have the first order (in space) GHEBE:

$$\tau^{1/2}\,{}_{-\infty}D_t^{1/2}T+T+\frac{1}{2}V\tau^{1/2}\left({}_{-\infty}D_t^{-1/2}\zeta\right)T=sF \qquad (55~~37~~)$$

Or:

$$\tau^{1/2}\,{}_{-\infty}D_t^{1/2}T + T + \frac{1}{2}\tau^{1/2}\,{}_{-\infty}D_t^{-1/2}\left(\underline{v}\cdot\nabla_h T - \kappa_h\nabla_h^2 T\right) = sF$$

(56~~38~~)

This equation is apparently similar to the usual transport equation. To see this, operate on both sides by $\tau^{-1/2}\,{}_{-\infty}D_t^{1/2}$, to obtain:

$$\frac{\partial T}{\partial t} + \underline{v}' \cdot \nabla T - \kappa' \nabla^2 T + \tau^{-1/2}\,{}_{-\infty}D_t^{1/2}T = sF'$$

(57~~39~~)

$$\underline{v}' = \frac{1}{2}\underline{v}; \qquad \kappa' = \frac{1}{2}\kappa; \qquad F' = \tau^{-1/2}\,{}_{-\infty}D_t^{1/2}F$$

Except for the factor ½, the half order derivative term and the "effective", (roughened) forcing, this is the usual transport equation. Nevertheless, although tempting, it would be wrong to think of this simply as a usual transport equation with an extra fractional term. The reason is that the extra term is not a small perturbation, it is dominant except at small spatial scales. On the contrary, it is rather the classical transport terms that are small perturbations to the main HEBE. Alternatively, without the $\frac{\partial T}{\partial t}$ term, eq. ~~41~~ 59 is a generalized fractional diffusion equation (e.g. [*Coffey et al.*, 2012]), although still with a key difference being that the fractional derivative is Weyl, not Riemann-Liouville (i.e. over the range $-\infty$ to *t*, not 0 to *t*).

Field Code Changed

Field Code Changed

3.5 Climate states, ~~Thermodynamic~~ equilibrium and the low frequency GHEBE

3.5.1 The equilibrium temperature distribution: ~~The~~ the HEBE ~~thermodynamic~~ climate~~equilibrium~~

The HEBE applies to time scales sufficiently short and to spatial scales sufficiently large that the horizontal temperature fluxes are too slow to be important, they are neglected. The first order correction (eqs. ~~38~~56, ~~39~~57) makes a small improvement by giving a more realistic treatment of the small scale horizontal transport. However, a long time after performing a step increase of the forcing, the time derivatives vanish and a new climate state is reached. If the temperature followed the pure HEBE, the spatial ~~pattern for thermodynamic~~ equilibrium temperature distribution would be determined by setting the HEBE time derivative to zero:

$$T_{eq,HEBE}\left(\underline{x}\right) = F_0 s\left(\underline{x}\right); \qquad F\left(t,\underline{x}\right) = F_0\Theta\left(t\right)$$

(58~~40~~)

Where the subscript "~~e~~*eq*" indicates the long time equilibrium (climate) FEBE limit. However, appendix A shows that – depending on the nature of the horizontal transport - at scales perhaps of the order of ~~millennia~~centuries, the horizontal heat fluxes will dominate the relaxation processes so that for very long times, this HEBE estimate is only approximate.

3.5.2 Equilibrium and approach to equilibrium in the inhomogeneous GHEBE

To understand the long time behaviour, we return to the GHEBE but perform a (long-time) binomial expansion of the half-order operator assuming that the transport terms dominate:

$$\begin{aligned}&\left(l\left(\underline{x}\right)\zeta\left(\underline{x}\right)+\tau\frac{\partial}{\partial t}\right)^{1/2}T=\left(l\zeta\right)^{1/2}\left(1+\left(l\zeta\right)^{-1}\tau\frac{\partial}{\partial t}\right)^{1/2}T\\ &\approx\left(l\zeta\right)^{1/2}T+\frac{1}{2}\frac{\partial}{\partial t}\left(\left(l\zeta\right)^{-1/2}\tau\right)T-\frac{1}{8}\frac{\partial^2}{\partial t^2}\left(\left(l\zeta\right)^{-1/2}\tau\left(l\zeta\right)^{-1}\tau\right)T+...\end{aligned}$$ (59~~41~~)

(from here on we drop the "*h*" subscripts on *l* and the gradient operator). Again, to be strictly valid, τ must be a constant so that $l\left(\underline{x}\right)\zeta\left(\underline{x}\right)$ and $\tau\frac{\partial}{\partial t}$ commute~~)~~. We have to be careful since the advection length and relaxation times are functions of position (but not time) so that the spatial operators don't commute. Keeping terms to first order in time, we obtain:

$$\left(l\zeta\right)^{1/2}T+T+\frac{1}{2}\frac{\partial}{\partial t}\left(\left(l\zeta\right)^{-1/2}\tau\right)T=sF$$ (60~~42~~)

To make progess, let's choose the transport operator so that its half powers are easy to interpret. The simplest approach is consider only diffusive transport and to use an isotropic fractional operator defined over the surface of the earth. For an arbitrary test function ρ, the corresponding order *H* fractional integral is:

$$\left(-\nabla^2\right)^{-H/2}\rho=I_{iso,d}^{H}\rho=\frac{1}{\Gamma\left(H\right)}\int_{\Omega}\frac{\rho\left(\underline{y}\right)d^d\underline{y}}{\left|\underline{x}-\underline{y}\right|^{d-H}}$$ (61~~43~~)

(for 0≤*H*≤*d*, where *d* is the dimension of space, here *d* = 2, see e.g. [*Schertzer and Lovejoy*, 1987], appendix A). This can be understood since in Fourier space, the Laplacian is $-\nabla^2\overset{F.T.}{\longrightarrow}\left|\underline{k}\right|^2$ and its inverse is $\left(-\nabla^2\right)^{-1}\overset{F.T.}{\longrightarrow}\left|\underline{k}\right|^{-2}$, the "Poisson solver". Note that eqs. ~~42~~60, ~~43~~ 61 involve ½ order inverse Laplacians which are *H* = 1 (rather than *H* = ½) isotropic integrals (eq. ~~43~~61). With the help of spherical harmonics, ~~Appendix D~~Appendix C generalizes the results of section 2.3 gives the corresponding operators and their fractional extensions on the surface of the sphere.

Applying eq. ~~43~~ 61 to the case *d* = 2 and *H* = 1 we have:

Formatted: Font: Symbol

$$\left(-\nabla^2\right)^{-1/2}\rho = \int_{\Omega} \frac{\rho\left(\underline{x}'\right)d^2\underline{x}'}{\left|\underline{x}-\underline{x}'\right|} \qquad (62~~44~~)$$

Therefore, let us define a diffusive type transport operator $l\zeta$ and its inverse $\left(l\zeta\right)^{-1}$ implicitly from its inverse half-order power:

$$\left(l\zeta\right)^{-1/2} = l^{-1}\left(-\nabla^2\right)^{-1/2}; \qquad \left(l\zeta\right)^{1/2} = \left(-\nabla^2\right)^{1/2} l = \left(-\nabla^2\right)^{-1/2}\left(-\nabla^2\right)l \qquad (63~~45~~)$$

Hence let us define the half-order operator by:

$$\left(l\zeta\right)^{-1/2} T\left(\underline{x}\right) = l\left(\underline{x}\right)^{-1}\int_{\Omega}\frac{T\left(\underline{x}'\right)d^2\underline{x}'}{\left|\underline{x}-\underline{x}'\right|} \qquad (64~~46~~)$$

With this definition the surface temperature equation 60 becomes:

$$\frac{1}{2}\frac{\partial}{\partial t}\left[l\left(\underline{x}\right)^{-1}\int_{E}\frac{\tau T\left(\underline{x}',t\right)d^2\underline{x}'}{\left|\underline{x}-\underline{x}'\right|}\right] + T\left(\underline{x},t\right) - \int_{E}\frac{\nabla^2\left(l\left(\underline{x}'\right)T\left(\underline{x}',t\right)\right)d^2\underline{x}'}{\left|\underline{x}-\underline{x}'\right|} = s\left(\underline{x}\right)F\left(\underline{x},t\right) \qquad (65~~47~~)$$

Where the range of the integration $\Omega = E$ is the entire surface of the earth. This equation has only superficial links to equations studied in the literature such as the "generalized fractional advection-dispersion equation" (e.g. [*Meerschaert and Sikorskii*, 2012], [*Hilfer*, 2000]). We can now consider the system reaching equilibrium after a step forcing $F(\underline{x},t) = F_0(\underline{x})\Theta(t)$, (increase by $F_0(\underline{x})$ "turned on" at $t = 0$). At long enough times, the earth reaches ~~thermodynamic~~ equilibrium ~~and~~, the time derivative term vanishes and we obtain the equation for the equilibrium (climatological) temperatures:

$$T_{eq}\left(\underline{x}\right) - \int_{E}\frac{\nabla^2\left(l\left(\underline{x}'\right)T_{eq}\left(\underline{x}'\right)\right)d^2\underline{x}'}{\left|\underline{x}-\underline{x}'\right|} = s\left(\underline{x}\right)F_0\left(\underline{x}\right) \qquad (66~~48~~)$$

To obtain an approximate solution, let's now assume that $T_{eq}\left(\underline{x}\right)$ differs from the climatological FEBE climate temperature ~~T_e~~$T_{eq,FEBE}(\underline{x})$ by a small perturbation $\delta T(\underline{x})$.

$$T_{eq}\left(\underline{x}\right) = T_{eq,HEBE}\left(\underline{x}\right) + \delta T\left(\underline{x}\right); \quad T_{eq,HEBE}\left(\underline{x}\right) = s\left(\underline{x}\right)F_0\left(\underline{x}\right) \qquad (67~~49~~)$$

then, using ~~T_e~~$T_{eq}(\underline{x}) \approx s$ ~~λ~~$(\underline{x})F_0(\underline{x})$ in the integral, we obtain the approximation:

Formatted: Font: Italic

$$T_{eq}\left(\underline{x}\right)\approx T_{eq,HEBE}\left(\underline{x}\right)+\delta T\left(\underline{x}\right);\qquad \delta T\left(\underline{x}\right)=\int_E \frac{\nabla^2\left(l\left(\underline{x}'\right)s\left(\underline{x}'\right)F_0\left(\underline{x}'\right)\right)d^2\underline{x}'}{\left|\underline{x}-\underline{x}'\right|} \qquad (68~~50~~)$$

$\delta T\left(\underline{x}\right)$ is the slow, diffusive correction to the "instantaneous" (fast, high frequency), HEBE climate sensitivity s~~λ~~($\underline{x}$) that is estimated at usual (e.g. decadal) scales. As expected, since this is the long time solution after a step perturbation, it doesn't depend on τ.

Horizontal transport of heat redistributes the energy fluxes locally, but since the GHEBE is linear, it shouldn't affect the overall (global) energy balance. Let us check this by direct calculation of the globally averaged temperature. Averaging eq. ~~48~~66, we obtain:

$$\overline{T_{eq}\left(\underline{x}\right)}-\int_E \overline{\frac{\nabla^2\left(l\left(\underline{x}'\right)T_{eq}\left(\underline{x}'\right)\right)d^2\underline{x}'}{\left|\underline{x}-\underline{x}'\right|}}=\overline{s\left(\underline{x}\right)F_0\left(\underline{x}\right)};\qquad \overline{f}=\frac{1}{A_E}\int_E f\left(\underline{x}\right)d^2\underline{x};\quad A_E=\int_E d^2\underline{x} \qquad (69~~51~~)$$

Where the spatial averaging operator (overbar) is defined for an arbitrary function *f*. The average of the horizontal heat flux term yields:

$$\frac{1}{A_E}\int_E\int_E \frac{\nabla^2\left(l\left(\underline{x}'\right)T_{eq}\left(\underline{x}'\right)\right)}{\left|\underline{x}-\underline{x}'\right|}d^2\underline{x}\,d^2\underline{x}'=K_E\int_E \nabla^2\left(l\left(\underline{x}'\right)T_{eq}\left(\underline{x}'\right)\right)d^2\underline{x}'=\int_{\delta E} d\underline{s}\cdot\nabla\left(l\left(\underline{x}'\right)T_{eq}\left(\underline{x}'\right)\right)=0 \qquad (70~~52~~)$$

Where K_E is an unimportant constant from the $\underline{x}$ integration, independent of $\underline{x}$'. The far right equality is an application of the divergence theorem on the surface *E* whose boundary is *δE*, $d\underline{s}$ is a vector parallel to the bounding line. But since the integration is over the whole earth surface (*E*), there is no boundary, hence the result. We conclude that while horizontal diffusion transports heat over the earth's surface, it does not affect the overall global radiation budget: $\overline{T_{eq}}=\overline{T_{eq,HEBE}}$.

4. Conclusions

Up until now, at macroweather and climate scales, the Earth's energy balance has been modelled using two classical approaches. On the one hand, Budyko - Sellers models assume the continuum mechanics heat equation~~ holds~~, this ~~yields~~ yielding a 1-D latitudinally varying climate state. On the other hand, there are the zero-dimensional box models that combine Newton's law of cooling with the assumption of an instantaneous temperature-storage relationship. Both models avoid the critical conductive - radiative surface boundary condition~~s~~; the former by ignoring heat storage, redirecting radiative

Formatted: Font: Italic

imbalances meridionally away from the equator, the latter by postulating a surface heat flux that is not simultaneously consistent with the heat equation and energy conservation across a conducting and radiating surface (part I).

This two part paper re-examined the classical heat equation with classical semi-infinite geometry. In the horizontally homogeneous case (part I), the fundamental novelty is the treatment of the conductive - radiative boundary conditions, here (part II), it is the use of Babenko's method to extend this to the more realistic horizontally inhomogeneous problem. In both cases, the semi-infinite subsurface geometry is only important over a shallow layer of the order of the diffusion depth where most of the storage occurs (roughly estimated as ≈ 100m in the ocean, ≈<10m over land, see table 1 and appendix A).

The key result was obtained by using standard Laplace and Fourier techniques. It was shown quite generally that the surface temperatures and heat fluxes are related by a half-order derivative relationship. This means that if Budyko-Sellers models are right - that the continuum mechanics heat equation is a good approximation to the Earth averaged over a long enough time – ~~then~~ that a consequence is that the energy stored is given by a power law convolution over its past history. This is a general consequence of the conductive - radiative surface boundary conditions in semi-infinite geometry and is very different from the box models that assume that the relationship between the temperature and heat storage is instantaneous. Although the system itself is classical, this result may be viewed as a nonclassical example of the Mori-Zwanzig mechanism in which system parameters that are not modelled explicitly (here, the subsurface temperatures) imply long (power law) memories for the modelled parameters (here, the surface temperatures). This is in contrast to conventional short (exponential) memory assumption. It implies that any part of the Earth system that exchanges energy both radiatively and conductively into a surface should be modelled with fractional rather than integer ordered derivatives. A far reaching consequence is that classical dynamical systems approaches based on integer ordered differential equations are not necessarily pertinent to the climate system.

If we ignore horizontal heat transport (part I), an immediate consequence of half order storage is that the temperature obeys the Half-order Energy Balance Equation (HEBE) rather than the classical first order ~~one~~ EBE. Depending on the space-time statistics of the anomaly forcing, the HEBE justifies the current Fractional EBE (FEBE) based macroweather (monthly, seasonal) temperature forecasts [*Lovejoy et al.*, 2015], [*Del Rio Amador and Lovejoy*, 2019], [*Del Rio Amador and Lovejoy*, 2020a; *Del Rio Amador and Lovejoy*, 2020b] that are effectively high frequency approximations to the FEBE). Similarly, the low frequency (asymptotic) power law part can produce climate projections with significantly lower uncertainties than current GCM based alternatives ([*Hebert*, 2017], [*Hébert et al.*, 2020] and work in progress directly using the HEBE, [*Procyk et al.*, 2020]).

~~The implied long time storage behaviour explains the success of sealing based climate projections~~[*Hébert et al.*, 2020; *Procyk et al.*, 2020] ~~and, the implied short time behaviour potentially explains the success of macroweather forecasts that exploit it~~[*Del Rio Amador and Lovejoy*, 2019; 2020a; *Del Rio Amador and Lovejoy*, 2020b]~~.~~ When the system is periodically forced, the response is shifted in phase - and borrowing from the engineering literature - the surface is characterized by a complex thermal impedance that we showed is equal to the (complex) climate sensitivity. In part I, we gave evidence that this quantitatively explains the phase lag (typically of about 25 days) between the annual solar forcing and temperature response.

In this second part, we investigated the consequences of horizontal heat transport, first in a homogeneous medium with inhomogeneous forcing ~~(section 2)~~ first on a plane and then – permitting a direct comparison with the usual Budyko-Sellers approach - on the sphere (section 2). In section 3 ~~and then~~we considered~~, more generally with~~ inhomogeneous material properties (including variable diffusion lengths, relaxation times, and climate sensitivities~~, section 3~~). While Laplace and Fourier techniques can still be used in time, they cannot be used in space. ~~and not so useful here, but the~~However, the extension to inhomogeneous media was nevertheless possible thanks to Babenko's powerful (but less rigorous) operator method. Whereas in part I, the homogeneous fractional space-time operator was given a precise meaning, here - following Babenko - the corresponding inhomogeneous operator was interpreted using binomial expansions for both the short and long time limits and yield 2D energy balance models. Part II thus allows us for the first time to extend energy balance models to 2-D, allowing the treatment of regional temporal anomalies.

The expansions depend both on the space and time scale and on a dimensional parameter: the typical horizontal transport speed (V), estimated as $\approx 10^{-4}$m/s (appendix A). The zeroth order expansion in time limit yielded the inhomogeneous HEBE, the first order correction yielded an equation that superficially resembled the usual heat equation but instead had a leading half - order time derivative term. Based on the analysis of NCEP reanalyses (appendix A), it was argued that at spatial scales larger than hundreds of kilometers, that these approximations are likely to be useful for years, decades, and perhaps longer. However, for studying climate states – defined for example as the ~~thermodynamic~~ equilibrium state for forcings that are increased everywhere in step function fashion – we required low, not high frequency expansions and these are based on fractional spatial operators. We defined inhomogeneous fractional diffusion operators in both flat space and on the sphere (~~appendix D~~appendix C), and derived equations for both the~~ therm~~ equilibrium~~odynamic~~ limit and the approach to the limit. We showed that (as expected) they conserved energy and that the low frequency climate sensitivity is somewhat different from that estimated at higher frequencies (from the EBE or HEBE).

The EBE and HEBE are the $H = 1$, $H = 1/2$ special cases of the Fractional EBE (FEBE) that was recently introduced as a phenomenological model [*Lovejoy et al.*, 2020]~~.~~ (see also [*Lovejoy*, 2019a], [*Lovejoy*, 2019b]) with empirical estimates $H \approx$ 0.4 - 0.5, i.e. very close to the HEBE. Although only a special case, the HEBE illustrates the general features of the FEBE fractional-order energy storage term and power law long memories, in ~~[*Lovejoy et al.*, 2020].~~ [*Lovejoy*, 2019a] discussed the statistical properties of the FEBE driven by Gaussian white noise (a model for the internal variability forcing) showing that the high frequency limit is a process called fractional Gaussian noise (fGn). In the special HEBE case with $H = 1/2$, the fGn temperature response has exactly a high frequency $1/f$ spectrum that is cut-off at the relaxation time (empirically of the order of a few years). [*Lovejoy*, 2019a] developed optimal predictors and determined the predictability skill.

Whereas the more general FEBE is essentially a phenomenological model up unti~~t~~l now justified by the hypothesized scale invariance of the energy storage mechanisms ([*Lovejoy et al.*, 2020]), the HEBE follows directly and quite generally from the continuum mechanics heat equation, thus giving it a more solid theoretical basis. However, the work here suggests another way to obtain the FEBE: to replace the classical heat equation by its fractional generalization, the fractional heat equation, a possibility that we explore elsewhere. ~~Part II allowed us for the first time to extend energy balance models to 2-D, allowing~~

~~the treatment of regional temporal anomalies. Depending on the space-time statistics of the anomaly forcing, the HEBE justifies the current Fractional EBE (FEBE) based macroweather (monthly, seasonal) temperature forecasts [*Lovejoy et al.*, 2015], [*Del Rio Amador and Lovejoy*, 2019]. Similarly, the low frequency (asymptotic) power law part can produce climate projections with significantly lower uncertainties than current GCM based alternatives (~~[*Hebert*, 2017; *Hébert et al.*, 2020] ~~and work in progress directly using the HEBE [*Procyk et al.*, 2020]with R. Procyk).~~

~~*This work was performed in the spirit of Budyko-Sellers models in which the Earth system is averaged over scales longer than typical lifetimes of planetary scale weather structures. Following Budyko-Sellers, the key physical assumption was that the resulting averaged system is a continuum system, thus justifying use of the general continuum mechanics heat equation. From this, the GHEBE and HEBE follow from the surface conductive-radiative boundary condition. In as much as GCMs (that are based on continuum mechanics) reproduce the same statistics as the noise – or anthropogenically forced FEBE and HEBE, the continuum hypothesis is plausible.*~~

Formatted: Font: Italic

As a final comment, we should mention that although this paper focused on the time varying anomalies with respect to a time independent climate state, our approach opens the door to new methods for determining full 2-D climate states (generalizations of the 1-D Budyko-Sellers type climates) but also to determining past and future climates and the transitions between them. This is because the definition of temperature "anomalies" is very flexible. For example, we could first apply the method to determining the existing climate by fixing the forcing at current values and solving the time independent transport equations. Then, the long term effect of changes such as step function increases in forcing could be determined from the GHEBE anomaly equation (section 3.5) which regionally corrects the local climate sensitivities for (slow) horizontal energy transport effects. —Nonlinear effects that can be modelled by temperature dependent forcings (i.e. $F\left(\underline{x},t\right)\rightarrow F\left(\underline{x},t,T\left(\underline{x},t\right)\right)$) can easily be introduced. Other nonlinear effects needed to account for Milankovitch cycles could thus easily be made, the primary difference being the half-order derivatives and the scaling that they imply. Indeed, the power law relaxation processes implied by the GHEBE suggests straightforward explanations for the observed power law climate regime spanning the range from centennial to Milankovitch scales.

Field Code Changed

Field Code Changed

5. Acknowledgements

I acknowledge discussions with L. Del Rio Amador, R. Procyk, R. Hébert, D. Clarke and C. Penland. This is a contribution to fundamental science; it was unfunded and there were no conflicts of interest. The data used in appendix A are from the NOAA website: https://www.esrl.noaa.gov/psd/data/gridded/data.ncep.reanalysis.html.

Field Code Changed

Appendix A: Empirical analysis of the horizontal structure

In order to apply our results to the Earth, we need some idea of the magnitudes of various terms in our equations. To start with, recall that our model is of the Earth system at macroweather and climate time scales i.e. all relevant quantities are averaged over the weather scales ≈ 10 days or longer. The resulting averaged system is then treated as a continuum and the general continuum mechanics heat equation is applied. In this, we essentially follow the Budyko - Sellers approach and consider that the diffusive transport is characterized by eddy (not molecular) diffusivities and that the vertical structure of this averaged continuum is homogeneous (although it may vary considerably from place to place in the horizontal, see section 2.3 for a scaling (multifractal) model). Unlike Budyko - Sellers that treat the vertical as negligibly thick – they don't consider it at all – our ~~key~~ main difference is that we assume that it has a thickness of the order of a few diffusion depths, and then we apply the key conductive- radiative surface boundary condition.

Probably the most important aspect is to estimate the relative importance of the temporal relaxation (and storage) terms $\tau\partial/\partial t$ in comparison to the horizontal transport terms $l_h\zeta$ with $\zeta=\left(\underline{\alpha}\cdot\nabla_h+l_h\left(-\nabla_h^2\right)\right)$ ~~(~~ (see eq. ~~25~~43). Indeed, for judging their relative importance, the key parameter is the ratio of the transport to relaxation terms *r*:

$$r=V\frac{\zeta T}{\left(\partial T/\partial t\right)}=\frac{\left(\underline{\alpha}\cdot\nabla_h+l_h\left(-\nabla_h^2\right)\right)T}{\left(\partial T/\partial t\right)};\qquad V=\frac{l_h}{\tau};\qquad \alpha=\frac{v}{V}\qquad (71\cancel{53})$$

Where α is the magnitude of the dimensionless advection velocity vector $\underline{\alpha}=\underline{v}/V$. When $r\ll 1$, the transport term is small compared to the temporal term, conversely when $r\gg 1$. In order to quantify this, it is convenient to consider the advective ("*a*") and diffusive ("*d*") terms as well as their derivatives individually:

$$\begin{aligned}
&r_a=V\frac{\zeta_{a,x}T+\zeta_{a,y}T}{\left(\partial T/\partial t\right)};\qquad \zeta_{a,x}T\approx\alpha_x\frac{\partial T}{\partial x};\qquad \zeta_{a,y}T\approx\alpha_y\frac{\partial T}{\partial y}\\
&r_d=V\frac{\zeta_{d,x}T+\zeta_{d,y}T}{\left(\partial T/\partial t\right)};\qquad \zeta_{d,x}T=l_h\frac{\partial^2 T}{\partial x^2};\qquad \zeta_{d,y}T=l_h\frac{\partial^2 T}{\partial y^2}
\end{aligned}\qquad (72\cancel{54})$$

In the macroweather regime, the temporal temperature fluctuation at time scale Δt is $\Delta T\left(\Delta t\right)\approx T_{\Delta t}$ where $T_{\Delta t}$ is the anomaly averaged over scale Δt; empirically this is valid over the macroweather regime i.e. up to 10 - 30 years in the industrial epoch

Field Code Changed

(see e.g. [*Lovejoy and Schertzer*, 2013], [*Lovejoy*, 2013], [*Lovejoy et al.*, 2017]). The typical fluctuation can be estimated by the RMS anomaly:

$$s_{\Delta t}\left(\underline{x}\right)=\left(\overline{T_{\Delta t}^{2}}\right)^{1/2}\approx s_{1}\left(\underline{x}\right)\left(\frac{\Delta t}{\Delta t_{1}}\right)^{H_{t}}$$

(73~~55~~)

Where the overbar is the average over all the anomalies in a time series at a single location $\underline{x}$. Δt_1 is a convenient reference time, here taken as 1 month. Empirically, the exponent $H_t \approx 0$ to -0.2; this is similar to the high frequency result $H_t = 0$ (i.e. for $\Delta t<\tau$) predicted from the HEBE with white noise forcing, valid for $\Delta t \approx<\tau$. Hence for our present purposes the typical time derivative is:

$$\frac{\partial T}{\partial t}\approx\frac{s_{\Delta t}}{\Delta t}$$

(74~~56~~)

This is the resolution Δt time derivative. Since typical north-south gradients are larger than typical east-west ones, the meridional (y) component of the transport is dominant, so that we will focus on it:

$$\frac{\partial T}{\partial y}\approx\frac{\left(\overline{\Delta T_{\Delta t}\left(\Delta y\right)^{2}}\right)^{1/2}}{\Delta y}=\frac{\Delta s_{\Delta t}\left(\Delta y\right)}{\Delta y};\qquad\frac{\partial^{2} T}{\partial y^{2}}\approx\frac{\Delta\left(\overline{\Delta T_{\Delta t}\left(\Delta y\right)^{2}}\right)^{1/2}}{\Delta y^{2}}=\frac{\Delta^{2} s_{\Delta t}\left(\Delta y\right)}{\Delta y^{2}}$$

(75~~57~~)

Hence the meirdional contributions to the ratios r_a, r_d are:

$$r_{a,y}=V\alpha\frac{\Delta t}{\Delta y}\Delta\log s_{\Delta t}\left(\Delta y\right)$$

(76~~58~~)

$$r_{d,y}=Vl_{h}\frac{\Delta t}{\Delta y^{2}}\left(\left(\Delta\log s_{\Delta t}\left(\Delta y\right)\right)^{2}+\Delta^{2}\log s_{\Delta t}\left(\Delta y\right)\right)$$

Where $\Delta\log s_{\Delta t}\left(\Delta y\right)=\frac{\Delta s_{\Delta t}\left(\Delta y\right)}{s_{\Delta t}}$, is the relative fluctuation in the RMS temperature at time scale Δt, spatial scale Δy and - since we are only interested in an order of magnitude - we took $\alpha \approx \alpha_y$. The estimate of the diffusive term uses a finite difference approximation to the Laplacian. l_h is horizontal ~~anomaly relaxation~~diffusion length and α is the nondimensional advection speed v/V ($V = l_h/\tau$, see below). To gauge the order of magnitudes, in the far right term of eq. ~~58~~76, we took the absolute value so that the result is an upper bound~~suppressed the signs~~.

Formatted: Font: 10 pt
Formatted: Font: 10 pt
Formatted: Font: 10 pt
Formatted: Font: 10 pt
Field Code Changed
Field Code Changed
Formatted: Font: 10 pt
Field Code Changed
Formatted: Font: Italic
Formatted: Font: Italic, Subscript
Formatted: Font: Italic
Formatted: Font: Italic, Subscript

~~To estimate l_h, consider the volumetric specific heat ρc. Ocean and land values are similar (respectively water: $\rho c \approx 4\mathrm{x}10^6$ and soil: $\rho c \approx 1\mathrm{x}10^6$ J/m^3). For λ, the global mean value is $\approx 0.8\pm0.4$ K/W/m^2, (using the CO_2 doubling value 3±1.5C, 90% confidence interval and 3.71 W/m^2 for CO_2 doubling) with regional values a factor of ≈ 2 higher or lower (IPCC AR5) yielding $\rho c\lambda \approx 3\mathrm{x}10^6$ s/m. The horizontal (eddy) diffusivity is $\kappa_h \approx 1$ m^2/s ([*Sellers*, 1969], [*North et al.*, 1981]). The vertical diffusivity is not used in the usual energy balance models, however in climate models, ocean values of $\kappa_v \approx 10^{-4}$ m^2/s are typical [*Houghton et al.*, 2001]. For soil, rough values of $\kappa_v \approx 10^{-6}$ m^2/s (wet) and $\kappa_v \approx 10^{-7}$ m^2/s (dry) are measured in [*Márquez et al.*, 2016] so that for soils, $l_v \approx 3 - 10$m.~~

~~Alternatively we can use $\kappa_v = \tau/(\rho c\lambda)^2$ and the global estimates of $\tau \approx 10^8$s ([*Hebert*, 2017], [*Procyk et al.*, 2020]work in progress with R. Procyk, or part I, section 3.3). From these, we obtain $\kappa_v \approx 10^{-5}$ m^2/s which is close to the model values. In conclusion, using $\kappa_v \approx 10^{-5} - 10^{-4}$ m^2/s yields $l_v \approx 30 - 100$m, $l_h \approx 10$ km. Consequently, the diffusive based velocity parameter is $V \approx l_h/\tau \approx 10^{-4}$ m/s.~~

~~The best transport model – diffusive, advective – or both - is not clear, therefore let us estimate the magnitude of the advective velocity v assuming that it dominates the transport. The appropriate value is not obvious since most models just use eddy diffusivity – not advection – for transport. One way - for example [Warren and Schneider, 1979] - is to note that typical meridional heat fluxes are of the order of 100 W/m^2 over meridional bands whose temperature gradients ΔT are several degrees K. If this heat is transported by advection, it implies $v \approx Q_a/(\rho c\Delta T) \approx 10^{-5} - 10^{-4}$m/s (eq. 4, part I), hence, using $V \approx 10^{-4}$m/s (above), we find $\alpha = v/V \approx 0.1 - 1$.~~

Quantity	Symbol	Values
Volumetric specific heat	ρc	water $\approx 4\mathrm{x}10^6$, soil $\approx 1\mathrm{x}10^6$ J/(m^{3}K).
Climate sensitivity	s	water $\approx 4\mathrm{x}10^6$, soil $\approx 1\mathrm{x}10^6$ J/(m^{3}K)
Relaxation time	τ	global $\tau \approx 10^8$s
Horizontal Diffusivity	κ_h	1 m^2/s
Vertical diffusivity	κ_v	ocean $\approx 10^{-4}$ m^2/s, soil $\approx 10^{-6}$ m^2/s, global $\approx 10^{-5}$ m^2/s
Diffusion depth	l_v	ocean 300m, soils $\approx 3 - 10$m, global $\approx 30 - 100$m
Diffusion length	l_h	ocean ≈ 30 km, land 3 km, global ≈ 10 km.
Diffusive velocity parameter	V	3x 10^{-3} – 3x 10^{-4} m/s
Nondimensional advection velocity	α	0.1 - 1

Table 1: Parameter estimates from part 1 section 3.1.2, see section 2.3 for some planetary scale estimates.

Formatted: Indent: First line: 0 cm
Formatted: Underline
Formatted: Centered
Formatted Table
Formatted ... [6]
Formatted ... [7]
Formatted: Font: 11 pt
Formatted: Indent: First line: 0 cm
Formatted ... [8]
Formatted ... [9]
Formatted: Font: 11 pt
Formatted ... [10]
Formatted ... [11]
Formatted ... [12]
Formatted ... [13]
Formatted ... [14]
Formatted ... [15]
Formatted ... [16]
Formatted ... [17]
Formatted ... [18]
Formatted ... [19]
Formatted: Font: 11 pt
Formatted ... [20]
Formatted ... [21]
Formatted: Indent: First line: 0 cm
Formatted ... [22]
Formatted ... [23]
Formatted ... [24]
Formatted ... [25]
Formatted ... [26]

Table 1 summarizes the~~With these~~ dimensional and nondimensional parameter estimates, the final step is to estimate values of the gradient and Laplacian terms (eq. ~~58~~76). Since s - and hence log s - are the amplitudes of temporal noises; these amplitudes vary stochastically from one spatial location to another. Due to the space-time~~tial~~ scaling of the temperature anomalies (analysed in [*Lovejoy and Schertzer*, 2013]), we expect that ~~their~~ the statistics of the logarithms (eq. 76) to follow power laws up to large scales. To quantify this, we used NCEP reanalysis data at 2.5° resolution from 1948 to present, and after removing the low frequency anthropogenic trend, we estimated the RMS temperature anomalies at each pixel; $s(\underline{x})$. In fig. 6, we then calculated spatial zonal and meridional fluctuations $\Delta \log s(\Delta x)$, $\Delta \log s(\Delta y)$, and from these their root mean square (RMS) values. From the figure, we see that to a good approximation:

$$\Delta \log s(\Delta x) \approx \left(\frac{\Delta x}{L_{EW}}\right)^{H_x} \qquad L_{EW} \approx 1.5x10^7 m$$

$$\Delta \log s(\Delta y) = \left(\frac{\Delta y}{L_{NS}}\right)^{H_y} \qquad L_{NS} \approx 3x10^6 m \qquad H_x \approx H_y \approx 0.5$$

(77~~59~~)

The fluctuations we used are Haar fluctuations, but because $H_x \approx H_y > 0$, they are nearly equal to difference fluctuations [*Lovejoy and Schertzer*, 2012]. We see that the zonal and meridional lines are roughly parallel: with a "trivial" horizontal anisotropy factor ≈ 5 (typical north-south fluctuations are 5 times larger than typical east-west ones). Although, $H = 1/2$ is the value corresponding to Brownian motion, the actual variability is highly intermittent (spiky), so that unlike the temporal fluctuations, these spatial increments are far from Gaussian; it is *not* Brownian motion. Multifractal analysis indicates that the intermittency parameter (the codimension of the mean) $C_1 \approx 0.16$ which is very high, reflecting the strong spatial fluctuations as we move from one climate zone to another [*Lovejoy and Schertzer*, 2013], [*Lovejoy*, 2018], [*Lovejoy*, 2019b].

Since the north-south gradients are much stronger than the east-west ones, we can estimate the gradients and Laplacians by using the y direction fluctuations: at scale Δy:

$$r_{a,y} = \frac{V\alpha\Delta t}{\Delta y}\left(\frac{\Delta y}{L_{NS}}\right)^{H_y} \qquad (78~~60~~)$$

$$r_{d,y} = \frac{V\Delta t}{\Delta y}\left(\frac{l_h}{\Delta y}\right)\left[\left(\frac{\Delta y}{L_{NS}}\right)^{2H_y} + \left(\frac{\Delta y}{L_{NS}}\right)^{H_y}\right] \qquad (79~~61~~)$$

Formatted: Indent: First line: 1 cm
Formatted: Font: 10 pt
Field Code Changed
Formatted: Font: 10 pt
Formatted: Font: 10 pt
Formatted: Font: (Default) +Body (Times New Roman)
Formatted: Font: Cambria
Formatted: Font: 9 pt
Formatted: Indent: First line: 1 cm
Field Code Changed
Field Code Changed

Since $L_{NS} \approx 3\text{x}10^6$m , over most of the range of Δy, $r_{d,y} \approx \frac{V\Delta t}{\Delta y}\left(\frac{l_h}{\Delta y}\right)\left(\frac{\Delta y}{L_{NS}}\right)^{H_y}$ so that the ratio of advection to diffusion is $\frac{r_c}{r_d} \approx \left(\frac{\alpha \Delta y}{l_h}\right)$ so that advection dominates diffusion for $\Delta y > \frac{l_h}{\alpha}$. Taking $\alpha \approx 1$, it is dominant for $\Delta y >\approx l_h$.

Using $l_h \approx 10^4$m, $L_{NS} \approx 3\text{x}10^6$m, $H_y = 1/2$, $V = 10^{-4}$ m/s we find approximately critical length scales that yields unit ratios:

$$\Delta y_{c,a} = 10^{-14}\Delta t^2; \qquad r_a\left(\Delta y_{c,a}\right) = 1$$

$$\Delta y_{c,d} = 10^{-2}\Delta t^{2/3}; \qquad r_d\left(\Delta y_{c,d}\right) = 1$$

(80~~62~~)

Where Δt is measured in seconds, Δy in meters. When the typical distances exceed these critical distances (i.e. when $\Delta y > \Delta y_c$), we have $r<1$ so that the temporal derivative terms dominate over the horizontal transport. For Δt = 1 month, we have $\Delta y_{c,a} \approx$ 0.1m, and $\Delta y_{c,d} \approx$ 200m, so that unless the distances are very small, the temporal (storage) terms are indeed dominant. Even over much longer time scales - e.g. $\Delta t \approx$30 years (~~10^{10}s~~10^9s), they dominate for distances greater than $\approx \Delta y_{c,a} \approx \Delta y_{c,d} \approx$ 10 km. Alternatively, we could estimate the time scales needed so that the critical transport scale is 1000km. From the same equations, we obtain estimates of 300 years (advection), 30,000 years (diffusion). Note however that in the anthropocene, for periods Δt ≈> 10 years, that the temporal fluctuations start to grow (i.e. the empirical relations eqs. ~~60~~78, ~~61~~ 79 will break down); nevertheless, the above scaling relations for the internal variability may hold to much longer times [*Lovejoy et al.*, 2013].

In summary, from eq. ~~62~~80, we conclude that for the larger scales >>≈10 km, that $r \ll 1$ and that the HEBE may apply except for time scales $\gg\tau$: the only explicit role of κ_h, κ_v, ρ, c is to determine the limits of validity of the HEBE via l_h, α. When the HEBE is valid, only the relaxation time τ and the climate sensitivity s~~λ~~ are relevant.

Appendix B: The HEBE cross-correlations

The temperature anomaly cross-correlation function (a matrix when the temperature is discretized on a grid), is commonly used in climate science, notably to determine Empirical Orthogonal Functions (EOFs). These can be determined from the HEBE (or GHEBE if needed) once a forcing model is given. Let us first consider that the climate sensitivities and relaxation times are deterministic characterizations of the local properties at points $\underline{x}_1$, $\underline{x}_2$. In this case, for the HEBE, any correlations between the temperature anomalies at those points will arise because of correlations in the forcing $F(\underline{x},t)$. We now consider simple deterministic and stochastic forcings.

Formatted: Font: 10 pt

Field Code Changed

Formatted: Font: 10 pt

Formatted: Indent: First line: 1 cm

Formatted: Font: Italic

a) Deterministic forcing, temporal averaging:

The simplest model is to take ~~complete~~ spatial ~~correlation~~ correlations obtained by temporally averaging~~,~~ following ~~with~~ a step function ($\Theta(t)$) forcing at $t = 0$, but different at each position $\underline{x}$:

$$F(\underline{x},t) = F_0(\underline{x})\Theta(t)$$

(81~~63~~)

The temporally averaged cross-correlation can be determined by:

$$T(\underline{x}_1,t)T(\underline{x}_2,t) = \frac{s(\underline{x}_1)F_0(\underline{x}_1)s(\underline{x}_2)F_0(\underline{x}_2)}{\tau(\underline{x}_1)\tau(\underline{x}_2)}\int_0^t\int_0^t G_{\delta,1/2}\left(\frac{t-u_1}{\tau(\underline{x}_1)}\right)G_{\delta,1/2}\left(\frac{t-u_2}{\tau(\underline{x}_2)}\right)du_1\,du_2$$

(82~~64~~)

Recalling that ~~$G_{1,1/2}$ (= G_Θ) is~~ the step response~~,~~, is the integral of $G_{\delta,1/2}$ ~~(= G_δ)~~ and since $G_{\Theta,1/2}(\infty) = 1$ we have:

$$\lim_{t_L\to\infty}\left[\frac{1}{t_L}\int_0^{t_L} G_{\Theta,1/2}\left(\frac{t}{\tau(\underline{x}_1)}\right)G_{\Theta,1/2}\left(\frac{t}{\tau(\underline{x}_2)}\right)dt\right] = 1$$

(83~~65~~)

Hence:

$$\overline{T(\underline{x}_1,t)T(\underline{x}_2,t)} = s(\underline{x}_1)F_0(\underline{x}_1)s(\underline{x}_2)F_0(\underline{x}_2)$$

(84~~66~~)

b) Stochastic forcing:

A convenient model of pure internal variability, is to assume that the forcing is statistically stationary in time with the following forcing cross-correlations:

$$R_F(\underline{x}_1,\underline{x}_2,\Delta t) = \langle F(\underline{x}_1,t)F(\underline{x}_2,t-\Delta t)\rangle$$

(85~~67~~)

(the “<.>” symbol indicates ensemble, statistical averaging). ~~This~~ The corresponding ~~implies a~~ stationary temperature cross-correlation:

$$R_T(\underline{x}_1,\underline{x}_2,\Delta t) = \langle T(\underline{x}_1,t)T(\underline{x}_2,t-\Delta t)\rangle$$

(86~~68~~)

Note the general symmetry property $R\left(\underline{x}_1,\underline{x}_2,-\Delta t\right)=R\left(\underline{x}_2,\underline{x}_1,\Delta t\right)$ ~~;~~ $R\left(\underline{x}_1,\underline{x}_2,-\Delta t\right)=R\left(\underline{x}_2,\underline{x}_1,\Delta t\right)$ so that we only need to determine R for $\Delta t>0$. For statistically stationary forcing, $R_T\left(\underline{x}_1,\underline{x}_2,\Delta t\right)$ is the anomaly cross-correlation needed - for example - for constructing Empirical Orthogonal Functions (EOFs).

Field Code Changed

The easiest way to relate R_F and R_T is via their spectra. Let us define the transform pairs:

$$\widehat{T(\omega)}=\int_{-\infty}^{\infty}e^{-i\omega t}T(t)dt;\qquad T(t)=\frac{1}{2\pi}\int_{-\infty}^{\infty}e^{i\omega t}\widehat{T(\omega)}d\omega$$

(87~~69~~)

similarly for the forcing F (the circonflex indicates Fourier Transform). Then:

$$\widehat{\left(\frac{d^H T}{dt^H}\right)}=\left(i\omega\right)^H\hat{T}$$

(88~~70~~)

(this is true for the Weyl fractional derivatives used here, [*Podlubny*, 1999]). So that the impulse response is:

$$G_{\delta,1/2}(t)=\frac{1}{2\pi}\int_{-\infty}^{\infty}\frac{e^{i\omega t}}{1+\left(i\omega\right)^{1/2}}d\omega$$

(89~~71~~)

Formatted: Equation

The solution to the HEBE at two different points $\underline{x}_1$, $\underline{x}_2$ is:

$$\hat{T}\left(\underline{x}_1,\omega_1\right)=s\left(\underline{x}_1\right)\frac{\hat{F}\left(\underline{x}_1,\omega_1\right)}{1+\left(i\omega_1\tau\left(\underline{x}_1\right)\right)^{1/2}}$$

$$\hat{T}^*\left(\underline{x}_2,\omega_2\right)=s\left(\underline{x}_2\right)\frac{\hat{F}^*\left(\underline{x}_2,\omega_2\right)}{1+\left(-i\omega_2\tau\left(\underline{x}_2\right)\right)^{1/2}}$$

(90~~72~~)

Where the asterix indicates complex conjugate. Multiplying and taking ensemble averages and assuming that the forcing – and hence responses - are statistical stationary, we obtain:

$$<\widehat{T^*}\left(\underline{x}_1,\omega\right)\hat{T}\left(\underline{x}_2,\omega'\right)>=\hat{R}_T\left(\underline{x}_1,\underline{x}_2,\omega\right)\delta\left(\omega-\omega'\right);\qquad \hat{R}_T\left(\underline{x}_1,\underline{x}_2,\omega\right)=\hat{R}_T^*\left(\underline{x}_2,\underline{x}_1,\omega\right)$$

(91~~73~~)

Where:

$$R_T\left(\underline{x}_1,\underline{x}_2,\Delta t\right)=\frac{1}{2\pi}\int_{-\infty}^{\infty}e^{i\omega\Delta t}\widehat{R}_T\left(\underline{x}_1,\underline{x}_2,\omega\right)d\omega$$

(92~~74~~)

Therefore:

$$R_T\left(\underline{x}_1,\underline{x}_2,\omega\right)=s\left(\underline{x}_1\right)s\left(\underline{x}_2\right)\hat{G}_T\left(\underline{x}_1,\underline{x}_2,\omega\right)\widehat{R}_F\left(\underline{x}_1,\underline{x}_2,\omega\right);$$

$$\hat{G}_T\left(\underline{x}_1,\underline{x}_2,\omega\right)=\frac{1}{\left(1+\left(-i\omega\tau\left(\underline{x}_1\right)\right)^{1/2}\right)\left(1+\left(i\omega\tau\left(\underline{x}_2\right)\right)^{1/2}\right)}$$

(93~~75~~)

A special case that is useful later, is when $\underline{x}_1=\underline{x}_2=\underline{x}$, which yields the spectrum E_T at the point $\underline{x}$:

$$E_T\left(\underline{x},\omega\right)\delta\left(\omega-\omega'\right)=\left\langle\hat{T}\left(\underline{x},\omega\right)\widehat{T^*}\left(\underline{x},\omega'\right)\right\rangle;\qquad E_T\left(\underline{x},\omega\right)=\widehat{R}_T\left(\underline{x},\underline{x},\omega\right)$$

Field Code Changed

(94~~76~~)

Using a partial fraction expansion of eq. ~~75~~93, we obtain:

$$\widehat{G}_T\left(\underline{x}_1,\underline{x}_2,\omega\right)=\frac{1}{\tau_1+\tau_2}\left[\frac{\tau_1+i\tau_g}{\left(1+\left(-i\omega\tau_1\right)^{1/2}\right)}+\frac{\tau_2-i\tau_g}{\left(1+\left(i\omega\tau_2\right)^{1/2}\right)}\right];\qquad \tau_g=sign\left(\omega\right)\left(\tau_1\tau_2\right)^{1/2}$$

(95~~77~~)

By inverting the Fourier transform, this can be used to determine the real space transfer function $G_T\left(\underline{x}_1,\underline{x}_2,\Delta t\right)$. Using contour integration, it is convenient to convert the inverse Fourier transforms into Laplace transforms for $\Delta t>0$:

$$G_T\left(\underline{x}_1,\underline{x}_2,\Delta t\right)=\frac{1}{\pi\left(\tau_1+\tau_2\right)}\left[\int_0^{\infty}e^{-x\left(\Delta t/\tau_2\right)}\frac{x^{1/2}}{1+x}dx+\left(\frac{\tau_2}{\tau_1}\right)^{1/2}\int_0^{\infty}e^{-x\left(\Delta t/\tau_2\right)}\frac{1}{1+x}dx-\left(\frac{\tau_1}{\tau_2}\right)^{1/2}\int_0^{\infty}e^{-x\left(\Delta t/\tau_1\right)}\frac{1}{1+x^{1/2}}dx\right]$$

(96~~78~~)

For $\Delta t<0$, use $G_T\left(\underline{x}_1,\underline{x}_2,-\Delta t\right)=G_T\left(\underline{x}_2,\underline{x}_1,\Delta t\right)$. The spatial cross-correlation, temporal autocorrelation function of the temperature is therefore:

$$R_T\left(\underline{x}_1,\underline{x}_2,\Delta t\right)=s\left(\underline{x}_1\right)s\left(\underline{x}_2\right)G_T\left(\underline{x}_1,\underline{x}_2,\Delta t\right)*R_F\left(\underline{x}_1,\underline{x}_2,\Delta t\right)$$ (97~~79~~)

Where the "*" indicates convolution.
The basic Laplace transforms in eq. ~~78~~ 96 can be expressed in terms of higher mathematical functions as follows (all for $t>0$):

$$G_{\delta,1/2}\left(t\right)=\frac{1}{\pi}\int_0^\infty \frac{x^{1/2}}{1+x}e^{-xt}dx=\frac{1}{\sqrt{\pi t}}-e^{t}erfc\left(\sqrt{t}\right)$$ (98~~80~~)

$$\frac{1}{\pi}\int_0^\infty \frac{e^{-xt}}{1+x}dx=\frac{1}{\pi}e^{t}\Gamma\left(0,t\right);\qquad \Gamma\left(0,t\right)=\int_t^\infty \frac{e^{-t}}{t}dt$$

$$\frac{1}{\pi}\int_0^\infty \frac{1}{1+x^{1/2}}e^{-xt}dx=\frac{1}{\sqrt{\pi t}}-e^{-t}erfi\left(\sqrt{t}\right)+\frac{e^{-t}}{\pi}E_I\left(t\right);\qquad erfi\left(z\right)=erf\left(iz\right)/i=\mathrm{Im}\left(ercf\left(-iz\right)\right);$$

$$E_I\left(t\right)=-\int_{-t}^\infty \frac{e^{-t}}{t}dt=-\Gamma\left(0,-t\right)+i\pi$$

The $i\pi$ comes from integrating half way around the pole at the origin. Note that both the Exponential Integral (E_I) and the incomplete Gamma functions have log divergences at the origin. If needed, these formulae can be combined to obtain a complete analytic expression for $G_T\left(\underline{x}_1,\underline{x}_2,\Delta t\right)$, which can then be used to determine the temperature correlations if the forcing correlations are known: $R_T\left(\underline{x}_1,\underline{x}_2,\Delta t\right)=s\left(\underline{x}_1\right)s\left(\underline{x}_2\right)G_T\left(\underline{x}_1,\underline{x}_2,\Delta t\right)*R_F\left(\underline{x}_1,\underline{x}_2,\Delta t\right)$ where the asterix is the temporal convolution.

The special case $\underline{x}_1=\underline{x}_2$ i.e. with $\tau_1=\tau_2=\tau$, is a little simpler:

$$G_T\left(\Delta t\right)=\frac{1}{\tau}g\left(\frac{\left|\Delta t\right|}{\tau}\right);\qquad g\left(\Delta t\right)=\frac{1}{2\pi}\int_0^\infty e^{-x\Delta t}\left(\frac{x^{1/2}}{1+x}+\frac{1}{1+x}-\frac{1}{1+x^{1/2}}\right)dx;\quad \Delta t>0$$ (99~~81~~)

Whose Fourier transform is:

$$\hat{G}_T\left(\underline{x},\underline{x},\omega\right)=\frac{1}{1+2\,\mathrm{Re}\left[\left(-i\omega\tau\right)^{1/2}\right]+\omega\tau}$$ (100~~82~~)

Evaluating the integral for $g(\Delta t)$ using the Laplace transform formulae (eq. ~~80~~98):

$$g(\Delta t)=\frac{1}{\pi}\left(e^{\Delta t}\Gamma(0,\Delta t)+e^{-\Delta t}\operatorname{Re}\left(\Gamma(0,-\Delta t)\right)\right)-\left(e^{\Delta t}erfc\sqrt{\Delta t}+e^{-\Delta t}Im\left(erfc\left(-i\sqrt{\Delta t}\right)\right)\right)$$ (101~~83~~)

(Δt>0). The small scale and asymptotic limits are thus:

$$g(\Delta t)=-\frac{\log\Delta t}{\pi}-\frac{1}{2}-\frac{\gamma_E}{\pi}+2\sqrt{\frac{\Delta t}{\pi}}-\frac{t}{2}-\left(\frac{t^2\log\Delta t}{2\pi}\right)+... \qquad \Delta t<<1$$

$$g(\Delta t)\approx\frac{1}{\Delta t\sqrt{\pi\Delta t}}-\frac{2}{\pi\Delta t^2}+\frac{15}{8\Delta t^3\sqrt{\pi\Delta t}}-... \qquad \Delta t>>1$$ (102~~84~~)

Note the small scale log divergence, this is important when the forcing is a white noise, see [*Lovejoy*, 2019a]. The temporal autocorrelation at the point $\underline{x}$ is thus:

$$R_T(\underline{x},\Delta t)=\frac{\lambda(\underline{x})^2}{\tau(\underline{x})}g\left(\Delta t/\tau(\underline{x})\right)*R_F(\underline{x},\Delta t); \qquad R(\underline{x},\Delta t)=R(\underline{x},\underline{x},\Delta t)$$

$$R_T(\underline{x},\Delta t)=\frac{s(\underline{x})^2}{\tau(\underline{x})}g\left(\Delta t/\tau(\underline{x})\right)*R_F(\underline{x},\Delta t); \qquad R(\underline{x},\Delta t)=R(\underline{x},\underline{x},\Delta t)$$ (103~~85~~)

However, in general, the Fourier relations are easier to deal with.

~~**Appendix C: Statistical Space-Time Factorization**~~

~~At high frequencies (i.e. $\Delta t<\tau$), and empirically over the macroweather regime up to a decade or more ([Lovejoy and de Lima, 2015]), both precipitation and temperature anomalies (at least approximately) respect a space-time symmetry called "space-time statistical factorization" ("STSF"). For example, for the autocorrelation function *R*, this implies~~ $R_{space-time}(\Delta\underline{x},\Delta t)=R_{space}(\Delta\underline{x})R_{time}(\Delta t)$~~. If obeyed, this factorization implies important simplications in regional macroweather forecasting: it is therefore interesting to investigate the implications HEBE for the STSF hypothesis.~~

~~The easiest way to approach the STSF is to consider that the forcing and relaxation times $\tau(\underline{x})$ and sensitivities $\lambda(\underline{x})$ are stochastic fields that are statistically homogeneous in space so that the correlation functions can be written: . If we assume that the forcing is statistically independent of the temperature, then, taking the high frequency limit of~~ $\hat{G}_T$ ~~in eq. 75:~~

$$\hat{G}_T\left(\underline{x},\underline{x}-\underline{\Delta x},\omega\right)\approx\frac{1}{\left(\tau\left(\underline{x}\right)\tau\left(\underline{x}-\underline{\Delta x}\right)\right)^{1/2}\omega}\qquad \cancel{(86)}$$

~~we obtain:~~

$$R_T\left(\underline{\Delta x},\omega\right)=<\left[\frac{\lambda\left(\underline{x}\right)\lambda\left(\underline{x}-\underline{\Delta x}\right)}{\left(\tau\left(\underline{x}\right)\tau\left(\underline{x}-\underline{\Delta x}\right)\right)^{1/2}}\right]>\frac{R_F\left(\underline{\Delta x},\omega\right)}{\omega}$$

$\cancel{(87)}$

~~From this, see that if the forcing factorizes then the temperature autocorrelation function also factorizes:~~

$\cancel{(88)}$

~~Where~~ $R_{\lambda\tau^{-1/2}}\left(\underline{\Delta x}\right)$ ~~is the autocorrelation function of~~ $\cancel{\lambda\tau^{-1/2}}$ ~~(the term in square brackets in eq. 87). From here, the inverse Fourier transform of and gives the real space version of the STSF symmetry. Notice that at the STSF hinges on the factorization approximation for~~ $\hat{G}_T\left(\underline{x},\underline{x}-\underline{\Delta x},\omega\right)$ ~~and at low ω, it breaks down.~~

Appendix ~~D~~C: Fractional Integration on the sphere

At long enough time scales, the spatial transport of heat is important and the spherical geometry of the Earth must be taken into account. The standard way (see section 2.3 and ~~e.g.~~ the reviews [*North et al.*, 1981], [*North and Kim*, 2017]) is to use spherical harmonics. In Appendix 5D of [*Lovejoy and Schertzer*, 2013] these were used to define fractional integrals on the sphere, necessary in order to produce the corresponding multifractal cloud and topography models (see also [*Landais et al.*, 2019]). Spherical harmonics are particularly convenient when the heat transport is diffusive, involving fractional Laplacians. In section 3.5.2, these were defined in real space by taking the domain of integration to be a sphere. In this appendix we discuss an alternative method of spherical fractional integration that may have theoretical and practical advantages.

The Laplacian on a sphere (∇_Ω^2) is the angular part of the Laplacian in spherical coordinates, it is obtained by expressing the Laplacian in spherical coordinates and setting the radial derivatives to zero:

$$\nabla_\Omega^2=\left[\frac{\partial}{\partial\mu}\left(1-\mu^2\right)\frac{\partial}{\partial\mu}+\frac{1}{\left(1-\mu^2\right)}\frac{\partial^2}{\partial\phi^2}\right];\quad \mu=\cos\theta \qquad (104\cancel{89})$$

Field Code Changed

Field Code Changed

where θ is the colatitude and ϕ is the longitude. The normalized eigenfunctions of ∇^2_Ω are the spherical harmonics $Y_{n,m}$:

$$Y_{n,m}(\mu,\phi)=\left[\frac{2n+1}{4\pi}\frac{(n-|m|)!}{(n+|m|)!}\right]^{1/2}P_{n,|m|}(\mu)e^{im\phi}\begin{pmatrix}(-1)^m; & m\geq 0\\ 1; & m<0\end{pmatrix};\qquad \mu=\cos\theta;\quad -n\leq m\leq n$$

(105~~90~~)

With m, n integer, $n\geq 0$ and $P_{n,m}$ is the associated Legendre polynomial. $Y_{n,m}$ satisfies:

$$-\nabla^2_\Omega Y_{n,m}(\mu,\phi)=n(n+1)Y_{n,m}(\mu,\phi)$$ (106~~91~~)

So that $n(n+1)$ are the eigenvalues. Since $|m|\leq n$ there are $2n+1$ degenerate eigenvalues and functions for each n.

The spherical harmonics form a complete orthogonal basis, so that any function $f(\mu,\phi)$ on the sphere can be uniquely expressed in terms of a spherical harmonic expansion:

$$f(\mu,\phi)=\sum_{n=0}^{\infty}\sum_{m=-n}^{n}F^{(0)}_{n,m}Y_{n,m}(\mu,\phi);\quad F^{(0)}_{n,m}=\int_0^{2\pi}\int_{-1}^{1}Y^*_{n,m}(\mu,\phi)f(\mu,\phi)\,d\mu\,d\phi$$ (107~~92~~)

Where ~~the~~ $F^{(0)}_{n,m}$ are the coefficients of the expansion without fractional integration (i.e. of order 0, indicated in the superscript). This suggests the following definition for a fractional spherical integration order H of a spherical harmonic:

$$\left(-\nabla^2_\Omega\right)^{-H/2}Y_{n,m}(\mu)=\left[n(n+1)\right]^{-H/2}Y_{n,m}(\mu);\quad n\geq 1$$, (108~~93~~)

for the HEBE, we take H = 1 which corresponds to the ½ power of the inverse Laplacian (see section 2.3 for the zonally averaged case that depends only on n). We have excluded the value n = 0 since when H>0, the filter $\left[n(n+1)\right]^{-H/2}$ divergences; since $Y_{0,0}(\mu,\phi)=\frac{1}{\sqrt{4\pi}}$, this component corresponds to the mean. Therefore the above definition is adequate for mean zero anomalies. Alternatively, the mean can be removed and taken care of separately, see below. With this definition, the fractional integral of the zero mean function f is:

$$\left(-\nabla_{\Omega}^{2}\right)^{-H/2} f\left(\mu,\phi\right)=\sum_{n=1}^{\infty}\sum_{m=-n}^{n} F_{n,m}^{(H)}Y_{n,m}\left(\mu,\phi\right);\quad F_{n,m}^{(H)}=\left[n\left(n+1\right)\right]^{-H/2}F_{n,m}^{(0)} \qquad (109~~94~~)$$

i.e. a filter in spherical harmonic space, analogous to the Fourier filter $\left|\underline{k}\right|^{-H}$ for an isotropic fractional integration in Cartesian coordinates.

The definition of the fractional Laplacian (eq. ~~93~~111, ~~94~~112) is adequate when the horizontal transport coefficients are constant, but in section 3.5, we saw that more generally, the half order divergence operator was written: $l\left(\mu,\phi\right)^{-1}\left(-\nabla_{\Omega}^{2}\right)^{-1/2}$ i.e. there was an extra multiplication by the spatially varying diffusion length $l\left(\mu,\phi\right)$. In flat (Cartesian) coordinates, such real space multiplications correspond to Fourier space convolutions so that this operator can also be conveniently expressed in Fourier space. However, with spherical harmonics, this simplicity is lost: although isotropic real space convolutions can still be performed by filtering the harmonics, real space multiplications no longer correspond to convolutions of harmonic coefficients, the closest spherical harmonic equivalent is much more complicated, it involves Clebsch-Gordon coefficients.

A method of fractionally integrating the mean (n = 0) component was developed for the purpose of multifractal modeling in Appendix 5D of [*Lovejoy and Schertzer*, 2013]. There, a different definition of fractional integrals on the sphere was proposed: a convolution with the function $\Theta^{-(2-H)}$, where Θ is the angle between two points subtended at the center of the sphere. The function $\Theta^{-(2-H)} / \Gamma(H/2)$ was numerically expanded in spherical harmonics and the convolution was again performed by filtering the coefficients (the constant $\Gamma(H/2)$ is needed so that the normalization is the same as for the definition eq. ~~92~~107). The main difference between the two definitions is that the latter can be directly applied to fields with nonzero means. With this definition, the H order fractional integral of a constant function on the sphere (representing the nonzero mean), is simply the value multiplied by $2^{-H/2}\sqrt{\pi}/\Gamma\left(H/2\right)\int_{0}^{2\pi}s^{-(2-H)}\sin s\,ds$ which for the HEBE H =1 case, reduces to $(1/2)^{1/2}Si(2\pi)$ where Si is the standard sine integral function. However for the coefficients $n\geq1$, numerical tests show that the two definitions are almost exactly the same; for example with H = 1, the spherical harmonic coefficients of $\Theta^{-(2-H)}$ are within 3% for all $n\geq1$ and the ratio converges rapidly to 1 for large n. The conclusion is that filtering the anomaly by $\left[n\left(n+1\right)\right]^{-H/2}$ and then multiplying the mean by the above factor is a practical method of fractionally integrating a function on the sphere.

6. References

Babenko, Y. I., *Heat and Mass Transfer*, Khimiya: Leningrad (in Russian), 1986.
Brunt, D., Notes on radiation in the atmosphere, *Quart. J. Roy. Meterol. Soc.* , *58*, 389-420, 1932.

Chenkuan, L., and Clarkson, K., Babenko's Approach to Abel's Integral Equations, *Mathematics 6*, 32 doi: doi:10.3390/math6030032, 2018.

Coffey, W. T., Kalmykov, Y. P., and Titov, S. V., Characteristic times of anomalous diffusion in a potential, in *Fractional Dynamics: Recent Advances*, edited by J. Klafter, S. Lim and R. Metzler, pp. 51-76, World Scientific, 2012.

Del Rio Amador, L., and Lovejoy, S., Predicting the global temperature with the Stochastic Seasonal to Interannual Prediction System (StocSIPS) *Clim. Dyn.* doi: org/10.1007/s00382-019-04791-4., 2019.

Del Rio Amador, L., and Lovejoy, S., Using scaling for seasonal global surface temperature forecasts: StocSIPS *Clim. Dyn.*, *under review*, 2020a.

Del Rio Amador, L., and Lovejoy, S., Long-range Forecasting as a Past Value Problem: Using Scaling to Untangle Correlations and Causality *Geophys. Res. Lett.*, *(submitted, Nov. 2020)*, 2020b.

Havlin, S., and Ben-Avraham, D., Diffusion in disordered media, *Adv. Phys.*, ***36***, 695-798, 1987.

Hebert, R. (2017), A Scaling Model for the Forced Climate Variability in the Anthropocene, MSc thesis, McGill University, Montreal.

Hébert, R., Lovejoy, S., and Tremblay, B., An Observation-based Scaling Model for Climate Sensitivity Estimates and Global Projections to 2100, *Climate Dynamics*, *(in press)*, 2020.

Hilfer, R. (Ed.), *Applications of Fractional Calculus in Physics* World Scientific, 2000.

Houghton, J. T., Ding, Y., Griggs, D. J., Noguer, M., van der Linden, P. J., Dai, X., Maskell, K., and Johnson, C. A. (Eds.), *Climate Change 2001: The Scientific Basis, Contribution of Working Group I to the Third Assessment Report of the Intergovernmental Panel on Climate Change*, Cambridge University Press, 2001.

Kobelev, V., and Romanov, E., Fractional Langevin Equation to Describe Anomalous Diffusion *Prog. of Theor. Physics Supp.*, *139*, 470-476, 2000.

Kulish, V. V., and Lage, J. L., Fractional-diffusion solutions for transport, local temperature and heat flux. , *ASME Journal of Heat Transfer*, *122* 372-376, 2000.

Landais, F., Schmidt, F., and Lovejoy, S., Topography of (exo)planets, *MNRAS 484*, 787–793 doi: 10.1093/mnras/sty3253, 2019.

Lionel, R., D., C. M., M., C., S., S., and M., G., Parameter estimation for energy balance models with memory *Proc. R. Soc. A*, *470* doi: doi.org/10.1098/rspa.2014.0349, 2014.

Lovejoy, S., What is climate?, *EOS*, *94, (1), 1 January*, p1-2, 2013.

Lovejoy, S., How accurately do we know the temperature of the surface of the earth? , *Clim. Dyn.* doi: doi:10.1007/s00382-017-3561-9, 2017.

Lovejoy, S., The spectra, intermittency and extremes of weather, macroweather and climate, *Nature Scientific Reports*, *8*, 1-13 doi: 10.1038/s41598-018-30829-4, 2018.

Lovejoy, S., Fractional Relaxation noises, motions and the stochastic fractional relxation equation *Nonlinear Proc. in Geophys. Disc.*, *https://doi.org/10.5194/npg-2019-39*, 2019a.

Lovejoy, S., *Weather, Macroweather and Climate: our random yet predictable atmosphere*, 334 pp., Oxford U. Press, 2019b.

Lovejoy, S., and Schertzer, D., Haar wavelets, fluctuations and structure functions: convenient choices for geophysics, *Nonlinear Proc. Geophys.* , *19*, 1-14 doi: 10.5194/npg-19-1-2012, 2012.

Lovejoy, S., and Schertzer, D., *The Weather and Climate: Emergent Laws and Multifractal Cascades*, 496 pp., Cambridge University Press, 2013.

Lovejoy, S., and de Lima, M. I. P., The joint space-time statistics of macroweather precipitation, space-time statistical factorization and macroweather models, *Chaos 25*, 075410 doi: 10.1063/1.4927223., 2015.

Lovejoy, S., Schertzer, D., and Silas, P., Diffusion on one dimensional multifractals, *Water Res. Res.*, *34*, 3283-3291, 1998.

Lovejoy, S., Schertzer, D., and Varon, D., Do GCM's predict the climate…. or macroweather?, *Earth Syst. Dynam.* , *4*, 1–16 doi: 10.5194/esd-4-1-2013, 2013.

Lovejoy, S., Del Rio Amador, L., and Hébert, R., Harnessing butterflies: theory and practice of the Stochastic Seasonal to Interannual Prediction System (StocSIPS), , in *Nonlinear Advances in Geosciences,* , edited by A. A. Tsonis, pp. 305-355, Springer Nature, 2017.

Lovejoy, S., del Rio Amador, L., and Hébert, R., The ScaLIng Macroweather Model (SLIMM): using scaling to forecast global-scale macroweather from months to Decades, *Earth Syst. Dynam.*, *6*, 1–22 doi: www.earth-syst-dynam.net/6/1/2015/, doi:10.5194/esd-6-1-2015, 2015.

Lovejoy, S., Procyk, R., Hébert, R., and del Rio Amador, L., The Fractional Energy Balance Equation, *Quart. J. Roy. Met. Soc.* , *(under revision)*, 2020.

Magin, R., Sagher, Y., and Boregowda, S., Application of fractional calculus in modeling and solving the bioheat equation, in *Design and Nature II*, edited by M. W. C. C. A. Brebbia, pp. 207-216, WIT Press, 2004.

Márquez, J. M. A., Bohórquez, M. A. M., and Melgar, S. G., Ground Thermal Diffusivity Calculation by Direct Soil Temperature Measurement. Application to very Low Enthalpy Geothermal Energy Systems, *Sensors (Basel)*, *16*, 306 doi: 10.3390/s16030306, 2016.

Meerschaert, M. M., and Sikorskii, A., *Stochastic Models for Fractional Calculus*, 2012.

Miller, K. S., and Ross, B., *An introduction to the fractional calculus and fractional differential equations*, 366 pp., John Wiley and Sons, 1993.

North, G. R., Cahalan, R. F., and Coakley, J., J. A. , Energy balance climate models, *Rev. Geophysics Space Phy.*, *19*, 91-121, 1981.

North, R. G., and Kim, K. Y., *Energy Balance Climate Models*, 369 pp., Wiley-VCH, 2017.

Podlubny, I., *Fractional Differential Equations*, 340 pp., Academic Press, 1999.

Procyk, R., Lovejoy, S., and Hébert, R., The Fractional Energy Balance Equation for Climate projections through 2100, *Earth Sys. Dyn. Disc.*, *under review* doi: org/10.5194/esd-2020-48 2020.

Schertzer, D., and Lovejoy, S., The dimension and intermittency of atmospheric dynamics, in *Turbulent Shear Flow*, edited by L. J. S. Bradbury, F. Durst, B.E. Launder, F.W. Schmidt, J.H. Whitelaw, pp. 7-33, Springer-Verlag, 1985.

Schertzer, D., and Lovejoy, S., Physical modeling and Analysis of Rain and Clouds by Anisotropic Scaling of Multiplicative Processes, *Journal of Geophysical Research*, *92*, 9693-9714, 1987.

Sellers, W. D., A global climate model based on the energy balance of the earth-atmosphere system, *J. Appl. Meteorol.*, *8*, 392-400, 1969.

Trenberth, K. E., Fasullo, J. T., and Kiehl, J., Earth's global energy budget, *Bull. Amer. Met.Soc.,*, 311-323 doi: DOI:10.1175/2008BAMS2634.1, 2009.

Warren, S. G., and Schneider, S. H., Seasonal simu-lation as a test for uncertainties in the parameterizations of a Budyko-Sellers zonal climate model, *J. Atmos. Sci.*, *36*, 1377-1391, 1979.

Weissman, H., S. Havlin, Dynamics in multiplicative processes, *Phys. Rev. B*, *37*, 5994-5996, 1988.

West, B. J., Bologna, M., and Grigolini, P., *Physics of Fractal Operators*, 354 pp., Springer, 2003.

Zhuang, K., North, G. R., and Stevens, M. J., A NetCDF version of the two-dimensional energy balance model based on the full multigrid algorithm, *SoftwareX*, *6*, 198–202 doi: https://doi.org/doi.org/10.1016/j.softx.2017.07.003, 2017.

Ziegler, E., and Rehfeld, K., TransEBM v. 1.0: Description, tuning, and validation of a transient model of the Earth's energy balance in two dimensions, *Geosci. Model Devel. Disc.* doi: https://doi.org/10.5194/gmd-2020-237, 2020.

Formatted: Indent: Left: 0 cm, Hanging: 1 cm

Figures

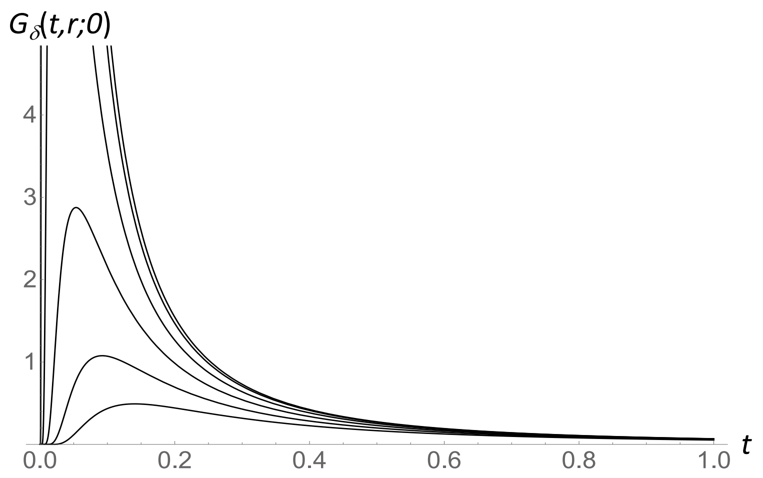

Fig. 1: The surface impulse response function ($G_\delta(t,r;0)$, eq. 12, i.e. Dirac in time and Dirac in space) as a function of nondimensional time (*t*) for nondimensional distance from the source increasing from *r* = 0 (top) to *r* = 1 in steps of 0.2 (top to bottom).

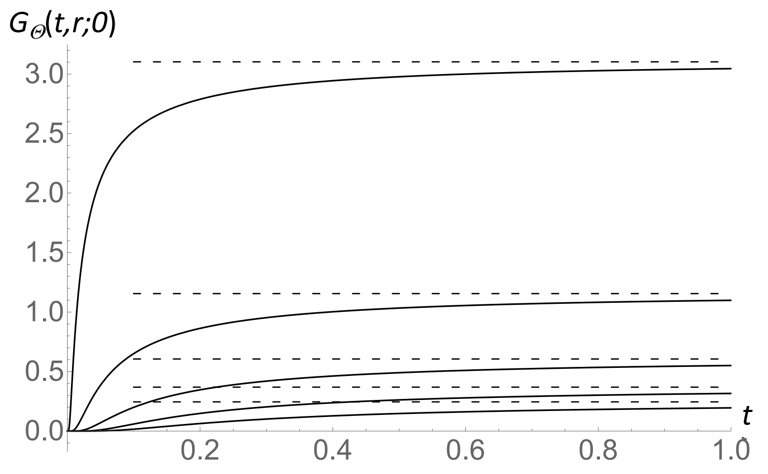

Fig. 2: The surface step response (time), Dirac (space) function ($G_{\Theta}\left(t,r;0\right)$, eq. 12) as a function of nondimensional time, each curve is for a different nondimensional distance from the source increasing from r = 0.2 (top) to r = 1 in steps of 0.2 (top to bottom). At each distance r, the temperature approaches ~~thermodynamic~~ equilibrium (= $G_{therm,\delta}(r)$, eq. 20) at large t (shown by dashed horizontal lines).

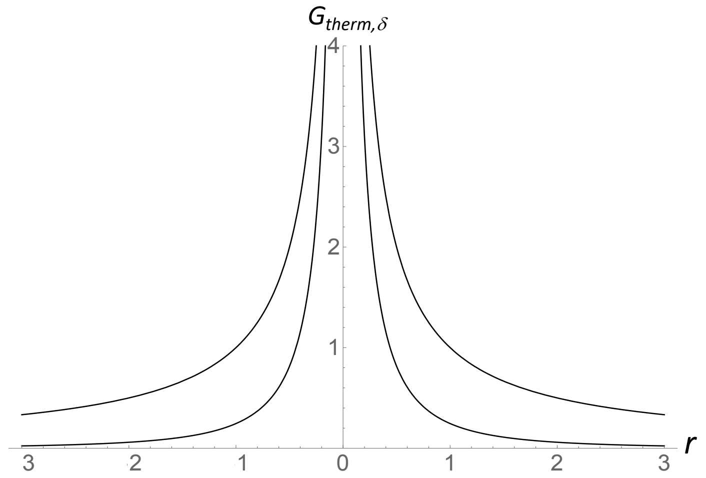

$G_{therm,\delta}$
4
3
2
1
r
3
2
1
0
1
2
3

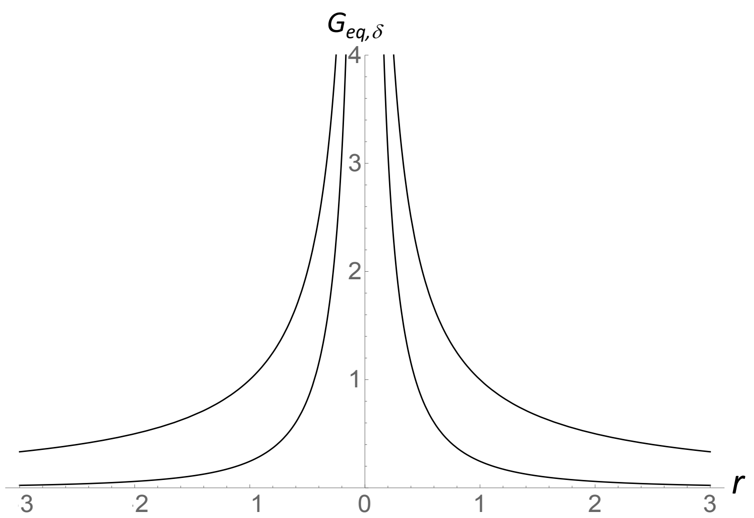

Fig. 3: A comparison of the spatial impulse response Green's functions for ~~thermal~~ equilibrium with surface forcing via conduction only (i.e. $\left.\frac{\partial T_{eq}}{\partial z}\right|_{z=0} = \delta\left(\underline{x}\right)$, no radiation), top = r^{-1}), and bottom, the same but with conduction – radiative forcing via the surface BC ($\left.\frac{\partial T_{eq}}{\partial z}\right|_{z=0} + T\left(r;0\right) = \delta\left(\underline{x}\right)$) that is asymptotically ≈ r^{-3} (eq. 21).

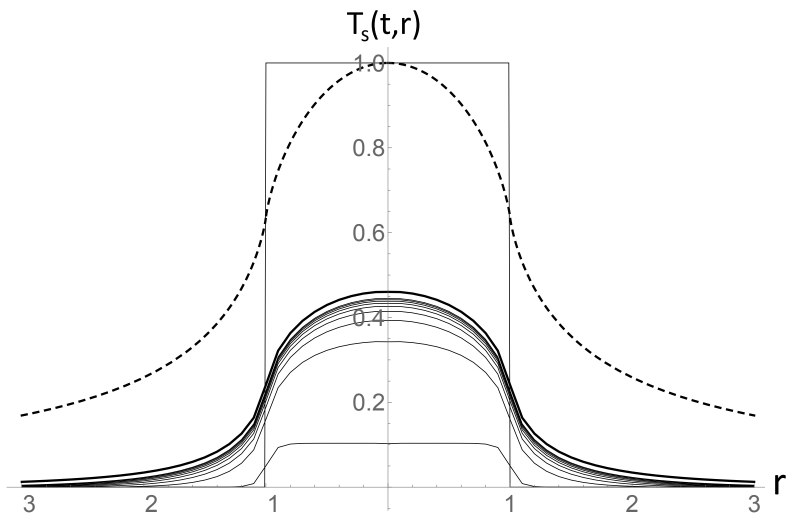

Fig. 4: This is the step response in time and (circular) step in space for conductive-radiative forcing. Lines for *t* = 0.01 (bottom), 0.2, 0.4, ... 1.6 (black, bottom to top, the thick black line is for $t = \infty$ (~~therm odynamic~~ equilibrium). The nondimensional forcing is the rectangle (from unit circular forcing). Also shown (top dashed) is the ~~thermodynamic~~ equilibrium when the forcing is purely due to unit conductive heating over the unit circle.

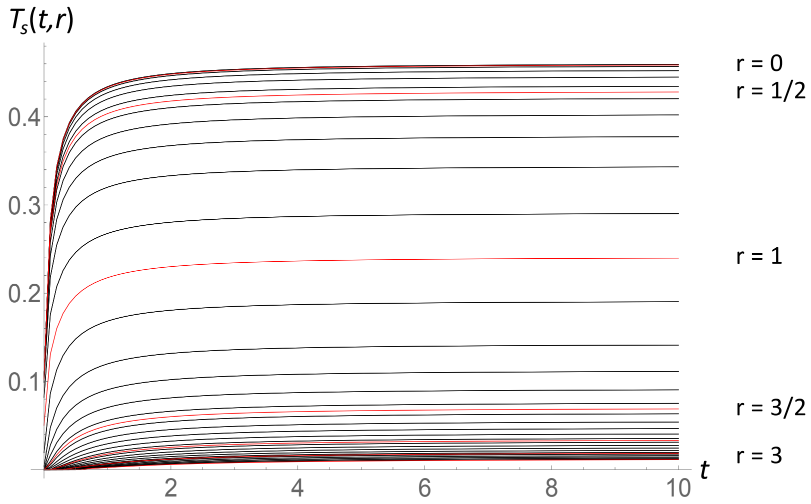

Fig. 5: The response to a unit intensity forcing in the unit circle. The temperature as a function of nondimensional time is given for different distances from the center top (*r* = 0) to bottom (*r* = 3), from the same data as before… red every 1/2, black every 0.1 (top, *r* = 0, bottom, *r* = 3).

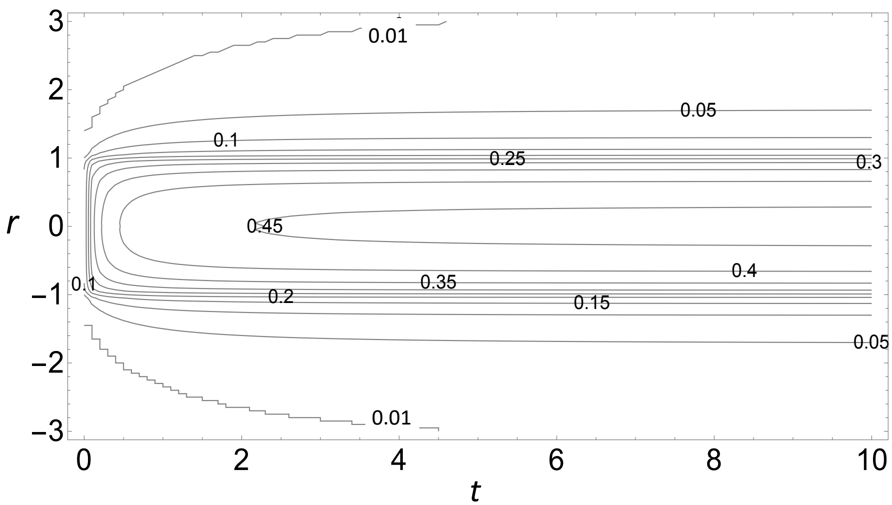

Fig. 6: Space - time contours for unit circle forcing as a function of nondimensional time (left to right) and nondimensional horizontal distance (vertical axis) and nondimensional time left to right.

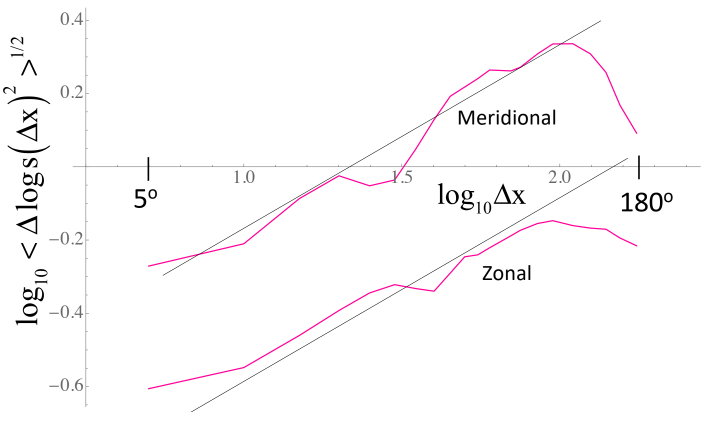

Fig. 7: The RMS fluctuations (at Δt = 1 month resolution) $\Delta \log s_{\Delta t}(\Delta x)$ (zonal, bottom), $\Delta \log s_{\Delta t}(\Delta y)$ (meridional, top) from NCAR reanalyses. The vertical scale is dimensionless, the horizontal scale is in $\log_{10}$ (degrees) with the minimum (5º) and maximum (180º) indicated in large, bold font. The black lines are reference lines (not regressions) with slopes $H_x = H_y = 0.5$.

Parameters	Symbol	Estimated Value
Specific heat per volume	ρc	$\approx 10^6$ J/m^3
Climate sensitivity	$s\lambda$	$\approx$ 1 K/(W/m^2)
Vertical diffusivity (ocean)	κ_v	$\approx 10^{-4}$ m^2/s
Vertical diffusivity (soil)	κ_v	$\approx 10^{-6}$ m^2/s
Horizontal diffusivity	κ_h	≈ 1 m^2/s
Vertical Diffusion depth (oceans)	$l_v = (\tau \kappa_v)^{1/2}$	≈ 100 m
Vertical Diffusion depth (soil)	$l_v = (\tau \kappa_v)^{1/2}$	$\approx$ 3 – 10m
Relaxation time	$\tau = \kappa_v (\rho c \lambda)^2$	**$\approx 10^8$ s**
Horizontal Diffusion length	$l_h = (\tau \kappa_h)^{1/2}$	$\approx 10^4$ m
Effective horizontal heat transport velocity	$\boldsymbol{V = l_h/\tau}$	**$\approx 10^{-4}$ m/s**
Effective advection velocity	v_h	$\approx 10^{-4}$ m/s
Nondimension advection velocity	α	0.1 - 1
Characteristic Zonal variation length	L_{EW}	$\approx 1.5 \times 10^7$ m
Characteristic Meridional variation length	L_{NS}	$\approx 3 \times 10^6$ m

Table 1: Empirical estimates of the parameters used in this paper; see appendix A for details.

Formatted: Font: Italic

Page 21: [1] Formatted	Shaun Lovejoy	11/9/20 10:03:00 PM

Font: Italic

Page 21: [1] Formatted	Shaun Lovejoy	11/9/20 10:03:00 PM

Font: Italic

Page 21: [2] Formatted	Shaun Lovejoy	11/10/20 10:59:00 AM

Font: Italic

Page 21: [2] Formatted	Shaun Lovejoy	11/10/20 10:59:00 AM

Font: Italic

Page 21: [2] Formatted	Shaun Lovejoy	11/10/20 10:59:00 AM

Font: Italic

Page 21: [2] Formatted	Shaun Lovejoy	11/10/20 10:59:00 AM

Font: Italic

Page 21: [3] Formatted	Shaun Lovejoy	11/12/20 11:02:00 AM

Font: Italic

Page 21: [3] Formatted	Shaun Lovejoy	11/12/20 11:02:00 AM

Font: Italic

Page 21: [3] Formatted	Shaun Lovejoy	11/12/20 11:02:00 AM

Font: Italic

Page 21: [3] Formatted	Shaun Lovejoy	11/12/20 11:02:00 AM

Font: Italic

Page 21: [3] Formatted	Shaun Lovejoy	11/12/20 11:02:00 AM

Font: Italic

Page 21: [3] Formatted	Shaun Lovejoy	11/12/20 11:02:00 AM

Font: Italic

Page 21: [3] Formatted	Shaun Lovejoy	11/12/20 11:02:00 AM

Font: Italic

Page 21: [3] Formatted	Shaun Lovejoy	11/12/20 11:02:00 AM

Font: Italic

Page 21: [3] Formatted	Shaun Lovejoy	11/12/20 11:02:00 AM

Font: Italic

Page 21: [3] Formatted	Shaun Lovejoy	11/12/20 11:02:00 AM

Font: Italic

Page 21: [3] Formatted Shaun Lovejoy 11/12/20 11:02:00 AM
Font: Italic

Page 21: [3] Formatted Shaun Lovejoy 11/12/20 11:02:00 AM
Font: Italic

Page 21: [3] Formatted Shaun Lovejoy 11/12/20 11:02:00 AM
Font: Italic

Page 21: [3] Formatted Shaun Lovejoy 11/12/20 11:02:00 AM
Font: Italic

Page 21: [3] Formatted Shaun Lovejoy 11/12/20 11:02:00 AM
Font: Italic

Page 21: [3] Formatted Shaun Lovejoy 11/12/20 11:02:00 AM
Font: Italic

Page 21: [3] Formatted Shaun Lovejoy 11/12/20 11:02:00 AM
Font: Italic

Page 21: [3] Formatted Shaun Lovejoy 11/12/20 11:02:00 AM
Font: Italic

Page 21: [3] Formatted Shaun Lovejoy 11/12/20 11:02:00 AM
Font: Italic

Page 21: [3] Formatted Shaun Lovejoy 11/12/20 11:02:00 AM
Font: Italic

Page 21: [3] Formatted Shaun Lovejoy 11/12/20 11:02:00 AM
Font: Italic

Page 21: [3] Formatted Shaun Lovejoy 11/12/20 11:02:00 AM
Font: Italic

Page 21: [3] Formatted Shaun Lovejoy 11/12/20 11:02:00 AM
Font: Italic

Page 21: [4] Formatted Shaun Lovejoy 11/10/20 1:55:00 PM
Font: Symbol

Page 21: [4] Formatted Shaun Lovejoy 11/10/20 1:55:00 PM
Font: Symbol

Page 21: [4] Formatted Shaun Lovejoy 11/10/20 1:55:00 PM
Font: Symbol

Font: Italic

Page 21: [5] Formatted **Shaun Lovejoy** **11/10/20 2:03:00 PM**

Font: Italic

Page 21: [5] Formatted **Shaun Lovejoy** **11/10/20 2:03:00 PM**

Font: Italic

Page 21: [5] Formatted **Shaun Lovejoy** **11/10/20 2:03:00 PM**

Font: Italic

Page 38: [6] Formatted **Shaun Lovejoy** **10/26/20 5:11:00 PM**

Font: 11 pt, No underline

Page 38: [6] Formatted **Shaun Lovejoy** **10/26/20 5:11:00 PM**

Font: 11 pt, No underline

Page 38: [7] Formatted **Shaun Lovejoy** **10/26/20 5:11:00 PM**

Font: 11 pt, No underline

Page 38: [7] Formatted **Shaun Lovejoy** **10/26/20 5:11:00 PM**

Font: 11 pt, No underline

Page 38: [8] Formatted **Shaun Lovejoy** **10/26/20 5:11:00 PM**

Font: 11 pt, No underline

Page 38: [8] Formatted **Shaun Lovejoy** **10/26/20 5:11:00 PM**

Font: 11 pt, No underline

Page 38: [9] Formatted **Shaun Lovejoy** **10/26/20 5:11:00 PM**

Font: 11 pt, No underline

Page 38: [9] Formatted **Shaun Lovejoy** **10/26/20 5:11:00 PM**

Font: 11 pt, No underline

Page 38: [10] Formatted **Shaun Lovejoy** **10/26/20 5:11:00 PM**

Font: 11 pt, No underline

Page 38: [10] Formatted **Shaun Lovejoy** **10/26/20 5:11:00 PM**

Font: 11 pt, No underline

Page 38: [11] Formatted **Shaun Lovejoy** **10/26/20 5:11:00 PM**

Font: 11 pt, No underline

Page 38: [11] Formatted **Shaun Lovejoy** **10/26/20 5:11:00 PM**

Font: 11 pt, No underline

Page 38: [12] Formatted	Shaun Lovejoy	10/26/20 5:12:00 PM

Font: (Default) +Headings (Times New Roman)

Page 38: [13] Formatted	Shaun Lovejoy	10/26/20 5:11:00 PM

Font: 11 pt, No underline

Page 38: [13] Formatted	Shaun Lovejoy	10/26/20 5:11:00 PM

Font: 11 pt, No underline

Page 38: [14] Formatted	Shaun Lovejoy	10/26/20 5:11:00 PM

Font: 11 pt, No underline

Page 38: [14] Formatted	Shaun Lovejoy	10/26/20 5:11:00 PM

Font: 11 pt, No underline

Page 38: [15] Formatted	Shaun Lovejoy	10/26/20 5:11:00 PM

Font: 11 pt, No underline

Page 38: [15] Formatted	Shaun Lovejoy	10/26/20 5:11:00 PM

Font: 11 pt, No underline

Page 38: [16] Formatted	Shaun Lovejoy	10/26/20 5:11:00 PM

Font: 11 pt, No underline

Page 38: [16] Formatted	Shaun Lovejoy	10/26/20 5:11:00 PM

Font: 11 pt, No underline

Page 38: [17] Formatted	Shaun Lovejoy	10/26/20 5:11:00 PM

Font: 11 pt

Page 38: [17] Formatted	Shaun Lovejoy	10/26/20 5:11:00 PM

Font: 11 pt

Page 38: [17] Formatted	Shaun Lovejoy	10/26/20 5:11:00 PM

Font: 11 pt

Page 38: [17] Formatted	Shaun Lovejoy	10/26/20 5:11:00 PM

Font: 11 pt

Page 38: [18] Formatted	Shaun Lovejoy	10/26/20 5:11:00 PM

Font: 11 pt, No underline

Page 38: [18] Formatted	Shaun Lovejoy	10/26/20 5:11:00 PM

Font: 11 pt, No underline

Page 38: [19] Formatted	Shaun Lovejoy	10/26/20 5:11:00 PM

Font: 11 pt, No underline

Page 38: [20] Formatted	Shaun Lovejoy	10/26/20 5:11:00 PM

Font: 11 pt, No underline

Page 38: [20] Formatted	Shaun Lovejoy	10/26/20 5:11:00 PM

Font: 11 pt, No underline

Page 38: [21] Formatted	Shaun Lovejoy	10/26/20 5:11:00 PM

Font: 11 pt, No underline

Page 38: [21] Formatted	Shaun Lovejoy	10/26/20 5:11:00 PM

Font: 11 pt, No underline

Page 38: [22] Formatted	Shaun Lovejoy	10/26/20 5:11:00 PM

Font: 11 pt

Page 38: [22] Formatted	Shaun Lovejoy	10/26/20 5:11:00 PM

Font: 11 pt

Page 38: [22] Formatted	Shaun Lovejoy	10/26/20 5:11:00 PM

Font: 11 pt

Page 38: [23] Formatted	Shaun Lovejoy	10/26/20 5:11:00 PM

Font: 11 pt, No underline

Page 38: [23] Formatted	Shaun Lovejoy	10/26/20 5:11:00 PM

Font: 11 pt, No underline

Page 38: [24] Formatted	Shaun Lovejoy	10/26/20 5:11:00 PM

Font: 11 pt, No underline

Page 38: [24] Formatted	Shaun Lovejoy	10/26/20 5:11:00 PM

Font: 11 pt, No underline

Page 38: [25] Formatted	Shaun Lovejoy	10/26/20 5:11:00 PM

Font: 11 pt, No underline

Page 38: [25] Formatted	Shaun Lovejoy	10/26/20 5:11:00 PM

Font: 11 pt, No underline

Page 38: [26] Formatted	Shaun Lovejoy	10/26/20 5:11:00 PM

Font: 11 pt, No underline

Page 38: [26] Formatted	Shaun Lovejoy	10/26/20 5:11:00 PM

Font: 11 pt, No underline

Overall Author Response to comments on “The Half-order Energy Balance Equation, Part 1: The homogeneous HEBE and long memories”:

The referees have made some suggestions for improvement, these will be made as indicated in the detailed responses below (in italics). I hope that the revised paper will be acceptable for publication. In addition, I have added 4 equations in section 3.1.1 that clarify the relationship with the usual Budyko-Sellers model, and also in the interest of clarity, I have added a short section 3.1.2 on the empirical model parameters.

Thanks,

Shaun Lovejoy

Anonymous Referee #1

Earth Syst. Dynam. Discuss.,https://doi.org/10.5194/esd-2020-12-RC1, 2020Interactive comment on“The Half-order EnergyBalance Equation, Part 1: The homogeneous HEBE and long memories” by Shaun Lovejoy

Peter Ashwin (Referee) p.ashwin@exeter.ac.ukReceived and published: 15 June 2020

This is an interesting and innovative manuscript that proposes the appropriate energy balance model that relates heat (S) and surface temperature (T) should involve a half order time derivative of T. It is a half-order energy balance equation (HEBE), a special case of a fractional order energy balance equation (FEBE) rather than the usual full order time derivative traditionally used for box (0D) and Budyko-Sellers (1D) models. The author convincingly argues that it this model is appropriate for longer timescale(10 day or more) variability, both empirically and from physical principles. This has consequences in expecting a longer memory of imposed forcing than one would expect of an integer order EBE; more precisely the response to step forcing has power law rather than exponential decay. The derivation assumes forcing at a conductive-radiative boundary condition and advection-diffusion of heat a semi-infinite domain: by using a Laplace-Fourier analysis the author obtains an integral form for the surface temperature that can be interpreted as a solution of a fractional differential equation. The case of periodic (annual/diurnal) forcing also considered and the surface thermal impedance is interpreted as a complex climate sensitivity – this is used to account for the observed phase lag between summer maximum forcing and surface maximum temperature.

Interactive comment on Earth Syst. Dynam. Discuss., https://doi.org/10.5194/esd-2020-12,2020.

Author: We thank the referee for his strong, positive review. As far as I can tell, he has understood the paper very well. He has no specific suggestions for changes.

Anonymous Referee #2

ESDDInteractivecommentPrinter-friendly versionDiscussion paper Earth Syst. Dynam. Discuss., https://doi.org/10.5194/esd-2020-12-RC2, 2020

Interactive comment on "The Half-order Energy Balance Equation, Part 1: The homogeneous HEBE and long memories" by Shaun Lovejoy
Anonymous Referee #2
Received and published: 28 June 2020

Review of "The Half-order Energy Balance Equation, Part 1: The homogeneous HEBE and long memories" by Lovejoy

Recommendation: Major revisions

This study derived a new version of the energy balance model based on non-integer derivatives. These models seamlessly contain long memory characteristics. This manuscript might be acceptable for publication in ESM after a major revision.

Author: We thank the referee for his/her comments that suggest a few clarifications. These are indicated in the detailed responses below (in italics).

1) Certain parts of the paper are confusing. For instance, the model is called a "zero dimensional" model though it has a vertical dimension. I assume this is because traditionally the vertical axis has been neglected and only a horizontal average considered. I strongly suggest to find a different terminology for this.

Author: We apologize for the admittedly confusing jargon, but we did not invent it! "Zero-dimensional" is the standard term for climate models without HORIZONTAL degrees of freedom. We do indicate this but we will gladly underline it and use alternative expressions when possible.

2) You refer many times to Part II. I think this is distracting; in my opinion it would make the paper easier to read to remove those references or to just have a short outlook on Part II in the conclusions section.

Author: We apologize if references to the second part of the paper are distracting. Many of these references were added after the initial submission at the explicit request of the editor Anders Levermann who thought that the linkage between the two parts was not strong enough. Since the editor was mostly concerned about adding linkages near the beginning of the paper, I tried to remove a few later on, although most of the references to the second part are quite pertinent.

The specific correspondence is on the site, I reproduce it here:

Editor Initial Decision: Start review and discussion after technical corrections (02 Apr 2020) by Anders Levermann
Comments to the Author:
Dear Shaun
See my comment to part no. 2. The two papers need to be clearly linked.
Bests,
Anders

The initial comment in part II alluded to above:
Editor Initial Decision: Start review and discussion after technical corrections (19 Mar 2020) by Anders Levermann
Comments to the Author:
Dear Shaun,
you have to reference the first part of the paper clearly in the very beginning of the paper, so that the reader can easily find it. I would actually prefer if you could reference it already in the abstract. I did not look very hard, but

I was not able to find the reference to the part 1 in the paper. Please help us here.
Bests,
Anders

3) Is your approach valid for all time scales? A long memory climate response should lead to infinite climate sensitivity. So your climate response operator is probably only valid for certain time scales.

Authors: As discussed in the paper, while the model itself may well be valid over a very wide range of time scales, it has two regimes: one shorter than the relaxation time and one longer. Both regimes are scaling and therefore both could be considered to have long memories. However there is a common - but restrictive - definition of long memory processes that is often applied to Gaussian processes (a divergent integral time scale). If this definition is used for the HEBE, and the forcing is assumed to be a Gaussian white noise, this definition will only apply to the scales below the relaxation scale. According to this definition, the different long-time scaling regime has short memory. Therefore we will clarify this distinction in the revised manuscript.

4) Line 15: BC needs to be defined.

Author: OK.

5) Line 26: I do not think "macroweather" is a widely known term. So please define.

Author: OK.

6) Line 32: "latitudinally" probably should be "zonally"

Author: OK.

7) I am confused by the z-coordinate system. It is not clear to me what z=0 means? Surface or top of the atmosphere? Also all z values seem to be negative. Also Figure1 does not help at all in that respect.

Author: On line 114 it was stated:

"We consider that vertical (radiative and conductive), and horizontal (conductive and advective) heat transport occurs on the surface and in the half-volume $(x,y,z<0)$ respectively. Although physically, this means that the atmosphere and ocean are modelled as regions with $z\leq 0$, as mentioned, only the vertical surface temperature derivative is ultimately needed and this is well defined if the surface layer is of the order of a few diffusion depths (hundreds of meters)."

As for figure 1, it clearly shows the positive z direction as "up" with radiation only in this region and with heat conduction into the $z<$ region. Could the referee be more specific about how to clarify this further?

In any case, I will add a short discussion about the physical meaning of $z=0$: the surface.

We have now rewritten the corresponding paragraph, we hope that it is clearer.

8) Line 175: Your linearization is either accurate or not, but not both.

Author: I reworked the sentence.

9) Line 266: What do you exactly mean by "top"?

Author: I mean at $z = 0$. However this was already stated in the parentheses following the word "top":

"At the top ($z = 0$), the system is forced by the conductive - radiative surface boundary condition…"

The sentence was reworked to make this clearer.

10) in (33) you develop an asymptotic expansion. Why do you stop at the 1/2 term? There are also higher order term which might lead to different orders on fractional derivatives.

Author: Eq. 33 does not stop at ½ order terms but rather at orders 3/2, 5/2 ($G_{0,1/2}$), 3, 3/2 ($G_{1,1/2}$), 3, 3/2 ($G_{2,1/2}$), they are consequences of the HEBE that has derivatives of orders ½ and 0, the terms are not associated with other fractional derivatives. In any case, I could easily have given the general n^{th} order term since it is in the literature. The high order terms are simply high and low frequency corrections to the scaling - they do not define their own separate scaling regimes. I will state this in the revised ms. However, the high and low frequencies are dominated by the ½ order part and this is supported by empirical analyses performed prior to the discovery of the HEBE. Indeed, the text immediately following eq. 33 states this:

> *"The asymptotic equation for the step response ($G_{1,1/2}$) shows that thermodynamic equilibrium is approached slowly: as $t^{-1/2}$. It is this power law step response (with empirical exponent 0.5±0.2) that was discovered semi-empirically by [Hebert, 2017], [Lovejoy et al., 2017] and was successfully used for climate projections through to 2100. Similarly, $\approx t^{0.4}$ behaviour was used for macroweather (monthly, seasonal) forecasts close to the short time $t^{1/2}$ expansion [Lovejoy et al., 2015], [Del Rio Amador and Lovejoy, 2019]."*

11) Line 350: I am not sure many ESM readers are very familiar with long memory. I suggest that explain why (37) implies long memory.

Author: Eq. 37 is simply the definition of a fractional derivative. Since such derivatives are based on power laws, it is common for fractional derivatives to be used in the context of long memory processes. I have added some material to clarify this.

Interactive comment on Earth Syst. Dynam. Discuss., https://doi.org/10.5194/esd-2020-12,2020.

The Half-order Energy Balance Equation, Part 1: The homogeneous HEBE and long memories

Shaun Lovejoy

Physics dept., McGill University, Montreal, Que. H3A 2T8, Canada

Correspondence to: Shaun Lovejoy (lovejoy@physics.mcgill.ca)

Field Code Changed

Abstract: The original Budyko-Sellers type 1-D energy balance models (EBMs) consider the Earth system averaged over long times and applies the continuum mechanics heat equation. When these and the more phenomenological ~~zero (horizontal) - dimensional~~ box models are extended to include time varying anomalies, they have a key weakness: neither model explicitly nor realistically treats the ~~surface radiative -~~ conductive - radiative surface boundary condition that is necessary for a correct treatment of energy storage.

In this first of a two part series, we apply standard Laplace and Fourier techniques to the continuum mechanics heat equation, solving it with the correct radiative - conductive boundary conditions ~~BC's~~ obtaining an equation directly for the surface temperature anomalies in terms of the anomalous forcing. Although classical, this equation is half – not integer – ordered: the "Half - ordered Energy Balance Equation" (HEBE). A quite general consequence is that although Newton's law of cooling holds, that the heat flux across surfaces is proportional to a half (not first) ordered time derivative of the surface temperature. This implies that the surface heat flux has a long memory, that it depends on the entire previous history of the forcing, the temperature- heat flux relationship is no longer instantaneous.

We then consider the case where the Earth is periodically forced. The classical case is diurnal heat forcing; we extend this to annual conductive – radiative forcing and show that the surface thermal impedance is a complex valued quantity equal to the (complex) climate sensitivity. Using a simple semi-empirical model of the forcing, we show how ~~this~~ the HEBE can account for the phase lag between the summer maximum forcing and maximum surface temperature Earth response.

In part II, we extend all these results to spatially inhomogeneous forcing and to the full horizontally inhomogeneous problem with spatially varying specific heats, diffusivities, advection velocities, climate sensitivities. We consider the consequences for macroweather (monthly, seasonal, interannual) forecasting and climate projections.

1 Introduction

Ever since [*Budyko*, 1969] and [*Sellers*, 1969] proposed a simple model describing the exchange of energy between the earth and outer space, energy balance models (EBMs) have provided a straightforward way of understanding past, present and possible future climates. The models usually have either zero or one spatial dimension representing respectively the globally or latitudinally averaged meridional temperature distribution (for a review, see ~~e.g.~~ [*McGuffie and Henderson-Sellers*, 2005], and [*North and Kim*, 2017]).

The fundamental EBM challenge is to model the way that imbalances in incoming short wave and outgoing long wave radiation are transformed into changes in surface temperatures. In an ~~equilibrium~~ energy balanced climate state, the vertical flux imbalances are transported horizontally. Here we are primarily interested in the anomalies with respect to this state. When an external flux (forcing) is added, some of this anomalous imbalance is radiated to outer space while some is converted into sensible heat and conducted into (or out of) the subsurface. This latter flux accounts for both energy storage as well as for surface temperature changes and attendant changes in long wave emissions. EBMs avoid explicit treatment of this critical surface boundary condition, treating it phenomenologically in ways that are flawed; in this two part paper, we show how they can easily be improved with significant benefits: first, the (idealized) homogeneous case (part I), and then the general horizontally inhomogeneous (2D) case (part II).

First consider ~~zero dimensional~~ box EBMs with zero horizontal dimensions, a model of the mean Earth temperature. These are based on two distinct assumptions: a) that the rate that heat (S) is exchanged between the earth and outer space (dS/dt) is proportional to the difference between the surface temperature (T) and its long term equilibrium value (T_{eq}): $dS/dt \propto (T_{eq}-T)$ (Newton's Law of Cooling, NLC) and b) that this rate is also proportional to the rate of change of surface temperature: $dS/dt \propto dT/dt$. Budyko-Sellers models are on firmer ground: they start with the basic continuum mechanics heat equation with advective and diffusive heat transport. Yet they have no vertical coordinate, and so are unable to correctly treat the surface conduction – radiation - energy storage issue. By restricting explicit treatment of energy transport to the horizontal, they resort to the ad hoc assumption that the vertical flux imbalances are redirected horizontally and meridionally. The original Budyko-Sellers models were of time independent climate states, there was no energy storage at all: the radiative imbalances were completely redirected. While this approximation may be reasonable for these long term states, they become problematic as soon the original models were extended to include temporal variations ([*Dwyers and Petersen*, 1975]). While these time varying extensions implicitly allow for subsurface energy storage, this implicit treatment is both unnecessary and unsatisfactory.

The basic physical problem is that anomalous radiative flux imbalances partly lead to heat conduction fluxes into the subsurface and partly to changes in longwave radiative fluxes. The part conducted into the subsurface is stored and may re-emerge, possibly much later. Starting with the heat equation, realistic and mathematically correct treatments, involve the introduction of a vertical coordinate and the use of conductive - radiative surface boundary conditions (BCs). If one considers the horizontally homogeneous 3-D problem in a semi-infinite medium with these mixed BCs and linearized long wave emissions, the problem is classical and can be straightforwardly solved using Laplace and Fourier techniques. Mathematically it turns out that the key is the surface layer that defines the surface vertical temperature gradient. The influence of ~~the~~ the subsurface ~~conditions are only important~~is only over a thin layer of the order of a few diffusion depths ~~(~~where most of the energy storage occurs~~)~~. This depth depends on the specific heat per volume as well as the diffusivity and is estimated to be typically of the order of 100m for the ocean (depending its turbulent diffusivity), and less over land (see appendix A, part 2).

The exact treatment of this homogeneous problem confirms that Newton's law of cooling holds, but shows that the classical box model relation between heat flux and the surface temperature is wrong: symbolically the correct relation is $dS/dt \propto d^H T/dt^H$ with $H = 1/2$ - not the phenomenological value $H = 1$. Physically, these fractional derivatives are simply convolutions, in this case involving power law storage (hence "memories"). The corresponding half-order energy balance equation (HEBE) has qualitatively much stronger storage than the short exponential memories associated with the standard integer ordered ($H = 1$) box model derivatives.

Half-order derivatives have appeared in heat and diffusion problems since at least [*Meyer*, 1960], [*Oldham and Spanier*, 1972], [*Oldham*, 1973], and [*Oldham and Spanier*, 1974]. An equation mathematically identical to the

Field Code Changed
Field Code Changed
Field Code Changed
Field Code Changed

homogeneous *H* = 1/2 special case of the FEBE was derived by [*Oldham*, 1973] as a short time approximation to electrolyte diffusion in a spherical geometry, and [*Oldham and Spanier*, 1974] anticipate our present application by noting that half-order derivatives can be applied to "not one but an entire class of boundary value problems…". Later, half-order derivatives were developed by [*Babenko*, 1986], and have been regularly exploited in engineering heat transfer problems, see e.g. [*Sierociuk et al.*, 2013], [*Sierociuk et al.*, 2015] and references therein. The method is probably not more generally known since most applications are with fairly standard heat flux boundary conditions and other more familiar techniques can be used.

More generally, fractional derivatives and their equations [*Podlubny*, 1999], have a history going back to Leibniz in the 17th century and their development has exploded in the last decades (for books on the subject, see e.g. [*Miller and Ross*, 1993], [*Podlubny*, 1999], [*Hilfer*, 2000], [*West et al.*, 2003], [*Tarasov*, 2010], [*Klafter et al.*, 2012], [*Klafter et al.*, 2012], [*Baleanu et al.*, 2012], [*Atanackovic et al.*, 2014]).

~~Although – perhaps surprisingly - the exact problem discussed here does not appear to have been treated until now, the mathematical origin and application of half order derivatives in heat transfer problems has been known since at least [*Babenko*, 1986], [*Podlubny*, 1999], and has been regularly exploited in engineering heat transfer problems, see e.g. [*Sierociuk et al.*, 2013], [*Sierociuk et al.*, 2015] and references therein. More generally, fractional derivatives and their equations have a history going back to Leibniz in the 17th century and their development has exploded in the last decades (for books on the subject, see e.g. [*Miller and Ross*, 1993], [*Podlubny*, 1999], [*Hilfer*, 2000], [*West et al.*, 2003], [*Tarasov*, 2010], [*Klafter et al.*, 2012], [*Klafter et al.*, 2012], [*Baleanu et al.*, 2012], [*Atanackovic et al.*, 2014]).~~

Interestingly, the explicit or implicit application of fractional derivatives to model the Earth's temperature - and more recently energy budget - has several antecedents arising from the wide range spatial scaling symmetries of atmospheric fields respected by the fluid equations, models and (empirically) by the atmospheric fields themselves (see the reviews [*Lovejoy and Schertzer*, 2013], [*Lovejoy*, 2019b]). Since this includes the velocity field - whose spatial scaling implies scaling in time - it implies that power laws should be more realistic than exponentials. At first, this led to power law Climate Response Functions (CRFs), [Rypdal, 2012; van Hateren, 2013], [*Rypdal and Rypdal*, 2014], [Rypdal et al., 2015] , [Hebert, 2017], [*Hébert et al.*, 2020]. However, without truncations, pure power law CRFs lead to divergences: the "runaway Green's function effect" [*Hébert and Lovejoy*, 2015], a model unstable to infinitesimal step function increases in forcing: the Equilibrium Climate Sensitivity is infinite. These can be tamed either by a high frequency truncation ([Hebert, 2017], [*Hébert et al.*, 2020]), or by restricting forcings to only those that return to zero *[Rypdal, 2016]*, [*Myrvoll-Nilsen et al.*, 2020]. However, [*Lovejoy*, 2019b], [*Lovejoy*, 2019a], [*Lovejoy et al.*, 2020], argued that it is not the CRF itself, but rather the earth's heat storage mechanisms that respect the scaling symmetry. This hypothesis implies that the corresponding storage (the derivative term) in the energy balance equation (EBE) is of fractional rather than integer order: the fractional energy balance equation (FEBE). Denoting the order of the derivative term in the equation by *H*, it was shown empirically that if the derivative was of order $H \approx 0.4$ - 0.5 (rather than the classical EBE value $H = 1$), that it could account for both the low frequency multidecadal memory [Hebert, 2017], [*Hébert et al.*, 2020] needed for climate projections, as well as the high frequency

Field Code Changed
Formatted: Font: 10 pt
Formatted: Font: 10 pt
Field Code Changed
Field Code Changed
Field Code Changed
Formatted: Indent: First line: 0 cm
Field Code Changed
Field Code Changed
Field Code Changed
Field Code Changed
Field Code Changed
Field Code Changed
Field Code Changed
Field Code Changed
Field Code Changed
Field Code Changed

macroweather (i.e. the regime at longer time scales than the lifetime of planetary structures, here, monthly to decadal) memory needed for monthly, seasonal and annual macroweather forecasts, [Lovejoy et al., 2015], [*Del Rio Amador and Lovejoy*, 2019; 2020a; *Del Rio Amador and Lovejoy*, 2020b]. Indeed, the FEBE CRF can be used directly to make climate projections that are compatible with the Coupled Model Intercomparison Project 5 (CMIP5) multi-model ensemble mean projections but with substantially smaller uncertainties ([*Procyk et al.*, 2020]~~work in progress with R. Procyk~~). Finally, it is possible to generalize the classical (3D) continuum equation to the Fractional Heat Equation from which the (inhomogeneous, 2D) FEBE governs the surface temperature (work in progress)~~[*Lovejoy et al.*, 2020]~~.

In spite of empirical and theoretical support, the FEBE is essentially a phenomenological global model; in this paper we show how – at least for the $H = 1/2$ special case- it can be placed on a firmer theoretical basis while simultaneously extending it to two spatial dimensions. Our model is for macroweather temperature anomalies i.e. at time scales longer than the lifetimes of planetary structures, typically 10 days. Following Budyko and Sellers, the system averaged over weather scales is considered to be a continuum justifying the application of the continuum mechanics heat equation. Our starting point is thus the same as the classical EBMs: radiative, advective and conductive heat transport using the standard continuum mechanics energy equation. Also following the classical approaches, the longwave black body radiation is treated in its linearized form.

This work is divided into two parts. The first part is ~~quite~~ classical, it focuses on the homogeneous heat equation pointing out the consequence that with semi-infinite geometry (depth) and with (realistic) conductive - radiative boundary conditions, that the surface temperature satisfies the homogeneous HEBE. We relate this to the usual box models, Budyko-Sellers models, and classical diurnal heating models including the notions of thermal admittance and impedance and complex climate sensitivities useful in understanding the annual cycle. We underscore the generality of the basic (long memory) storage mechanism. The second part extends this work to the horizontal, first to the homogeneous case (but with inhomogeneous forcing, including a direct comparison with the classical latitudinally varying 1-D Budyko-Sellers model on the sphere), and then - using Babenko's method - to the general inhomogeneous case. Part II also contains several appendices that discuss empirical parameter estimates, spatial statistics useful for Empirical Orthogonal Functions and understanding the horizontal scaling properties as well as the changes needed to account for spherical geometry.

2. The Transport Equations

2.1 Conductive and advective heat fluxes

In most of what follows, the earth's spherical geometry plays no role, we use Cartesian coordinates with the z axis pointing upwards and horizontal coordinates $\underline{x} = (x,y)$ (~~see~~ however in section II.2.3 and appendix II.C of part II), we treat the latitudinally varying case on a sphere~~appendix D, part II~~). The horizontal is essentially the same the Budyko-Sellers model: horizontal diffusive and advective heat fluxes are atmospheric column averages lying on the surface ($z = 0$). What is new is ~~We consider that~~the treatment of the vertical with ~~(~~radiative and conductive~~)~~ fluxes crossing the surface either into the subsurface (downward, the negative z direction where it can propagate to $-\infty$), or to outer space (upward, $z > 0$) so that heat

Formatted: Font: Italic

Field Code Changed

Formatted: Font: Italic

is effectively stored ~~,~~ in the half-volume $(x,y,z<0)$~~and horizontal (conductive and advective) heat transport occurs on the surface and in the half-volume (x,y,z<0) respectively~~. Although ~~physically~~in principle~~,~~ this means that all~~the atmosphere and ocean are modelled~~ ~~as~~ the semi-infinite region~~s with~~ $z\leq 0$ is modelled, we will see that ultimately ~~as mentioned,~~ only the vertical surface temperature derivative is ~~ultimately~~ needed and this is well defined ~~if~~ as long as the surface layer is of the order of a few diffusion depths (tens or hundreds of meters). Later, we show that the main equations only explicitly depend on the local relaxation times and climate sensitivities, the vertical and horizontal transport details are only implicit. Finally, the fields are assumed to be in the macroweather regime i.e. they have been averaged over the weather – macroweather transition scale (about 10 days) or longer, and possibly for tens or hundreds of kilometers in space (the space-time limits are not yet clear). Since ten ~~this~~ days is the typical lifetime of planetary atmospheric structures, much of the actual turbulent atmospheric transport processes are averaged out, giving some justification to the parametrization.

We start with energy transport by diffusion: Fick's law $\underline{Q}_d=-\rho c\kappa\nabla T$ where Q_d is the diffusive heat flux vector, κ is the thermal diffusivity, ρ the density, c the specific heat, and $T(\underline{x},z,t)$ the temperature. Following standard energy balance models, we use eddy diffusivities that are different in ~~we use different~~the horizontal ("h") and vertical ("v"), ~~coefficients~~ $\kappa_h(\underline{x})$, $\kappa_v(\underline{x})$:

$$\underline{Q}_d=-\rho c\kappa_h\nabla_h T-\rho c\kappa_v\frac{\partial T}{\partial z}\hat{z};\quad \nabla_h=\frac{\partial}{\partial x}\hat{x}+\frac{\partial}{\partial y}\hat{y} \tag{1}$$

Field Code Changed

(the circonflex indicates unit vectors). To include advection, we consider the heat equation for a fluid in a horizontal velocity field $\underline{v}_h$:

Formatted: Normal

$$c\rho\frac{DT}{Dt}=-\nabla\cdot\underline{Q}_d;\quad \frac{DT}{Dt}=\frac{\partial T}{\partial t}+\underline{v}_h\cdot\nabla T \tag{2}$$

Where D/Dt is the advective derivative. The heat equation is therefore:

$$c\rho\frac{\partial T}{\partial t}=-c\rho\underline{v}_h\cdot\nabla_h T+\nabla_h\cdot\left(\rho c\kappa_h\nabla_h T\right)+\frac{\partial}{\partial z}\left(\rho c\kappa_v\frac{\partial T}{\partial z}\right) \tag{3}$$

Field Code Changed

If $c\rho$ = constant and using the continuity equation, $\nabla\cdot\left(c\rho\underline{v}_h\right)=0$ and we can write:

Field Code Changed

$$c\rho\frac{\partial T}{\partial t}=-\nabla\cdot\left(\underline{Q}_a+\underline{Q}_d\right);\qquad \underline{Q}_a=c\rho\underline{v}_h\left(T-T_0\right);\qquad \underline{Q}_d=-\rho c\kappa_h\nabla_h T-\rho c\kappa_v\frac{\partial T}{\partial z}\hat{z} \tag{4}$$

Field Code Changed

Q_a is the advective heat flux and T_0 is a constant reference temperature (it disappears when the divergence is taken). ~~Taking $v = v_h$, we made the standard assumption that the advection is in the horizontal plane.~~ This is the classical fluid heat equation, it can readily be verified that it conserves energy (integrate both sides over a volume and then use the divergence theorem). $\kappa_h(\underline{x})$, $\kappa_v(\underline{x})$, $v_h(\underline{x})$ are taken to be independent of t and z, they are part of the climate state and are empirically determined so as to reproduce the time independent climate temperature distribution. In future work, they could be given their own time-varying anomalies.

2.2 Radiative heat fluxes

At the surface, there is an incoming energy flux $R_{\downarrow}$:

$$R_{\downarrow}(\underline{x},t)=Q_0(\underline{x})+F(\underline{x},t) \tag{5}$$

Where F is the anomalous forcing and $Q_0(\underline{x})$ is the local solar radiation:

$$Q_0(\underline{x})=S(\underline{x})\left(1-\alpha(\underline{x})\right)$$

$$Q_0(\underline{x})=QS(\underline{x})a(\underline{x}) \tag{6}$$

Q is the mean top of the atmosphere flux (≈341 W/m^2), $S(\underline{x})$ is the dimensionless local solar constant with local coalbedo a ~~α~~$(\underline{x})$ (in the notation of [*North and Kim*, 2017]) and the time dependent part of the radiative balance is specified by the additional incoming energy flux, the "forcing" $F(\underline{x},t)$. Although in this paper we mostly ignore temporal albedo variations (see however section 3.3), they are important for studying temperature-albedo feedbacks and climate transitions. If needed, even if they include a (potentially nonlinear) temperature dependence, they are easy to incorporate. For example, they could be included in F by using $a(\underline{x},t)=a_0(\underline{x})+a_1(\underline{x},t,T(\underline{x},t))$ in place of a ~~α~~$(\underline{x})$ in eq. 6 and $F(\underline{x},t)=F_0(\underline{x},t)+QS(\underline{x})a_1(\underline{x},t,T(\underline{x},t))$ in place of F in eq. 5.

As usual, $F(\underline{x},t)$ includes solar, volcanic and anthropogenic forcings. However since macroweather includes random internal variability, $F(\underline{x},t)$ also includes a stochastic internal variability component. Finally, for macroweather scales shorter than a year, F could also include the annual cycle and therefore possible cyclical albedo variations due to seasonally varying cloudiness (section 3.3). Alternatively T and F can be deseasonalized in the usual way to yield standard monthly climate "normals" so that the mean anomalies are zero over the climate normal reference period.

$R_{\downarrow}(\underline{x},t)$ is partially balanced by the outgoing $R_{\uparrow}(\underline{x},t)$ that depends on the surface temperature and the effective emissivity $\varepsilon(\underline{x})$:

$$R_{\uparrow}(\underline{x},t)=\sigma\varepsilon(\underline{x})T(\underline{x},0,t)^4 \tag{7}$$

where σ is Stefan-Boltzmann constant. The $R_\downarrow$, $R_\uparrow$ imbalance drives the system, it implies that heat diffuses across the surface which is the top boundary condition needed to solve eq. 3 for $T(\underline{x},z<0,t)$:

$$\left.\left(\sigma\varepsilon\left(\underline{x}\right)T\left(\underline{x},z,t\right)^4+\rho c\kappa_v\left(\underline{x}\right)\frac{\partial T\left(\underline{x},z,t\right)}{\partial z}\right)\right|_{z=0}=Q_0\left(\underline{x}\right)+F\left(\underline{x},t\right) \qquad (8)$$

The derivative term $\rho c\kappa_v \partial T/\partial z\big|_{z=0}=Q_s$ is the conductive (sensible) heat flux across the surface, into the earth, see fig. 1. The radiative fluxes thus impose a "mixed" conductive - radiative boundary condition involving both T and $\partial T/\partial z$ (they are a special case of "Robin" boundary conditions [*Hahn and Ozisk*, 2012]). If we add the initial condition $T\left(\underline{x},z,t=0\right)=0$ (or later, $T\left(\underline{x},z,t=-\infty\right)=0$) and the Dirichlet boundary condition at great depth $T\left(\underline{x},z=-\infty,t\right)=0$ and assume that the system is periodic or infinite in the horizontal, then, in principle, these are enough to determine the temperature for $T(\underline{x},z<0,t>0)$ (or eventually, $T\left(\underline{x},z,t=-\infty\right)=0$). Instead of avoiding this conductive - radiative BC below we show how it directly yields an equation for the surface temperature.

Field Code Changed

2.3 The Climatological and anomaly fields

Let us now decompose the heat flux and temperature into time independent (climatological) and time varying (anomaly) components: Q_c, T_c and Q, T. As usual, we linearize the outgoing black body radiation, although we do so around the spatially varying surface temperature $T_c(\underline{x},z=0)$ (i.e. not the global average temperature) which yields spatially varying coefficients:

$$R_\uparrow\left(T_c\left(\underline{x},0\right)+T\left(\underline{x},0,t\right)\right)\approx R_\uparrow\left(T_c\left(\underline{x},0\right)\right)+\frac{T\left(\underline{x},0,t\right)}{s\left(\underline{x}\right)} \qquad (9)$$

Field Code Changed

(T_c+T is the actual temperature), with climate sensitivity:

$$s\left(\underline{x}\right)=\frac{1}{4\sigma\varepsilon\left(\underline{x}\right)T_c\left(\underline{x},0\right)^3} \qquad (10)$$

Field Code Changed

~~The linearization is accurate s~~Since typical macroweather temperature anomalies are only a few degrees, the black body emission is quite linear with the temperature anomaly. However due to feedbacks, ~~this formula for~~ the proportionality coefficient – the climate sensitivity ~~–~~ – as estimated in eq. 10 is not accurate; below, we simply consider ~~sr λ((~~$\underline{x}$) to be an empirically determined function of position.

Formatted: Font: Italic

The incoming radiation at the location $\underline{x}$ drives the system. The radiative imbalance ΔR going into the subsurface is therefore equal to the conductive flux Q_s into the surface; it specifies the conductive-radiative surface boundary condition for T_c and the anomalies T:

$$\Delta R = Q_s; \qquad \Delta R = R_{\downarrow} - R_{\uparrow}; \qquad Q_s = -Q_{d,z} \tag{11}$$

Where $Q_{d,z}$ is the (upward) vertical component of the heat flux at the surface given by Fick's law: $Q_{d,z} = -\rho c \kappa_v \left.\frac{\partial T}{\partial z}\right|_{z=0}$. The conductive - radiative surface boundary conditions for the time independent climate and anomaly temperatures is therefore:

$$\left.\left(R_{\uparrow}\left(T_c\left(\underline{x},z\right)\right) + \rho c \kappa_v \frac{\partial T_c\left(\underline{x},z\right)}{\partial z} \right)\right|_{z=0} = Q_0\left(\underline{x}\right)$$

$$\left.\left(\frac{T\left(\underline{x},z,t\right)}{s} + \rho c \kappa_v \frac{\partial T\left(\underline{x},z,t\right)}{\partial z} \right)\right|_{z=0} = F\left(\underline{x},t\right) \tag{12}$$

s~~λ~~, ρ, c and κ are all presumed to be functions of $\underline{x}$. Note: the conductive heat flux is a sensible heat flux; the boundary condition involves its vertical component that represents heat stored in the subsurface. While eqs. 11, 12 involve the vertical temperature derivative at the surface (i.e. over an infinitesimal layer), $l_v = s$~~λ~~$\rho c \kappa_v$ defines the diffusion depth (typically ≈ 10 - 100m in thickness, see part II); so that physically the model need only be realistic over this fairly shallow depth where most of the heat is stored.

Now, in the temperature eq. 3, replace T by T_c+T. The equation for the time independent climate part is:

$$c\rho \frac{\partial T_c}{\partial t} = 0 = -\rho c \underline{v}_h \cdot \nabla_h T_c + \nabla_h \cdot \left(\rho c \kappa_h \nabla_h T_c\right) + \frac{\partial}{\partial z}\left(\rho c \kappa_v \frac{\partial T_c}{\partial z}\right) \tag{13}$$

and for the time-varying anomalies:

$$c\rho \frac{\partial T}{\partial t} = -\rho c \underline{v}_h \cdot \nabla_h T + \nabla_h \cdot \left(\rho c \kappa_h \nabla_h T\right) + \frac{\partial}{\partial z}\left(\rho c \kappa_v \frac{\partial T}{\partial z}\right) \tag{14}$$

These equations must now be solved using boundary conditions eqs. 11, 12 for respectively T_c, T and $T_c = T = 0$ at $z = -\infty$ (all t), and $T\left(\underline{x},z,t=0\right) = 0$ (or see below, $T\left(\underline{x},z,t=-\infty\right) = 0$).

The separation into one equation for the time invariant climate state and another for the time-varying anomalies is done for convenience. As long as the outgoing long wave radiation is approximately linear over the whole range of temperatures (as is commonly assumed in EBMs), this division involves no anomaly smallness assumptions nor assumptions concerning their time averages; the choice of the reference climate depends on the application. Below, we choose anomalies defined in the standard way (although not necessarily with the annual cycle removed, section 3.3), this is adequate for monthly and seasonal forecasts as well as 21st century climate projections. However, a different choice might be more appropriate for modelling transitions between different climates including possible chaotic behaviours.

2.4 The climatological temperature distribution and Budyko-Sellers models

In order to simplify the problem, starting with [*Budyko*, 1969] and [*Sellers*, 1969], the usual approach to obtaining T_c is somewhat different. First, the climatological temperature field is only defined at $z = 0$, i.e. $T_c(\underline{x}) = T_c(\underline{x},0)$. Without a vertical coordinate, the climatological radiative imbalance $Q_0(\underline{x}) - R_\uparrow(T_c(\underline{x}))$ no longer forces the system via the vertical surface derivative (eq. 11), instead the imbalance is conventionally redirected in the meridional direction away from the equator (fig. 2).

To see how this works, return to eq. 4 for the climatological component and put $\frac{\partial}{\partial z} = 0$:

$$\underline{Q}_c(\underline{x}) = \underline{Q}_{c,a}(\underline{x}) + \underline{Q}_{c,d}(\underline{x}) + sign(y)\left(Q_0(\underline{x}) - R_\uparrow\left(T_c(\underline{x})\right)\right)\hat{y} \qquad (15)$$

(in this formulation, one usually uses the latitude angle instead of the meridional coordinate y see part II, section 2.3~~appendix D~~). The direction of the redirected vertical flux is always away from the equator ($y = 0$; hence $sign(y)$), in any event, zonal fluxes will cancel when averaged over latitudinal bands.

The usual Budyko-Sellers type models then average $\underline{Q}_c$ over lines of constant latitude yielding a 1-D model:

$$\overline{\underline{Q}}_c(y) = \left(\rho c\left(v_y \overline{T}_c - \kappa_h \frac{\partial \overline{T}_c}{\partial y}\right) + sign(y)\left(Q_0(y) - R_\uparrow\left(\overline{T}_c\right)\right)\right)\hat{y} \qquad (16)$$

(overbar indicates averaging over all longitudes, x).

In the more popular Seller's version, the basic horizontal transport is due to the eddy thermal diffusivity, the κ_h term. There may also be a small advection velocity v but it is not considered to be a true physical velocity but only an ad hoc parameter needed to prevent κ_h from being negative (~~[*Sellers*, 1969],~~ [*Sellers*, 1969]), the standard presentation (~~see also~~ [*North et al.*, 1981],) avoids the problem by using the diffusivity, see section 3.1). The horizontal eddy diffusivity κ_h is often taken as the sum of contributions from water, water vapor and air. In the pure Budyko version, there is no eddy diffusivity, the heat flux is assumed to be proportional to the temperature difference with respect to a reference (e.g. mean) value; $(\underline{Q})_y \propto (T - T_0)$.

Comparing this with eq. 4 for Q_a, we see that this implies that Budyko horizontal heat fluxes are purely advective.

The final step to obtaining the energy equation is to take the divergence:

Field Code Changed

$$\nabla \cdot \underline{\overline{Q}}_c = \frac{\partial \overline{Q}_c}{\partial y} = -\rho c \frac{\partial \overline{T}_c}{\partial t} \tag{17}$$

Budyko and Sellers only considered the time independent case and obtained:

$$\frac{\partial \underline{\overline{Q}}_c(y)}{\partial y} = 0$$
$$\underline{\overline{Q}}_c(y) = const \tag{18}$$

By appropriately choosing a reference temperature (usually the global average), the constant can be adjusted for convenience. Somewhat later, [*Dwyers and Petersen*, 1975] considered the time independent case (eq. 17) which is second order in *y*. Subsequently the model has been widely used for studying different past and future climates and the corresponding transitions. Note that the $\rho c \frac{\partial \overline{T}_c}{\partial t}$ term corresponds to energy storage; in the time independent case there is no storage.

3. The classical origin of the fractional operators: conductive-radiative boundary conditions in a semi-infinite domain

3.1 The zero dimensional homogeneous heat equation

3.1.1 The ~~nondimensional anomaly equations~~key parameters

Formatted: Heading 3

No matter how the climate temperature equation is solved, the equation for the time dependent anomaly temperature remains eq. 14. We now rewrite it in a way that brings out the critical mathematical properties. Since ρc and κ_v are only functions of $\underline{x}$, eq. 14 can be rewritten:

$$\left(\frac{\partial}{\partial t} - \kappa_v \frac{\partial^2}{\partial z^2}\right) T = -\underline{v} \cdot \nabla_h T + \kappa_h \nabla_h^2 T; \qquad \underline{v} = \underline{v}_h - \underline{v}_d; \quad \underline{v}_d = \frac{1}{\rho c} \nabla_h \left(\kappa_h \rho c\right) \tag{19}$$

Where we have defined an effective diffusion velocity $\underline{v}_d$ and effective advection velocity $\underline{v}$. Eq. 19 must be solved with the boundary conditions in eq. 12.

The roles of the various terms are clearer if the equation is nondimensionalized. For this, we note that if we include the boundary conditions, the anomaly temperature is entirely determined by the dimensional quantities κ, *s* ~~λ~~, ρ and *c*. From these, there exists a unique dimensional combination $\tau(\underline{x})$ with dimensions of time, we will see that this controls the relaxation of the system back to thermodynamic equilibrium, it is a “relaxation time”. Using κ_v yields:

$$\tau=\kappa_v\left(\rho c\lambda\right)^2; \qquad l_v=\left(\tau\kappa_v\right)^{1/2}=\kappa_v\rho c\lambda \tag{20}$$

where $l_v(\underline{x})$ is the vertical relaxation length of the surface energy balance processes. In the next section, ~~part II, table 1and section 3.3~~ we give some rough parameter estimates. We may also define the horizontal diffusion length l_h, speed V, nondimensional (square root) diffusivity ratio β and nondimensional advection vector $\underline{\alpha}$:

$$\underline{\alpha}=\frac{\underline{v}}{V}; \quad V=\frac{l_h}{\tau}; \quad l_h=\left(\tau\kappa_h\right)^{1/2}=\beta\kappa_h\rho cs; \quad \beta=\left(\frac{\kappa_v}{\kappa_h}\right)^{1/2} \tag{21}$$

The continuity equation for energy becomes $\nabla\cdot\left(\frac{\beta}{s}\underline{\alpha}\right)=0$. For global (zero dimensional) models, τ has been estimated as 2 – 5 years which is comparable to the classical exponential relaxation time scales mentioned above ([*Hebert*, 2017], [*Procyk et al.*, 2020]) ~~[Lovejoy et al., 2018]work in progress with R. Procyk),~~ *and in section 3.3 we estimate* $\tau\approx$ *2.75 years.*

In order to understand the classical origin of fractional derivatives, it is helpful to consider the homogeneous Seller-type (diffusive transport) heat equation where τ, l_v and l_h are constants and can thus be used to nondimensionalize the operators. *t* is therefore in ~~units~~ terms of relaxation times, $\underline{x}$ in terms of diffusion lengths l_h and z in ~~units~~ terms of diffusion depths l_v. By taking *s* ~~λ~~ = 1, we effectively have a forcing *F* with dimensions of temperature. In part I, we consider only the “zero dimensional” equation where the “zero” refers to the number of horizontal dimensions (i.e. only vertical, *z* and time *t*). ~~We use the following notation: the first argument is *t* then horizontal space, then a semicolon followed by the depth *z*. Circonflexes denote Laplace (time) and Laplace-Fourier (time and horizontal space) transforms.~~

With these dimensional parameters, we can write the equations as:

$$\underline{Q}_h=-\frac{l_h}{s}\nabla_h T+\frac{\underline{\alpha}}{s}\left(T-T_0\right); \quad Q_z=-\frac{l_v}{s}\frac{\partial T}{\partial z} \tag{22}$$

Formatted: Font: Italic

Commented [SL1]: Comment on balance versus equilibrium somewhere

Formatted: Font: Symbol

Field Code Changed

Field Code Changed

Commented [SL2]: check

Field Code Changed

$$\tau\frac{\partial T}{\partial t}=-\zeta T-l_v s\frac{\partial Q_z}{\partial z};\qquad \zeta=l_h s\nabla_h\cdot\left(\frac{\underline{\alpha}-l_h\nabla_h}{s}\right)\qquad \zeta T=l_h s\nabla_h\cdot\underline{Q}_h \tag{23}$$

Where ζ is the dimensionless horizontal transport operator. We have ignored the reference temperature T_0 by either taking it to be zero or by assuming $\nabla_h\cdot\left(s^{-1}\underline{\alpha}\right)=0$ which is true if β = constant.

If the advection is chosen appropriately, then we may write the horizontal transport operator in the form:

$$\zeta=-s\nabla_h\cdot\left(\frac{l_h}{s}\right)\nabla_h;\quad \underline{\alpha}=s\nabla_h\left(\frac{l_h}{s}\right) \tag{24}$$

This is convenient for comparing the HEBE with the 1-D B-S equations on a sphere in part II section 2.3, and avoids the unphysical negative diffusivities reported by Sellers.

$$\zeta=-sR\nabla_h\cdot D_F\nabla_h;\quad D_F=\frac{l_h\left(\underline{x}\right)}{Rs\left(\underline{x}\right)}=\kappa_h\frac{\beta\rho c}{R} \tag{25}$$

Where D_F is a HEBE diffusion constant per radian and R is the earth radius.

3.1.2 Parameter estimates

Before proceeding, it is useful to get a feel for typical values of the parameters in the equations. In part II, section 2.3 and appendix II.A we combine these parameter estimates with analyses of monthly space-time temperature anomalies in order to analyse which terms in the equations are dominant at different time scales, the following are order of magnitude estimates.

A key parameter is the horizontal diffusion length $l_h=\left(\tau\kappa_h\right)^{1/2}=\beta\kappa_h\rho cs$ (eq. 21). It can be estimated from the horizontal diffusivity κ_h, and the volumetric specific heat ρc, the sensitivity s, and vertical diffusivity κ_v, or alternatively from κ_h and τ.

a) Volumetric specific heat ρc: Ocean and land values are similar: water and soil: respectively $\rho c \approx 4\text{x}10^6$, $\approx 1\text{x}10^6$ J/(m^{3}K).

b) Climate sensitivity s: Using the CO_2 doubling value 3±1.5K, 90% confidence interval and 3.71 W/m^2 for CO_2 doubling, the global mean value is $s \approx 0.8\pm0.4$ K/W/m^2, with regional values a factor of ≈ 2 higher or lower (IPCC AR5) yielding $\rho cs \approx 3\text{x}10^6$ s/m.

Formatted: Equation
Field Code Changed
Formatted: Font: Symbol
Formatted: Font: Italic
Field Code Changed
Formatted: Equation
Field Code Changed
Formatted: Equation
Field Code Changed
Formatted: Font: Not Italic
Formatted: Font: Italic
Formatted: Font: Not Italic
Formatted: Font: Not Italic
Formatted: Font: Cambria, English (UK)
Formatted: Heading 3, Indent: First line: 0 cm
Field Code Changed

c) Relaxation time τ: Based on responses to anthropogenic forcings since 1880, [*Hebert*, 2017], [*Hébert et al.*, 2020; *Procyk et al.*, 2020], give the global estimate $\tau \approx 10^8$s ($\approx$ 4 years). This is comparable to the relaxation times for global box models.

d) Horizontal Diffusivity κ_h: As detailed in Part II, section 2.3, [*North et al.*, 1981], [*North and Kim*, 2017] uses a diffusion constant per radian analogous to D_F eq. 25 combined with global scale climatological forcing and temperature data to estimate a global thermal conductivity $K = 4.1\text{x}10^6$ Wm^{-1}K^{-1} from which we estimate the horizontal (eddy) diffusivity as $\kappa_h = K/(\rho c) \approx 1$ m^2/s. [*Sellers*, 1969] gives values about 100 times larger for the ocean.

e) Vertical diffusivity κ_v: The vertical diffusivity is not used in the usual energy balance models, however in climate models, ocean values of $\kappa_v \approx 10^{-4}$ m^2/s are typical [*Houghton et al.*, 2001]. For soil, rough values are $\kappa_v \approx 10^{-6}$ m^2/s (wet) and $\kappa_v \approx 10^{-7}$ m^2/s (dry) are measured in [*Márquez et al.*, 2016]. Alternatively we can use $\kappa_v = \tau/(\rho cs)^2$ and the global estimates of $\tau \approx 10^8$s to obtain $\kappa_v \approx 10^{-5}$ m^2/s which is close to the model values.

f) Diffusion depth l_v: Using $l_v = \kappa_v \rho cs$ we find for the ocean and soils respectively $l_v \approx 300$m, $\approx 3 - 10$m. Using the global estimates $\kappa_v \approx 10^{-5} - 10^{-4}$ m^2/s yields $l_v \approx 30 - 100$m.

g) Diffusion length l_h: Using $l_h = (\kappa_h \kappa_v)^{1/2} \rho cs$, $l_h \approx 30$ km (ocean), 3 km (land). Using $l_h = (\tau \kappa_h)^{1/2}$ and $\kappa_h \approx 1$ m^2/s yields a global estimate $l_h \approx 10$ km.

h) Diffusive based velocity parameter V: $V \approx l_h/\tau \approx 3\text{x}\,10^{-3} - 3\text{x}\,10^{-4}$ m/s.

i) Nondimensional advection velocity α: The best transport model – diffusive, advective – or both - is not clear, therefore let us estimate the magnitude of the advective velocity v assuming that it dominates the transport. The appropriate value is not obvious since most models just use eddy diffusivity – not advection - for transport. One way - for example [Warren and Schneider, 1979] - is to note that typical meridional heat fluxes are of the order of 100 W/m^2 over meridional bands whose temperature gradients ΔT are several degrees K. If this heat is transported by advection, it implies $v \approx Q_a/(\rho c \Delta T) \approx 10^{-5} - 10^{-4}$m/s (eq. 4), hence, using $V \approx 10^{-4}$m/s (above), we find $\alpha = v/V \approx 0.1 - 1$.

3.1.3 The nondimensional equations

With z, t in dimensionless form, the homogeneous zero dimensional heat equation is:

$$\left(\frac{\partial}{\partial t} - \frac{\partial^2}{\partial z^2}\right) T(t;z) = 0 \qquad (26\cancel{23})$$

We use the following notation: the first argument is t then horizontal space, then a semicolon followed by the depth z. ~~Circonflexes denote Laplace (time) and Laplace-Fourier (time and horizontal space) transforms.~~ The transfer is confined to the

Formatted: Font: Italic

Formatted: Font: Italic

Field Code Changed

Field Code Changed

Field Code Changed

Formatted: Indent: First line: 1 cm

Formatted: Heading 3

Field Code Changed

semi-infinite region $z \le 0$ with boundary conditions: $T(t;-\infty)=0$ (bottom). ~~At the top (z = 0), t~~The system is forced by the conductive - radiative surface boundary condition at z = 0 (the top):

$$\left.\frac{\partial T}{\partial z}\right|_{z=0}+T(t;0)=F(t) \qquad (27~~24~~)$$

For initial conditions, in this section, the forcing is "turned on" at $t>0$ (i.e. $T(t;z)=0$ for $t \le 0$), allowing use of Laplace transforms (see section 3.3 for Fourier methods).

Performing a Laplace transform ("L.T.") of the heat equation we obtain:

$$\left(\frac{d^2}{dz^2}-p\right)\hat{T}(p;z)=-T(0;z)=0 \qquad (28~~25~~)$$

Where the circonflex indicates the Laplace transform in time (with conjugate variable p). Solving:

$$\hat{T}(p;z)=A(p)e^{\sqrt{p}z}+B(p)e^{-\sqrt{p}z} \qquad (29~~26~~)$$

Where A, B are determined by the BC's. Since we require the temperature at depth ($z<<0$) to remain finite, we must have B = 0, hence:

$$\hat{T}(p;z)=A(p)e^{\sqrt{p}z} \qquad (30~~27~~)$$

To determine $A(p)$, we Laplace transform the surface boundary condition:

$$\left.\frac{d\hat{T}}{dz}\right|_{z=0}+\hat{T}(p;0)=\hat{F}(p); \qquad F(t)\overset{L.T.}{\leftrightarrow}\hat{F}(p) \qquad (31~~28~~)$$

yielding:

$$A(p)=\frac{\hat{F}(p)}{1+\sqrt{p}} \qquad (32~~29~~)$$

It is more convenient to determine the response $G_\delta(t;z)$ to the impulse forcing $F(t)=\delta(t)$; the impulse Green's function.

Using eq. ~~26~~30, ~~28~~ 32 we obtain:

$$\widehat{G_\delta}\left(p;z\right)=\frac{e^{\sqrt{p}z}}{1+\sqrt{p}};\qquad F\left(t\right)=\delta\left(t\right)\overset{L.T.}{\leftrightarrow}\hat{F}\left(p\right)=1$$

(33~~30~~)

The above assumes that the subsurface is infinitely deep. If instead it has a finite thickness L, and we take the bottom boundary condition as $T\left(t;-L\right)=0$ (rather than $T\left(t;-\infty\right)=0$), then $B\left(p\right)\approx O\left(e^{-2L\sqrt{p}}\right)$ and $\widehat{G_\delta}\left(p;0\right)=\frac{1}{1+\sqrt{p}}-\frac{2e^{-2L\sqrt{p}}\sqrt{p}}{\left(1+\sqrt{p}\right)^2}+O\left(e^{-4L\sqrt{p}}\right)$ so that the influence of the bottom condition on the surface decreases exponentially fast as its depth L increases. Physically, as long as the depth is of the order of a few diffusion depths (estimated as ≈ 100m in the ocean, ≈ 10m for land), the semi-infinite geometry assumption is unimportant. In the following, we therefore ignore any finite thickness corrections.

Taking the inverse Laplace transform of eq. ~~29~~ 33 we obtain the integral representation:

$$G_\delta\left(t;z\right)=\frac{1}{\pi}\int_{-\infty}^{\infty}\frac{\zeta e^{-\zeta^2 t}}{1+\zeta^2}\left(-\sin z\zeta+\zeta\cos z\zeta\right)d\zeta\overset{L.T.}{\leftrightarrow}\widehat{G_\delta}\left(p;z\right)=\frac{e^{\sqrt{p}z}}{1+\sqrt{p}}$$

(34~~31~~)

($z\leq 0$; where we have used contour integration on the Bromwich integral).

3.1.~~2~~ 4 The surface temperature

For the surface, the integral (eq. ~~30~~34) can be expressed with the help of higher mathematical functions:

$$G_{0,1/2}\left(t;0\right)=G_\delta\left(t;0\right)=\frac{1}{\sqrt{\pi t}}-e^t\,erfc\sqrt{t}=\overset{L.T.}{\leftrightarrow}\widehat{G}_{0,1/2}\left(p;0\right)=\widehat{G_\delta}\left(p;0\right)=\frac{1}{1+\sqrt{p}};\quad erfc\left(z\right)=\frac{2}{\sqrt{\pi}}\int_z^\infty e^{-s^2}ds$$

(35~~32~~)

$G_\delta\left(t;0\right)$ is the H = 1/2 impulse response Green's function,~~Mittag-Leffler function (sometimes called a "generalized exponential", ~~ also denoted $G_{0,1/2}$, the "0" for 0th integral of the impulse, the "1/2" for the order of the derivative for its equation, see below), it is sometimes called a "generalized exponential", itself expressed in terms of Mittag-Leffler functions.

For long times after an impulse, the response $G_\delta\left(t;0\right)\approx t^{-3/2}$ (t≫1, eq. ~~33~~ 37 below) so that the system rapidly returns to its original temperature. It is more interesting to consider the response of the system to a step (Heaviside) forcing $F(t)=\Theta(t)$ (=

Field Code Changed

Formatted: Font: Not Italic

Field Code Changed

Formatted: Font: Not Italic

Field Code Changed

Commented [SL3]: G is the Green's function expressed in terms of ML functions…

1, for $t>0$, = 0 for $t\le 0$) after which the system eventually attains a new thermodynamic equilibrium. Since $\Theta(t)=\int_0^t \delta(u)\,du$, we have the step response $G_\Theta(t;z)=\int_0^t G_\delta(u;z)\,du$ (also denoted $G_{1,1/2}$, eq. ~~32~~36), and $G_\Theta(t;0)\approx 1-\frac{1}{\sqrt{\pi t}}$ (eq. ~~33~~37) i.e., a slow power law approach to thermodynamic equilibrium. Figs. 3, 4 show this at different times and depths. With unit step forcing, the boundary condition (eq. ~~23~~27) indicates that the fraction of the heat flux that is transformed into long wave radiation is equal to the temperature with unit forcing. Therefore the $z = 0$ curve in fig. 3 shows that at first, all the forcing flux is conducted into the subsurface, but that this fraction rapidly vanishes as the surface approaches equilibrium. At equilibrium, the temperature has increased so that the short and long wave fluxes are once again in balance and there is no longer any conductive flux.

For future reference, we give the corresponding step response $G_{1,1/2} = G_\Theta$ which is the integral of $G_{0,1/2}$ that describes relaxation to energy balance (for this model, thermodynamic equilibrium) when F is a step function. Similarly, the ramp (linear forcing) response $G_{2,1/2}$ is the integral of the step response, the second integral of the Dirac:

$$G_{1,1/2}(t)=\int_0^t G_{0,1/2}(s)\,ds=1-e^t\,\mathrm{erfc}\left(t^{1/2}\right)\quad G_{1,1/2}(t)=G_{\Theta,1/2}(t)=\int_0^t G_{0,1/2}(s)\,ds=1-e^t\,\mathrm{erfc}\left(t^{1/2}\right) \qquad (36~~33~~)$$

$$G_{2,1/2}(t)=\int_0^t G_{1,1/2}(s)\,ds=1-2\sqrt{\frac{t}{\pi}}+t-e^t\,\mathrm{erfc}\left(t^{1/2}\right)$$

For small and large t:

$$G_{0,1/2}(t)=G_{\delta,1/2}(t)\approx \begin{cases} \frac{1}{\sqrt{\pi t}}-1+2\sqrt{\frac{t}{\pi}}-t+\frac{4}{3}t\sqrt{\frac{t}{\pi}}-\dots & t<<1 \\ \frac{1}{2t\sqrt{\pi t}}-\frac{3}{4}\frac{1}{t^2\sqrt{\pi t}}+\dots & t>>1 \end{cases} \qquad (37~~34~~)$$

$$G_{1,1/2}(t)=G_{\Theta,1/2}(t)\approx \begin{cases} 2\sqrt{\frac{t}{\pi}}-t+\frac{4}{3}\frac{t^{3/2}}{\sqrt{\pi}}-\dots & t<<1 \\ 1-\frac{1}{\sqrt{\pi t}}+\frac{1}{2t\sqrt{\pi t}}-\dots & t>>1 \end{cases}$$

Field Code Changed

Field Code Changed

Commented [SL4]: Thermal equil. Or just "equil."?

Field Code Changed

Field Code Changed

$$G_{2,1/2}(t) \approx \begin{cases} \frac{4}{3}t\sqrt{\frac{t}{\pi}} - \frac{t^2}{2} + \frac{8}{15}t^2\sqrt{\frac{t}{\pi}} - \frac{t^3}{6} + \ldots & t << 1 \\ t + 1 - 2\sqrt{\frac{t}{\pi}} - \frac{1}{\sqrt{\pi t}} + \frac{1}{2t\sqrt{\pi t}} - \ldots & t >> 1 \end{cases}$$

The asymptotic equation for the step response ($G_{1,1/2}$) shows that ~~thermodynamic~~ equilibrium is approached slowly: as $t^{-\cancel{1}\underline{3}/2}$. It is this power law step response (~~with~~ empirical<u>ly with</u> ~~exponent~~ $\approx t^{-\cancel{0}1.5}$ ~~±0.2~~) that was discovered semi-empirically by [*Hebert*, 2017], [*Lovejoy et al.*, 2017]<u>,</u> [*Lovejoy et al.*, 2020] and was successfully used for climate projections through to 2100 [*Hébert et al.*, 2020]. Similarly, $\approx t^{-0.4}$ behaviour was used for macroweather (monthly, seasonal) forecasts close to the short time $t^{-1/2}$ expansion [*Lovejoy et al.*, 2015], [*Del Rio Amador and Lovejoy*, 2019].

If we take this as a model of the global temperature, we can use the ramp Green's function to estimate the ratio of the equilibrium climate response (ECS) to the transient climate response (TCR), we find: $TCR / ECS = G_{2,1/2}(\Delta t) / \Delta t$ where Δt is the nondimensional time over which (for the TCR) the linear forcing acts. Using τ = 4 years, and the standard Δt = 70 years for the TCR ramp, we find the plausible ratio TCR/ECS ≈ 0.78.

3.1.~~3~~ <u>5</u> Comparison with temperature forcing boundary conditions

It is interesting to compare this with the classical surface boundary condition when the system is forced by the surface temperature, an alternative – periodic surface heat forcing - is discussed in section 3.3. If the surface (z = 0) boundary condition $T_{force}(t)$ is imposed:

$$T_{temp}(t;0) = T_{force}(t) \qquad (\underline{38}\cancel{35})$$

then there will be vertical surface gradients that imply that heat is conducted through the surface. To obtain the impulse response Green's function, we take $T_{force}(t) = \delta(t)$ and repeating the Laplace transform approach, we obtain $A(p)$ = 1 (eq. ~~27~~ <u>31</u> with no derivative term). This yields the following Laplace Transform pairs for the impulse and step Green's function:

$$\begin{aligned} G_{temp,\delta}(t;z) &= \frac{ze^{-z^2 t}}{2\sqrt{\pi t^3}} \overset{L.T.}{\leftrightarrow} \hat{G}_{temp,\delta}(p;z) = e^{\sqrt{p}z} \\ G_{temp,\Theta}(t;z) &= 1 + erf\left(\frac{z}{2\sqrt{t}}\right) \overset{L.T.}{\leftrightarrow} \hat{G}_{temp,\delta}(p;z) = \frac{e^{\sqrt{p}z}}{p} \end{aligned} \qquad (\underline{39}\cancel{36})$$

Field Code Changed

Formatted: Font: Italic

Formatted: Superscript

Formatted: Superscript

Formatted: Superscript

Formatted: Superscript

In the context of the Earth's temperature, using heat conduction, (not temperature) boundary conditions, [*Brunt*, 1932] obtained the analogous classical formula noting that "this solution is given in any textbook".

These classical Green's functions provide useful comparisons with the conductive - radiative BC's. For example, integrating eq. ~~30~~ 34 with respect to time and simplifying, we obtain:

$$\Delta G_{\Theta}(t;z) = G_{\Theta,temp}(t;z) - G_{\Theta}(t;z) = \frac{1}{\pi}\int_{-\infty}^{\infty}\frac{e^{-\zeta^2 t}e^{iz\zeta}d\zeta}{(1+i\zeta)}; \qquad \begin{matrix} t \ge 0 \\ z \le 0 \end{matrix} \qquad (40~~37~~)$$

Since the step response G_Θ describes the approach to thermodynamic equilibrium, $\Delta G_{\Theta}(t;z)$ (fig. 5) succinctly expresses the differences between the temperature and conductive - radiative forced boundary conditions. The leading large t approximation to the integral in eq. ~~36~~ 40 is $\Delta G_{\Theta}(t;z) \approx e^{-\frac{z^2}{4t}} / \sqrt{\pi t}$ so that as the figure shows, although they both slowly approach each other and eventually attain thermodynamic equilibrium, that the differences are important (especially in the diffusion layer, $z \approx <1$) and they decay very slowly with time and depth, we discuss this further in section 3.3.

3.1.~~4~~ 6 Surface temperatures, Fractional derivatives and the HEBE

Let us now introduce the H^{th} order fractional derivative ${}_{t_0}D_t^H$ to represent the fractional derivative order H of an arbitrary function f over the domain from t_0 to t:

$${}_{t_0}D_t^H f = \frac{1}{\Gamma(1-H)}\int_{t_0}^{t}(t-s)^{-H} f'(s)ds; \qquad f'(s) = \frac{df}{ds}; \qquad 0 \le H \le 1 \qquad (41~~38~~)$$

Fractional derivatives of order H are most commonly interpreted in the Riemann-Liouville or Caputo sense ([*Podlubny*, 1999]) defined by $t_0 = 0$ in the above (for $H\le 1$, the main case of interest here, the distinction is not important). Fractional derivatives and their inverses, fractional integrals (with $H<0$) are thus power law weighted convolutions; fractional integrals of noises are often associated with long memory stochastic processes. Many studies have found long memories in macroweather ([*Blender and Fraedrich*, 2003], [*Bunde et al.*, 2005], [*Rybski et al.*, 2006], [*Varotsos et al.*, 2013]) and a Gaussian noise forced model (fractional Gaussian noise) have been proposed as models of internally forced (macroweather) temperature variability ([*Rypdal and Rypdal*, 2014], [*Lovejoy*, 2015], [*Del Rio Amador and Lovejoy*, 2019], [*Del Rio Amador and Lovejoy*, 2020b]). ~~This~~ Most ~~Riemann-Liouville (R-L) formulation~~applications of fractional derivatives ~~is~~ are ~~useful~~ for forcings that start at $t = t_0 = 0$ (i.e. $F = 0$ for $t\le 0$), see [*Miller and Ross*, 1993], ~~[*Podlubny*, 1999].~~ [*Podlubny*, 1999] and are ~~The R-L definition is~~ convenient for deterministic forcings, however ~~it~~ they singularizes $t = 0$ whereas we often wish to include periodic or

Formatted: Font: Italic

Formatted: Font: Italic

Formatted: Subscript

statistically stationary internal stochastic forcings so that $F(-\infty)=0$ (or in the periodic case, the mean over a cycle = 0) is more convenient, in which case we take $t_0=-\infty$ and hence $T_s(t=-\infty)$=0 (or periodic). As discussed in [*Lovejoy*, 2019a], this corresponds to the semi-infinite range "Weyl" fractional derivative. Deterministic, stochastic and periodic forcings can be combined into a single framework simply by using the Weyl derivatives with for example the deterministic part of the forcing starting at t = 0 (with the deterministic $F(t)$ = 0 for $t\le 0$) and the stochastic forcing at $t=-\infty$. These ~~R-L and Weyl~~ fractional derivatives have the following transformation properties:

$$\begin{aligned} {}_0D_t^H &\overset{L.T.}{\leftrightarrow} p^H \\ {}_{-\infty}D_t^H &\overset{F.T.}{\leftrightarrow} (i\omega)^H \end{aligned}$$ (42~~39~~)

Where ω is the Fourier conjugate to t, (see e.g. [*Miller and Ross*, 1993], [*Podlubny*, 1999]). In this part I (except for section 3.3), we consider deterministic forcings, putting t_0 = 0 in eq. ~~37~~41, we using ${}_0D_t^{1/2} \overset{L.T.}{\leftrightarrow} \sqrt{p}$ (H = 1/2 in eq. ~~38~~42), we obtain the HEBE for the surface temperature Green's function:

$$\left({}_0D_t^{1/2}+1\right)G_\delta(t;0)=\delta(t) \overset{(L.T.)}{\leftrightarrow} \left(\sqrt{p}+1\right)\hat{G}_\delta(p;0)=1$$ (43~~40~~)

This proves that the surface temperatures implied by the heat equation with conductive - radiative boundary conditions can be determined directly from the HEBE using the same Green's function. For the dimensional equations, the surface temperature therefore satisfies the dimensional HEBE:

$$\tau^{1/2}\,{}_0D_t^{1/2}T_s+T_s=sF(t); \qquad T_s(t)=\lambda\int_0^t G_\delta\left(\frac{t-u}{\tau};0\right)F(u)\frac{du}{\tau}$$ (44~~41~~)

(where the surface temperature is $T_s(t)=T(t;0)$).

This HEBE equation for the surface temperature could be regarded as a significant nonclassical example of the Mori-Zwanzig formalism, ([*Gottwald et al.*, 2017], [*Mori*, 1965], [*Zwanzig*, 1973], [*Zwanzig*, 2001]), and empirical model reduction formalisms [*Ghil and Lucarini*, 2020], whereby memory effects arise if we only look at one part of the system, ignoring the others. In the HEBE, the surface temperature is analogously expressed directly in terms of the forcing, ignoring the subsurface degrees of freedom. Although such memories are usually considered exponential and hence small, the HEBE shows that the classical continuum heat equation has on the contrary, strong power law memories. This points to serious limitations to conventional dynamical systems approaches to climate science that assume that the dynamical equations are integer ordered

Commented [SL5]: Note for 0<H<1, RL, Caputo and WEyl are nearly same…

Field Code Changed

Field Code Changed

Field Code Changed

with exponential memories. The HEBE shows that the fundamental radiatively exchanging components of the climate system will generally be characterized by long memories, associated with fractional rather than integer ordered derivatives. We develop this insight elsewhere.

[*Gottwald et al.*, 2017; *Mori*, 1965]

3.2 The HEBE, zero dimensional and box models and Newton's law of Cooling

Phenomenological models of the temperature based on the energy balance across a homogeneous surface may represent either the whole earth or only a subregion. The former are global "zero dimensional" energy balance models (sometimes called "Global Energy Balance Models", GEBMs (see the review~~s~~ [*McGuffie and Henderson-Sellers*, 2005]) whereas in the latter, they may represent the balance across the surface of a homogeneous subsection, a "box". The boxes have spatially uniform temperatures that store energy according to their heat capacity, density and size. Often several boxes are used, mutually exchanging energy, and the basic idea can be extended to column models. Since the average earth temperature can be modelled either as a single horizontally homogeneous box, or by two or more vertically superposed boxes, in the following, "box model" refers to both global and regional models.

A key aspect of these models is the rate at which energy is stored and at which it is exchanged between the boxes. Stored heat energy is transferred across a surface and it is generally postulated that its flux obeys Newton's law of cooling (NLC). The NLC is usually only a phenomenological model, it states that a body's rate of heat loss is directly proportional to the difference between its temperature and its environment. In these horizontally homogeneous models, it is only the heat energy/area (= S) that is important so that the NLC can be written:

$$Q_s = \frac{dS}{dt} = \frac{1}{Z}\left(T_{eq} - T\right) \qquad (45~~42~~)$$

S is the heat in the body and Q is the heat flux across the surface into the body (see fig. 6). T_{eq} is the equilibrium temperature, and Z is a transfer coefficient, ~~sometimes called~~ the "thermal impedance" (units: m^2K/W), its reciprocal Y is the surface "thermal admittance" see the next section). Identifying the equilibrium temperature with $T_{eq}(t) = s\,\cancel{\lambda}\,F(t)$ and using the dimensional surface boundary condition (eq. 12), it is easy to check that a direct consequence of the HEBE's conductive - radiative boundary condition is that it also satisfies the NLC:

$$Q_{s,HEBE} = \frac{dS_{HEBE}}{dt} = \rho c \kappa_v \left.\frac{\partial T}{\partial z}\right|_{z=0} = \frac{\left(T_{eq} - T\right)}{\lambda}; \qquad T_{eq} = \lambda F \qquad (46~~43~~)$$

Unlike the usual phenomenological box applications that simply postulate the NLC, the HEBE satisfies it as a consequence of its energy conserving surface boundary condition. Comparing eqs. 41, 42, we may also conclude that thermal impedance $Z = s\,\cancel{\lambda}$.

Formatted: Font: Italic

Formatted: Font: Italic

While the HEBE and box models obey the NLC, their relationships between the surface heat flux $Q_s = dS/dt$ and the surface temperature T are quite different. For example, for forcings starting at time $t = t_0$, using the HEBE we have:

$$Q_{s,HEBE} = \frac{dS_{HEBE}}{dt} = \frac{\tau^{1/2}}{\lambda} {}_{t_0}D_t^{1/2}T; \quad \tau = \rho c \lambda l_v; \quad l_v = \kappa_v \rho c \lambda$$

$$Q_{s,HEBE} = \frac{dS_{HEBE}}{dt} = \frac{\tau^{1/2}}{s} {}_{t_0}D_t^{1/2}T; \quad \tau = \rho c s l_v; \quad l_v = \kappa_v \rho c s \qquad (47~~44~~)$$

Although this relation between surface heat fluxes and temperatures has been known for some time ([*Babenko*, 1986], [*Podlubny*, 1999], see e.g. [*Sierociuk et al.*, 2013], [*Sierociuk et al.*, 2015] for applications), to my knowledge, it has never been applied to conduction - radiative models, nor has it been combined with the NLC to yield the homogeneous HEBE. In comparison, box models satisfy:

$$Q_{s,box} = \frac{dS_{box}}{dt} = \frac{\tau_{box}}{\lambda}\frac{dT}{dt}; \quad \tau_{box} = \rho c \lambda L; \quad L = \frac{C}{\rho c}$$

$$Q_{s,box} = \frac{dS_{box}}{dt} = \frac{\tau_{box}}{s}\frac{dT}{dt}; \quad \tau_{box} = \rho c s L; \quad L = \frac{C}{\rho c} \qquad (48~~45~~)$$

Where L is the effective thickness of the surface layer and C is the specific heat per area, τ_{box} is the classical EBE relaxation time. [*Geoffroy et al.*, 2013] used a two box model to fit outputs of a dozen GCM and found $\tau_{box} \approx 4.1\pm1.1$ years (the mean and spread of 12 models) and ≈ 40 - 800 years for the second box whereas the [*IPCC*, 2013] recommends a 2 box model with relaxation scales $\tau_{box} = 8.4$ and 409 years, with the FEBE, [*Procyk et al.*, 2020] finds $H = 0.38\pm0.05$, $\tau = 4.7\pm2.3$ years.

The HEBE and box heat transfer models can conveniently be compared and contrasted by placing them both in a more general common framework. Define the H^{th} order heat storage as:

$$S_H(t) = \frac{\tau^H}{\lambda\Gamma(1-H)}\int_{t_0}^{t} T(s)(t-s)^{-H}ds; \quad 0 \le H \le 1 \qquad (49~~46~~)$$

If we take $T(t_0) = 0$ (this is equivalent to fixing the reference of our anomalies), then integrating by parts:

$$S_H(t) = \frac{\tau^{H-1}}{\lambda\Gamma(1-H)}\int_{t_0}^{t} T'(s)(t-s)^{1-H}ds; \quad 0 \le H \le 1 \qquad (50~~47~~)$$

Formatted: Font: Italic

Formatted: Font: Symbol

Putting $H = 1$ yields the simple: $S_1(t) = T(t)/\lambda$ so that $S_1 = S_{box}$.

Over the interval t_0 to t, the fractional derivative of order H is defined as the ordinary derivative of the 1-H order fractional integral:

$$ {}_{t_0}D_t^H T = \frac{d}{dt}\left({}_{t_0}D_t^{H-1}T\right) = \frac{d}{dt}\left[\frac{1}{\Gamma(1-H)}\int_{t_0}^{t}(t-s)^{-H}T(s)ds\right]; \quad 0 \le H \le 1 \qquad (51~~48~~) $$

Therefore $S_{1/2} = S_{box}$ and:

$$ \frac{dS_H}{dt} = \lambda^{-1}\tau^H\,{}_{t_0}D_t^H T; \qquad \begin{array}{l} H_{HEBE} = 1/2; \quad \tau_{FEBE} = l_v \rho c \lambda \\ H_{box} = 1; \quad \tau_{box} = L\rho c\lambda \end{array} \qquad (52~~49~~) $$

Combining this with the NLC, in both cases we obtain:

$$ \tau^H\,{}_{t_0}D_t^H T + T = \lambda F \qquad (53~~50~~) $$

Hence the box and HEBE models are special cases of the Fractional order Energy Balance Equation (FEBE [*Lovejoy*, 2019b], [*Lovejoy*, 2019a]). Whereas the box model changes its heat content instantaneously with its current temperature ($T(t)$), at any moment, the energy stored in the HEBE model depends on the past temperatures, and since their weights fall off slowly – there is a long memory – it potentially depends on the temperature and hence energy stored in the distant past. Box or column models all have surfaces that exchanges heat both radiatively and conductively so that – contrary to standard practice – these surfaces should instead exchange heat fractionally with $H = 1/2$ not $H = 1$. Note that when we consider box interfaces with purely conductive heat exchanges (without radiative transfer e.g. between a "deep ocean" and "mixed layer" in global two box model), then the thermal contact conductance that characterizes the interface is needed.

At a theoretical level, the advantage of the HEBE is that unlike the box models, it is a direct consequence of the standard (energy conserving) continuum heat equation combined with standard energy conserving surface boundary conditions. It is therefore natural to ask if the $H = 1$ heat transfer (i.e. $dS_1/dt = (C/s\cancel{\lambda})dT/dt$) can be derived from the heat transport equation. Returning to the nondimensional boundary condition ($\left.\frac{\partial T}{\partial z}\right|_{z=0} + T(t;0) = F(t)$) it is easy to verify, that in order to recover $H = 1$ heat transfer, one must instead use $\left.\frac{\partial^2 T}{\partial z^2}\right|_{z=0} + T(t;0) = F(t)$. We therefore conclude that box model $H = 1$ transfer is *not* simultaneously compatible with heat equation and energy balance boundary conditions.

Formatted: Font: Italic

To summarize: we are currently in the unsatisfactory position of having zero and one dimensional (box and Budyko-Sellers) energy balance equations neither of which satisfy the correct radiative - conductive surface boundary conditions. For the box models, the consequence is that the energy storage processes have rapid (exponential) rather than slow (power law) relaxation. For the Budyko-Sellers models, the consequence is that at best, they are 1-D and even with this restriction, their time dependent versions have derivatives of the wrong order (~~see the discussion in~~ part II, section 2.3). In comparison, the zero dimensional HEBE is a consequence of correcting the Budyko-Sellers boundary conditions. It satisfies the NLC and corrects the order H reducing it from the phenomenological value H = 1, to H = 1/2. As a bonus, in part II we see that the HEBE can easily be extended from zero to two spatial dimensions, enlarging the scope of energy balance models while simultaneously eliminating these weaknesses.

3.3 Thermal impedance and Complex climate sensitivities and the annual cycle

3.3.1 Conductive versus conductive - radiative boundary conditions

Up until now, we have discussed forcing that is "turned on" at t = 0, this allowed for convenient solutions using Laplace transform methods. However, for forcing that is periodic or that is a stationary noise (i.e. the internal variability) Fourier techniques are more useful.

The first applications of Fourier techniques to the problem of radiative and conductive heat transfer into the Earth, was by [*Brunt*, 1932] and [*Jaeger and Johnson*, 1953] who considered the (weather regime) diurnal cycle. We already mentioned that [*Brunt*, 1932] also considered step function heat forcing, that he claimed might be a plausible model of the diurnal cycle near sunset or sunrise. However, in zero - dimensional models, the long time temperatures after step heat flux forcings are divergent (but not in 2D models, see part II) so that later in his paper Brunt considered periodic diurnal heat flux forcing with no net heat flux across the surface and used Fourier methods instead. In this classical diurnally forced problem, the periodic temperature response lags the forcing by a phase shift of $\pi/4$ = 3 hours. If we apply the same shift to the annual cycle – assuming that the Earth is forced by heat flux into its subsurface – the corresponding lag is 1.5 months ≈ 46 days which is generally too long (we shall see that it corresponds to an infinite relaxation time).

Following [*Brunt*, 1932] and [*Jaeger and Johnson*, 1953], let us consider the response to a single Fourier component forcing (this is equivalent to Fourier analysis of the equation). In this case, assuming a periodic temperature response and substituting this into the 1-D dimensional heat equation (time and depth, i.e. the dimensional version of eq. 22), we find that the variation of amplitude with depth is:

$$T(t;z) = T_s e^{i\omega t} e^{\sqrt{\frac{i\omega}{\kappa_v}}z}; \quad z \le 0 \qquad (54\cancel{51})$$

Where T_s is the amplitude of the surface temperature oscillations, it depends on the nature of the forcing, here on the boundary conditions ("*s*" for "surface"). Following Brunt, using the classical heat surface heat forcing $F_s e^{i\omega t}$ as the surface boundary condition (with this forcing, $F_s = Q_s$ is the heat crossing the surface entering the system in the downward direction, see figs. 1, 6) we find:

$$\rho c \kappa_v \left.\frac{\partial T_{heat}}{\partial z}\right|_{z=0} = F_s e^{i\omega t} \qquad (55~~52~~)$$

("heat" for heat forcing), we obtain:

$$T_{s,heat} = \frac{F_s}{\sqrt{i\omega(\rho c)^2 \kappa_v}} = Z(\omega) F_s; \qquad Z(\omega) = \frac{\lambda}{\sqrt{i\omega\tau}}$$

$$T_{s,heat} = \frac{F_s}{\sqrt{i\omega(\rho c)^2 \kappa_v}} = Z(\omega) F_s; \qquad Z(\omega) = \frac{s}{\sqrt{i\omega\tau}} \qquad (56~~53~~)$$

Where, $Z(\omega)$ is the complex frequency dependent thermal impedance, the reciprocal of the thermal admittance. For a given surface heat flux, $Z(\omega)$ quantifies the surface temperature response (we have written the impedance with the help of s ~~λ~~ in order to nondimensionalize the denominator). Thermal impedance and admittance are standard in areas of heat transfer engineering and were introduced into the problem of diurnal Earth heating by [*Byrne and Davis*, 1980]. From $Z(\omega)$, we can thus easily understand the key [*Brunt*, 1932], [*Jaeger and Johnson*, 1953] result: that $\arg(Z(\omega)) = \arg(i^{-1/2}) = -\pi/4$ ("arg" indicates the phase).

So far, this approach has only been applied to weather scales (the diurnal cycle). Let's now apply the same approach but with an eye to longer macroweather timescales, notably the annual cycle. The climate sensitivity is an emergent macroweather quantity that is determined by numerous feedbacks that over the weather scales are quite nonlinear but over macroweather scales are considerably averaged (and at least for GCMs, [*Hébert and Lovejoy*, 2018]) are already fairly linear. In any event, for the annual cycle we use radiative - conductive boundary conditions rather than the pure conductive ones used by Brunt.

Using conductive - radiative surface BCs with external forcing $F_s e^{i\omega t}$ yields:

Formatted: Font: Italic

$$F_s = Q_s + Q_{s,rad} = \lambda^{-1}\left(1+(i\omega\tau)^{1/2}\right)T_s$$

$$Q_{s,rad} = \lambda^{-1}T_s \qquad F(t) = F_s e^{i\omega t}$$

$$Q_s = \rho c \kappa_v \left.\frac{\partial T}{\partial z}\right|_{z=0} = \lambda^{-1}(i\omega\tau)^{1/2} T_s$$

$$F_s = Q_s + Q_{s,rad} = s^{-1}\left(1+(i\omega\tau)^{1/2}\right)T_s$$

$$Q_{s,rad} = s^{-1}T_s \qquad F(t) = F_s e^{i\omega t}$$

$$Q_s = \rho c \kappa_v \left.\frac{\partial T}{\partial z}\right|_{z=0} = s^{-1}(i\omega\tau)^{1/2} T_s$$

(57~~54~~)

Where here F_s is the radiative (downward) forcing radiative flux and Q_s and $Q_{s,rad}$ are the surface conductive (into the subsurface) and long wave radiative emission (away from the surface) fluxes respectively. Solving, we obtain the same depth dependence (eq. ~~50~~54), but with the amplitude of the surface oscillations given by:

$$T_s = \lambda(\omega)F_s; \qquad \lambda(\omega) = Z(\omega) = \frac{\lambda}{1+(i\omega\tau)^{1/2}}$$

$$T_s = s(\omega)F_s; \qquad s(\omega) = Z(\omega) = \frac{s}{1+(i\omega\tau)^{1/2}}$$

(58~~55~~)

Where we have introduced the complex climate sensitivity s ~~λ~~(ω) which by definition is equal to the complex thermal impedance Z(ω). In the context of the Earth's energy balance, it is more useful to think in terms of sensitivities than impedances so that below we use s~~λ~~(ω). With this, we obtain:

$$Q_s = \frac{s(\omega)}{s}(i\omega\tau)^{1/2}F_s; \qquad Q_{s,rad} = \frac{s(\omega)}{s}F_s$$

(59~~56~~)

Formatted: Font: Italic

Since Arg($i^{1/2}$) = π/4 (= 45°), we see that as mentioned earlier, the conductive and long wave radiative fluxes are out of phase by 45°, but the phase of the temperature lags the forcing by Arg(λ(ω)), which only reaches 45° in the large τ limit (see fig. 7). Note that we could have deduced eq. ~~55~~ 59 directly by Fourier analysis of the HEBE using $F.T.\left({}_{-\infty}D_t^{1/2}\right)=\left(i\omega\right)^{1/2}$, but the above allowed us to compare the results with the classical model. The Fourier method allows us to extend the complex climate sensitivity to the more general FEBE:

$$\lambda_H\left(\omega\right)=\frac{\lambda}{1+\left(i\omega\tau\right)^H}\quad s_H\left(\omega\right)=\frac{s}{1+\left(i\omega\tau\right)^H} \qquad (60~~57~~)$$

the usual EBE is the H = 1 special case.

3.3.2 Empirical estimates of complex climate sensitivities

Figs. 7, 8 compare the phases and amplitudes of λ(ω) for the classical and conductive - convective boundary conditions (H = 1/2) HEBE as well as the H = 1 EBE. The plots use ω = 2π *rad/yr*. From fig. 7, we see that taking the empirical value ~~of~~ τ ~~in the range 2 -~~ ≈ 5 years ([*Procyk et al.*, 2020]), that the HEBE lag is a little over a month~~,~~. ~~a result that is close to the observed lag between the summer solstice and maximum temperatures over most land areas.~~ From the detailed maps in [Donohoe et al., 2020] (see also [*Ziegler and Rehfeld*, 2020]) we estimate that in the extratropical regions, over land, the summer temperature maximum is typically 30 - 40 days after the solstice, but only 20 - 30 days after the maximum forcing (insolation) and for ocean, 60 - 70 days after the solstice but only 30 - 40 days after the maximum insolation. The HEBE ~~a~~ result ~~that~~ is thus close to the observed lag between the summer solstice and maximum temperatures over most land areas.

In contrast, if we use [*Brunt*, 1932]'s classical ~~The~~ the heat forcing result (~~π/~~we obtain π/4 = 1.5 months = 46 days which~~),~~ is already too long for most of the globe and the H = 1 EBE result (close to 3 months = 91 days) is much too long. [*North et al.*, 1983; *North and Kim*, 2017]Over the ocean, the lag is typically longer than over land probably because of the strong albedo periodicity associated with seasonal ocean cloud cover~~.~~ [Stubenrauch et al., 2006], [Donohoe et al., 2020]. This delays the summer solstice forcing maximum over the ocean, potentially explaining the extra lag.

~~This delays the summer solstice forcing maximum over the ocean, potentially explaining the extra ocean lag.~~

Although a complete analysis with modern data is out of our present scope, we can get a feel for the realism of this approach by using the ~~latitudinally~~ zonally averaged~~-~~ [*North and Coakley*, 1979] Sellers model discussed in the review [*North et al.*, 1981], updated in [*North et al.*, 1983] where most of the earth follows the EBE phase lags of ≈90 days. The model uses a 2nd order Legendre polynomial to take into account the latitudinal variations and a sinusoidal annual cycle with empirically fit parameters that effectively ~~latitudinally~~ zonally average over land and ocean. Empirical parameters are given for the albedo, top of the atmosphere insolation, temperature and outgoing IR radiation such that the global temperature maximum lags the solstice by 32.5 days~~.~~ [*North and Coakley*, 1979], [*North et al.*, 1983]. An [*Zhuang et al.*, 2017; *Ziegler and Rehfeld*, 2020]updated 2-D version of the Sellers model has used it to estimate phase lags with respect to the solstice finding lags of ≈ 90 days over oceans and ≈30-40 days over land ([*Zhuang et al.*, 2017], [*Ziegler and Rehfeld*, 2020]).

Formatted: Font: Italic

Formatted: Indent: First line: 1 cm

Before continuing, recall that the zero-dimensional theory discussed here assumes that all radiative flux imbalances are all stored, it ignores the divergence of the horizontal heat transport which according to [*Trenberth et al.*, 2009] – is small even though the ~~due to the meridional gradients~~heat fluxes— may be significant. Although at least for temperature anomalies, we argue that this effect is mostly important at small scales, the magnitude of horizontal heat divergence at macroweather scales ~~transport~~ is not well known and is presumably quite variable from place to place depending on (inhomogeneous) local ~~horizontal~~ transport parameters (see part II). A simple way to parameterize the transport is to maintain the assumption that the Earth has homogeneous parameters and to assume that the transport is due to horizontally inhomogeneous forcing. In part II, we show that for a horizontal wavenumber k, the effect of horizontal transport is to modify the storage term as $\left(i\omega\tau\right)^{1/2} \rightarrow \left(i\omega\tau+\left(l_h k\right)^2\right)^{1/2}$, therefore for pure periodic horizontal forcing:

$$Q_{s,h}=\frac{s_h(\omega)\left(i\omega\tau+\left(l_h k\right)^2\right)^{1/2}}{s}F_s;\qquad Q_{s,rad}=\frac{s_h(\omega)}{s}F_s;\qquad s_h(\omega)=\frac{s}{1+\left(i\omega\tau+\left(l_h k\right)^2\right)^{1/2}}$$

$$Q_{s,h}=\frac{\lambda_h(\omega)\left(i\omega\tau+\left(l_h k\right)^2\right)^{1/2}}{\lambda}F_s;\qquad Q_{s,rad}=\frac{\lambda_h(\omega)}{\lambda}F_s;\qquad \lambda_h(\omega)=\frac{\lambda}{1+\left(i\omega\tau+\left(l_h k\right)^2\right)^{1/2}}\qquad (61~~58~~)$$

("*h*" for "horizontal inhomogeneity; in [*Lovejoy et al.*, 2020] there is an analogous calculation for the FEBE with $H \neq 1/2$). In North et al's 1-D model, the top of the atmosphere forcing is exactly a cosine variation i.e. with a single wavenumber k = 1 cycle around the Earth. The only differences are that we neglected the curvature of the Earth and assumed that the Earth's transport properties are constant. We nevertheless use eq. ~~57~~ 61 as an approximation for the horizontal transport.

Formatted: Font: Italic

From the data in table 1 of [*North et al.*, 1981] , we may deduce:

$$\begin{aligned} F_s &= \left(212\pm 28\right)e^{-3.27i}\sin\theta; && W/m^2 \\ Q_{s,rad} &= 38e^{-3.65i}\sin\theta; && W/m^2 \qquad (62~~59~~) \\ T_s &= 15.5e^{-3.70i}\sin\theta; && K \end{aligned}$$

Where the forcing F_s is the product of the solar constant with the co-albedo (= 1- albedo) and θ is the latitude and the phases are taken with respect to the winter solstice. The variation (about ±13%) in the amplitude of F_s is due to the latitudinal variation of the coalbedo. In the model, the long wave radiation $Q_{s,rad}$ and the surface temperature response T_s have exact sinθ dependencies. The phases (in radians) are taken with respect to the winter solstice so that the summer solstice has a phase π = 3.14 rads, (in the northern hemisphere, June 21). Due to the coalbedo variations, the actual forcing has a phase = 3.27 rads peaking on June 28th. Also, the phase of the temperature and longwave emissions are larger = 3.70 rad, 3.65 rad corresponding to maxima on July 26th, July 23rd respectively (all results are appropriately symmetric for the southern hemisphere and for the cold lag following the winter solstice). The near identity of the phases of temperatures and long wave responses (a three day difference, probably not empirically significant), is already support for the model that predicts that they should be in phase. We also note that these lags (of 28, 25 days) are considerably shorter than the 46 day lag (Aug 12th) that would have been obtained had we applied Brunt's heat conductive forcing.

We can use these data to estimate the climate sensitivity, relaxation time τ and horizontal conduction term l_hk by using the following:

$$\lambda = \frac{T_s}{Q_{s,rad}} = 0.41 + 0.02i \approx 0.41; \quad K/\left(W/m^2\right)$$

$$\lambda_h(\omega) = \frac{T_s}{F_s} = (0.068 \pm 0.009) + (0.031 \pm 0.004i); \quad K/\left(W/m^2\right)$$

$$i\omega\tau + (l_h k)^2 = \left(\frac{F_s}{Q_{s,rad}} - 1\right)^2 = (13.20 \pm 4.6) + (17.3 \pm 5.1)i$$

$$s = \frac{T_s}{Q_{s,rad}} = 0.41 + 0.02i \approx 0.41; \quad K/\left(W/m^2\right)$$

$$s_h(\omega) = \frac{T_s}{F_s} = (0.068 \pm 0.009) + (0.031 \pm 0.004i); \quad K/\left(W/m^2\right)$$

(63~~60~~)

$$i\omega\tau + (l_h k)^2 = \left(\frac{F_s}{Q_{s,rad}} - 1\right)^2 = (13.20 \pm 4.6) + (17.3 \pm 5.1)i$$

From this (with ω = 2π/*yr*), we obtain:

$$\tau = 2.75 \pm 0.8\, yrs$$
$$l_h k = 3.63 \pm 0.64$$

(64~~61~~)

The relaxation time is within the rough bounds deduced by considering atmosphere - ocean coupling time scale (≈ 2 years, Hebert et al 2020), low frequency climate records (≈ ~~5~~ 4.7±2.3 years~~.~~, [*Procyk et al.*, 2020]~~work with R. Procyk~~), and the high frequency EBE relaxation times ≈ 4.1±1.1 years [*Geoffroy et al.*, 2013]. We also see that the ratio of the storage to transfer is 17.3/13.2 ≈ 1.3 so that most of the heat is indeed stored so that the above homogeneous theory is plausible. The nondimensional $l_h k$ characterizes the typical horizontal transport over the period of a year. Rather than interpreting it deterministically in terms of a global scale horizontal variation over a homogeneous earth, we consider it a nondimensional empirical parameter that we will try to clarify in future work. In any case, the horizontal transport and storage are in quadrature so that the effect of the transport on the magnitude of sensitivity is smaller: $\left|(i\omega\tau)^{1/2}+1\right| / \left|\left(i\omega\tau+(l_h k)^2\right)^{1/2}+1\right| \approx 0.88$ (i.e. about 12%) but the change in the phase is more substantive (≈ 15 days). We can note that the EBE $H = 1$ value (ignoring transport, with τ = 2.75 years) gives 87 days i.e. a maximum on September 21st which is much too late (fig. 7).

The static climate sensitivity s~~λ~~ should be purely real; its imaginary part is indeed small, it corresponds to 3 days and is probably within the error of the model and empirical estimates, it will be ignored below. s~~λ~~ can be converted to *K/*(CO_{2eq} *doubling*) by multiplying it by the canonical value 3.71 W/m^2/ (CO_{2eq} *doubling*) to yield 1.51 *K/*(CO_{2eq} *doubling*) which is at the lower part of the IPCC 90% confidence range (3±1.5 K/ (CO_{2eq} *doubling*)). Since both the methodology and the empirical parameter estimates could be updated and improved, the result is encouraging. In future, instead of assuming latitudinal constancy with a sinusoidal latitudinal dependence, gridded data could be used and the horizontal conduction approximation (the $l_h k$ term) could be improved.

Formatted: Font: Italic

4. Conclusions

This first paper of two parts proposes a new 2D energy balance equation for macroweather scales: ten days and longer. It follows the classical energy balance models pioneered by [*Budyko*, 1969] and [*Sellers*, 1969], and assumes that the dynamics can be adequately modelled by the continuum mechanics heat equation – by advection and diffusion. As reviewed in [*McGuffie and Henderson-Sellers*, 2005], [*North and Kim*, 2017], the classical models treat the parts of the atmosphere and ocean that radiatively interact with outer space as a zero thickness, two dimensional surface. The complex radiative processes that occur in the vertical direction are only treated implicitly. The dimensionality is then further reduced by zonal averaging. While this original time independent model may be reasonable for the long term (time invariant) climate states, it is inadequate for treating time varying anomalies. The key improvement in realism was by made explicitly introducing a vertical coordinate z. Yet, when this was done, it turned out that a detailed vertical model was still unnecessary: all that was required was the existence of a surface layer whose thickness was of the order of the diffusion depth. This is where most of the energy storage occurs and it determines vertical temperature derivative at the surface and hence the vertical conductive heat flux. This sensible heat flux is the crucial link between the local radiative imbalances that drive the system, the heat that is stored and the heat that is transported horizontally. Whereas the Budyko-Sellers models have zero thicknesses, our model has a finite but possibly small thickness; it need only be thick enough to account for energy storage and to determine the surface vertical temperature derivative.

In this first part, we considered only homogeneous zero-dimensional models. These are completely classical, yet as far as we know, have not been solved with conductive – (linearized) radiative boundary conditions. Using standard Laplace and Fourier techniques, we solved the full depth-time heat equation and showed that it's Green's function was identical to a half-order fractional differential equation that directly gives the surface temperature. Although half-order derivatives have occasionally been used in the context of the heat equation, (at least since [*Oldham and Spanier*, 1972; *Oldham and Spanier*, 1974], [*Babenko*, 1986]), the resulting half-order energy balance equation (the HEBE) is apparently new. Mathematically, the result is a direct consequence of the heat equation, the semi-infinite medium and conductive - radiative surface boundary conditions. The consequences are surprisingly far reaching. For example, the familiar integer ordered differential equations have exponential Green's functions, short memories. In contrast, the more general fractional ordered equations such as the HEBE have Green's functions that are "generalized exponentials", based on power laws and long memories. A general consequence is that while the HEBE respects Newton's law of cooling - i.e. that heat fluxes across a surface are proportional to temperature differences - that the relationship between this heat flux and the surface temperature is quite different: it involves a half order derivative rather than first order one. The energy stored is no longer instantaneously determined by the surface temperature, but rather by the entire prior forcing history. Irrespective of the details, we thus *expect* Earth heat storage processes to generally have long memories.

We also obtained general results on the Earth's response to periodic forcings. Ever since [*Brunt*, 1932], Fourier techniques have used the heat equation to model the Earth's temperature response when subjected to a diurnal heat flux forcing. We extend this from the weather regime to macroweather regime, from diurnally periodic heat forcing to annually periodic radiative - conductive forcing. An immediate consequence is that the surface thermal impedance - equal to the climate sensitivity – is a complex number whose phase determines the lag between the maximum of the forcing (shortly following the summer solstice) and the temperature maximum. Using a simple latitudinally averaged model with empirical parameters, we estimated this complex climate sensitivity and showed how this could readily account for the observed 22-25 day lag, estimating the (static) climate sensitivity at $s\cancel{\lambda} \approx 0.41$ K/(W/m^2) and relaxation time $\tau \approx 2.75$ years.

Formatted: Font: Italic

In part II, we extend these zero dimensional results to the horizontal. We first continue to use Laplace and Fourier techniques to treat the case of homogenous Earth parameters, but with inhomogeneous forcing. We then – with the help of Babenko's method, extend this to the full inhomogeneous problem with horizontally varying relaxation times, diffusivities, specific heats, climate sensitivities and forcings.

5. Acknowledgements

I acknowledge discussions with L. Del Rio Amador, R. Procyk, R. Hébert, D. Clarke and C. Penland. This is a contribution to fundamental science; it was unfunded and there were no conflicts of interest.

6. References

Atanackovic, M., Pilipovic, S., Stankovic, B., and Zorica, D., *Fractional Calculus with applications in mechanics: variations and diffusion processes*, 313 pp., Wiley, 2014.

Babenko, Y. I., *Heat and Mass Transfer*, Khimiya: Leningrad (in Russian), 1986.

Baleanu, D., Diethelm, K., Scalas, E., and Trujillo, J. J., *Fractional Calculus: Models and Numerical Methods*, 400 pp., World Scientific, 2012.
Blender, R., and Fraedrich, K., Long time memory in global warming simulations, *Geophys. Res. Lett.* , ***30***, 1769, 2003.
Brunt, D., Notes on radiation in the atmosphere, *Quart. J. Roy. Meterol. Soc.* , *58*, 389-420, 1932.
Budyko, M. I., The effect of solar radiation variations on the climate of the earth, *Tellus*, *21*, 611-619, 1969.
Bunde, A., Eichner, J. F., Kantelhardt, J. W., and Havlin, S., Long-term memory: a natural mechanism for the clustering of extreme events and anomalous residual times in climate records, *Phys. Rev. Lett.* , *94*, 1-4 doi: 10.1103/PhysRevLett.94.048701, 2005.
Byrne, G. F., and Davis, J. R., Thermal inertia, thermal admittance, and the effect of layers, *Remote Sensing of Environment*, *9*(4), 295-300 doi: 10.1016/0034-4257(80)90035-8, 1980.
Del Rio Amador, L., and Lovejoy, S., Predicting the global temperature with the Stochastic Seasonal to Interannual Prediction System (StocSIPS) *Clim. Dyn.* doi: org/10.1007/s00382-019-04791-4., 2019.
Del Rio Amador, L., and Lovejoy, S., Using scaling for seasonal global surface temperature forecasts: StocSIPS *Clim. Dyn.*, *under review*, 2020a.
Del Rio Amador, L., and Lovejoy, S., Long-range Forecasting as a Past Value Problem: Using Scaling to Untangle Correlations and Causality *Geophys. Res. Lett.*, *(submitted, Nov. 2020)*, 2020b.
Donohoe, A., Dawson, E., Mcmurdie, L., Battisti, D. S., and Rhines, A., Seasonal asymmetries in the lag between insolation and surface temperature, *J. of Clim.*, *33*, 3921-3945 doi: 10.1175/jcli-d-19-0329.1, 2020.
Dwyers, H. A., and Petersen, T., Time-dependent energy modelling, *J. Appl. Meteor.*, *12*, 36-42, 1975.
Geoffroy, O., Saint-Martin, D., Olivié, D. J., Voldoire, A., Bellon, G., and Tytéca, S., Transient climate response in a two-layer energy-balance model. part i: Analytical solution and parameter calibration using cmip5 aogcm experiments, *Journal of Climate*, *26*, 1841–1857, 2013.
Ghil, M., and Lucarini, V., The physics of climate variability and climate change, *Reviews of Modern Physics*, *92(3)*, 035002 doi: https://doi.org/10.1103/RevModPhys.92.035002, 2020.
Gottwald, G. A., Crommelin, D. T., and Franzke, C. L. E., Stochastic Climate Theory, in *Nonlinear and Stochastic Climate Dynamics*, edited by C. L. E. Franzke and T. J. OKane, pp. 209–240, Cambridge University Press, 2017.
Hahn, D. W., and Ozisk, M. N., *Heat Conduction*, 3rd edition ed., Wiley, 2012
Hebert, R. (2017), A Scaling Model for the Forced Climate Variability in the Anthropocene, MSc thesis, McGill University, Montreal.
Hébert, R., and Lovejoy, S., The runaway Green's function effect: Interactive comment on "Global warming projections derived from an observation-based minimal model" by K. Rypdal, *Earth System Dyn. Disc.* , *6*, C944–C953, 2015.
Hébert, R., and Lovejoy, S., Regional Climate Sensitivity and Historical Based Projections to 2100, *Geophys Res Lett.*, *45*, 4248-4254 doi: 10.1002/2017GL076649, 2018.
Hébert, R., Lovejoy, S., and Tremblay, B., An Observation-based Scaling Model for Climate Sensitivity Estimates and Global Projections to 2100, *Climate Dynamics*, *(in press)*, 2020.
Hilfer, R. (Ed.), *Applications of Fractional Calculus in Physics* World Scientific, 2000.
Houghton, J. T., Ding, Y., Griggs, D. J., Noguer, M., van der Linden, P. J., Dai, X., Maskell, K., and Johnson, C. A. (Eds.), *Climate Change 2001: The Scientific Basis, Contribution of Working Group I to the Third Assessment Report of the Intergovernmental Panel on Climate Change*, Cambridge University Press, 2001.
IPCC, *Climate Change 2013: The Physical Science Basis. Contribution of Working Group I to the Fifth Assessment Report of the Intergovernmental Panel on Climate Change.*, Cambridge University Press: Cambridge, 2013.
Jaeger, J. C., and Johnson, C. H., Note on diurnal temperature variation, *Pure Appl. Geophys.* , *24*, 104-106, 1953.
Klafter, J., Lim, S., and Metzler, R. (Eds.), *Fractional Dynamics: Recent Advances*, World Scientific, Singapore, 2012.
Lovejoy, S., Using scaling for macroweather forecasting including the pause, *Geophys. Res. Lett.*, *42*, 7148–7155 doi: DOI: 10.1002/2015GL065665, 2015.
Lovejoy, S., Fractional Relaxation noises, motions and the stochastic fractional relxation equation *Nonlinear Proc. in Geophys. Disc.*, *https://doi.org/10.5194/npg-2019-39*, 2019a.
Lovejoy, S., *Weather, Macroweather and Climate: our random yet predictable atmosphere*, 334 pp., Oxford U. Press, 2019b.

Lovejoy, S., and Schertzer, D., *The Weather and Climate: Emergent Laws and Multifractal Cascades*, 496 pp., Cambridge University Press, 2013.
Lovejoy, S., Del Rio Amador, L., and Hébert, R., Harnessing butterflies: theory and practice of the Stochastic Seasonal to Interannual Prediction System (StocSIPS), , in *Nonlinear Advances in Geosciences,* , edited by A. A. Tsonis, pp. 305-355, Springer Nature, 2017.
Lovejoy, S., del Rio Amador, L., and Hébert, R., The ScaLIng Macroweather Model (SLIMM): using scaling to forecast global-scale macroweather from months to Decades, *Earth Syst. Dynam.*, *6*, 1–22 doi: www.earth-syst-dynam.net/6/1/2015/, doi:10.5194/esd-6-1-2015, 2015.
Lovejoy, S., Procyk, R., Hébert, R., and del Rio Amador, L., The Fractional Energy Balance Equation, *Geophy. Res. Lett.*, *(in preparation, Sept. 2018)*, 2018.
Lovejoy, S., Procyk, R., Hébert, R., and del Rio Amador, L., The Fractional Energy Balance Equation, *Quart. J. Roy. Met. Soc.* , *(under revision)*, 2020.
Márquez, J. M. A., Bohórquez, M. A. M., and Melgar, S. G., Ground Thermal Diffusivity Calculation by Direct Soil Temperature Measurement. Application to very Low Enthalpy Geothermal Energy Systems, *Sensors (Basel)*, *16*, 306 doi: 10.3390/s16030306, 2016.
McGuffie, K., and Henderson-Sellers, A., *A Climate Modelling Primer*, Third Edition ed., John Wiley & Sons, Ltd 2005
Meyer, R. F. (1960), A heat-flux-meter for use with thin film surface thermometers : a report*Rep.*, National Research Council of Canada, Ottawa.
Miller, K. S., and Ross, B., *An introduction to the fractional calculus and fractional differential equations*, 366 pp., John Wiley and Sons, 1993.
Mori, H., Transport, Collective Motion, and Brownian Motion, *Progress of Theoretical Physics*, *33(3)*, 423–455 doi: https://doi.org/10.1143/PTP.33.423, 1965.
Myrvoll-Nilsen, E., Sørbye, S. H., Fredriksen, H.-B., Rue, H., and Rypdal, M., Statistical estimation of global surface temperature response to forcing under the assumption of temporal scaling, *Earth Syst. Dynam.*, *11*, 329–345 doi: https://doi.org/10.5194/esd-11-329-2020, 2020.
North, G. R., and Coakley, J. A., Differences between seasonal and mean annual energy balance model calculations of climate and climate sensitivity, *J, . Atmos.Sci.*, *36* 1189-1204, 1979.
North, G. R., Cahalan, R. F., and Coakley, J., J. A. , Energy balance climate models, *Rev. Geophysics Space Phy.*, *19*, 91-121, 1981.
North, G. R., Mengel, J. G., and Short, D. A., Simple Energy Balance Model Resolving the Seasons and the Continents Application to the Astronomical Theory of the Ice Ages *J. Geophys. Res.* , *88*, 6576-6586, 1983.
North, R. G., and Kim, K. Y., *Energy Balance Climate Models*, 369 pp., Wiley-VCH, 2017.
Oldham, K. B., Diffusive transport to planar, cylindrical and spherical electrodes, *J Electroanal Chem Interfacial Electrochem.*, *41*, 351–358, 1973.
Oldham, K. B., and Spanier, J., A general solution of the diffusion equation for semi infinite geometries, *J Math Anal Appl 39*, 665–669, 1972.
Oldham, K. B., and Spanier, J., *The Fractional Calculus*, Academic Press, reprinted by Dover, 2006, 1974.
Podlubny, I., *Fractional Differential Equations*, 340 pp., Academic Press, 1999.
Procyk, R., Lovejoy, S., and Hébert, R., The Fractional Energy Balance Equation for Climate projections through 2100, *Earth Sys. Dyn. Disc.*, *under review* doi: org/10.5194/esd-2020-48 2020.
Rybski, D., Bunde, A., Havlin, S., and von Storch, H., Long-term persistance in climate and the detection problem, *Geophys. Resear. Lett.*, *33*, L06718-06711-06714 doi: doi:10.1029/2005GL025591, 2006.
Rypdal, K., Global temperature response to radiative forcing: Solar cycle versus volcanic eruptions, *J. Geophys. Res.*, *117*, D06115 doi: 10.1029/2011JD017283, 2012.
Rypdal, K., Global warming projections derived from an observation-based minimal model, *Earth Syst. Dynam.*, *7*, 51–70., 2016.
Rypdal, K., Rypdal, M., and Fredriksen, H., Spatiotemporal Long-Range Persistence in Earth's Temperature Field: Analysis of Stochastic-Diffusive Energy Balance Models, *J. Climate*, *28*, 8379–8395. doi: doi:10.1175/JCLI-D-15-0183.1, 2015.
Rypdal, M., and Rypdal, K., Long-memory effects in linear response models of Earth's temperature and implications for future global warming, *J. Climate*, *27 (14)*, 5240 - 5258 doi: doi: 10.1175/JCLI-D-13-00296.1, 2014.

Field Code Changed

Sellers, W. D., A global climate model based on the energy balance of the earth-atmosphere system, *J. Appl. Meteorol.*, *8*, 392-400, 1969.

Sierociuk, D., Dzielinski, A., Sarwas, G., Petras, I., Podlubny, I., and Skovranek, T., Modelling heat transfer in heterogeneous media using fractional calculus, *Philos. Trans. R. Soc. A Math. Phys. Eng. Sci.* , *371: 20120146* doi: org/10.1098/rsta.2012.0146, 2013.

Sierociuk, D., Skovranek, T., Macias, M., Podlubny, I., Petras, I., Dzielinski, A., and Ziubinski, P., Diffusion process modeling by using fractional-order models, *Applied Mathematics and Computation 257*, 2–11 doi: org/10.1016/j.amc.2014.11.028, 2015.

Stubenrauch, C. J., Chédin, A., Rädel, G., Scott, N. A., and Serrar, S., Cloud Properties and their seasonal and diurnal variability from TOVS Path-B, *J. of Clim.*, *19*, 5531-5553 doi: org/10.1175/JCLI3929.1, 2006.

Tarasov, V. E., *Fractional Dynamics: Applications of Fractional Calculus to Dynamics of Particles, Fields and Media*, Higher Education Press, 2010.

Trenberth, K. E., Fasullo, J. T., and Kiehl, J., Earth's global energy budget, *Bull. Amer. Met.Soc.,*, 311-323 doi: DOI:10.1175/2008BAMS2634.1, 2009.

van Hateren, J. H., A fractal climate response function can simulate global average temperature trends of the modern era and the past millennium, *Clim. Dyn.* , *40*, 2651 doi: https://doi.org/10.1007/s00382-012-1375-3, 2013.

Varotsos, C. A., Efstathiou, M. N., and Cracknell, A. P., On the scaling effect in global surface air temperature anomalies. , *Atmos. Chem. Phys.* , *13 (10)*, 5243-5253, 2013.

Warren, S. G., and Schneider, S. H., Seasonal simu-lation as a test for uncertainties in the parameterizations of a Budyko-Sellers zonal climate model, *J. Atmos. Sci.*, *36*, 1377-1391, 1979.

West, B. J., Bologna, M., and Grigolini, P., *Physics of Fractal Operators*, 354 pp., Springer, 2003.

Zhuang, K., North, G. R., and Stevens, M. J., A NetCDF version of the two-dimensional energy balance model based on the full multigrid algorithm, *SoftwareX*, *6*, 198–202 doi: https://doi.org/doi.org/10.1016/j.softx.2017.07.003, 2017.

Ziegler, E., and Rehfeld, K., TransEBM v. 1.0: Description, tuning, and validation of a transient model of the Earth's energy balance in two dimensions, *Geosci. Model Devel. Disc.* doi: https://doi.org/10.5194/gmd-2020-237, 2020.

Zwanzig, R., Nonlinear generalized Langevin equations, *Journal of Statistical Physics,*, *9(3)*, 215–220 doi: https://doi.org/10.1007/BF01008729, 1973.

Zwanzig, R., *Nonequilibrium Statistical Mechanics* Oxford University Press, 2001.

Formatted: Indent: Left: 0 cm, Hanging: 1 cm

Figures

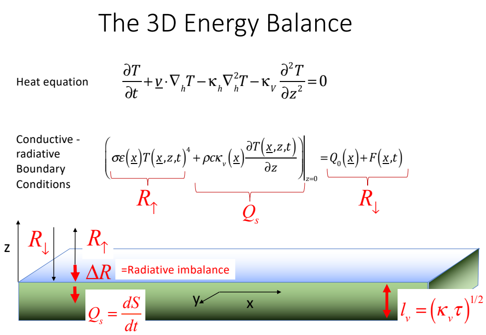

Fig. 1: A schematic diagram showing the correct 3D energy balance equations with conductive - radiative surface boundary conditions. Q_s is the heat flux across the surface into the subsurface, S is the energy stored in the subsurface per unit surface area. The picture illustrates the thin surface layer (whose thickness is of the order of the diffusion depth, l_v with relaxation time τ, eq. 20) in which the radiative exchanges between the earth and outer space occur.

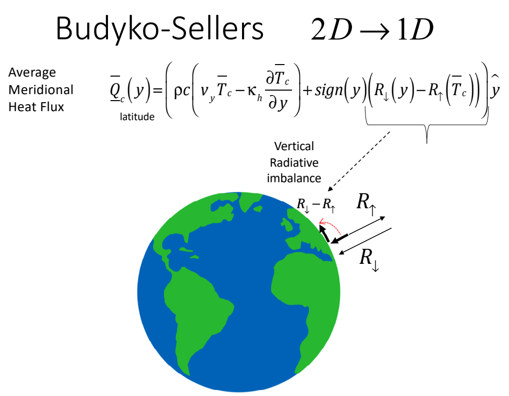

Fig. 2: A schematic diagram showing the Budyko-Sellers 1D energy balance equation obtained by latitudinal averaging and by redirecting the vertical imbalance away from the equator.

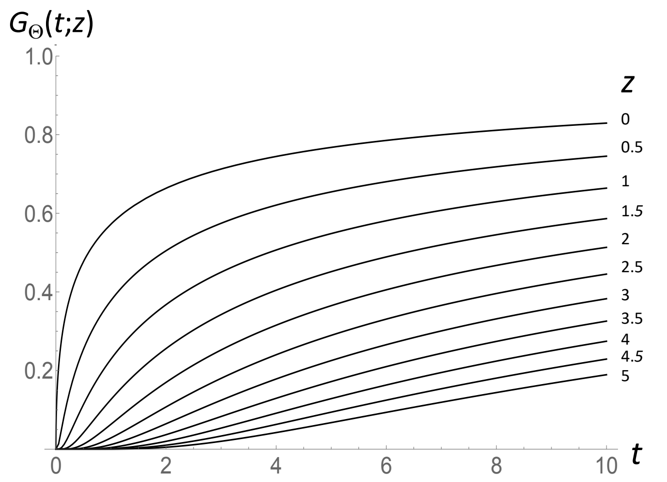

Fig. 3: The nondimensional temperature as a function of nondimensional time for various nondimensional depths with a step forcing; $G_\Theta(t;z)$ (obtained by integrating eq. ~~30~~ 34 in time). The (top) surface curve can be interpreted as the fraction of the forcing that is conductive. At first all the forcing is conductive with no radiation, eventually all the fluxes are radiative, the system reaches a new thermodynamic equilibrium and there is no conductive heat flux.

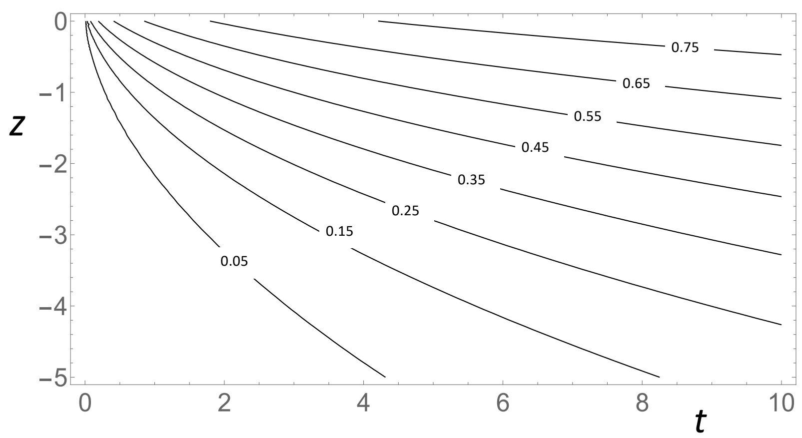

Fig. 4: Contours of nondimensional temperature as a function of nondimensional time and depth after a step function forcing ($G_\Theta(t;z)$).

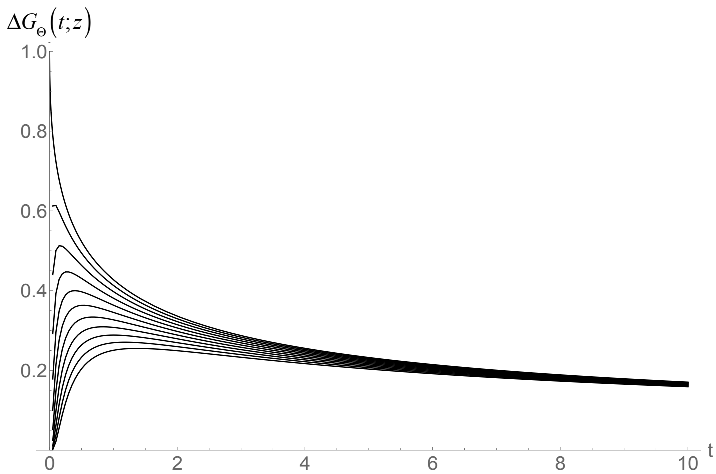

Fig. 5: The difference $\Delta G_{\Theta}(t;z)$ between the classical (temperature forced) and radiative forced step response functions over the diffusion depth (nondimensional z = 0 to -1). The top is shows the surface (z = 0), the curves from top to bottom are at depths z =0., -0., -0.2, -0.3,…-1. While the difference is large over the relaxation time (up to nondimensional t = 1), we see that they both slowly converge to thermodynamic equilibrium at large *t*.

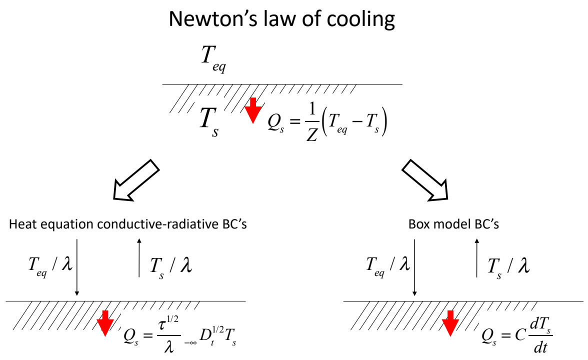

Fig. 6: A schematic showing Newton's law of cooling (NLC) that relates the temperature difference across a surface to the heat flux crossing the surface, Q_s (into the surface). T_{eq} is the fixed outside temperature, heat will flow as long as the surface temperature $T_s \neq T_{eq}$, Z is the thermal impedance (equal here to the climate sensitivity λ). To apply the NLC, we need to relate the heat flux to the surface temperature. The lower left shows the consequence of applying heat equation with conductive – radiative BC's, the lower right shows the phenomenological assumption made by box models. The arrows represent heat fluxes, hence the factor λ in the denominators. The system is assumed to be horizontally homogeneous and that the subsurface is much thicker than the diffusion depth.

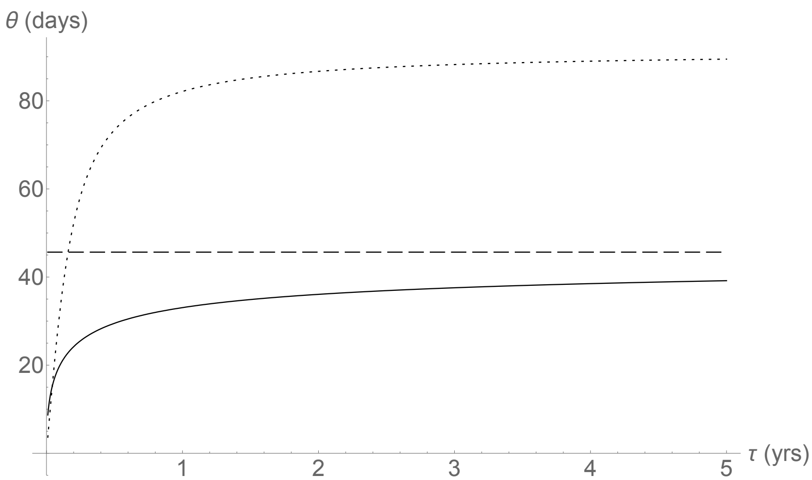

Fig. 7: The temperature phase lag (in months, the negative of argument of the complex climate sensitivity), using the complex climate sensitivity and annual cycle forcing (i.e. with $\omega = 2\pi$ *rads/yr*) with τ in years. The line with short dashes (top) is the usual EBE (H = 1), the solid line is the (H = 1/2) HEBE and the line with long dashes is the classical heat forcing model which is the large τ HEBE limit. All curves ignore any net horizontal heat transport. The data analyzed here yield $\tau \approx 2.75\pm0.8$ years but the actual phase is somewhat shorter due to horizontal heat transport.

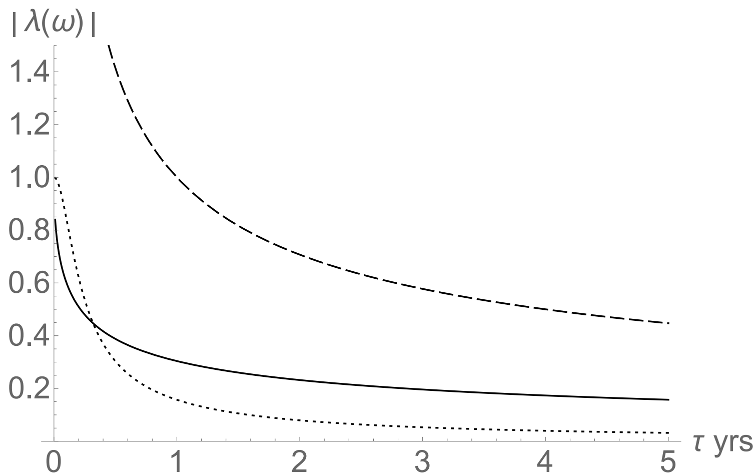

Fig. 8: Same as fig. 7 except for the amplitude of the complex climate sensitivity to annual cycle forcing (i.e. with $\omega = 2\pi$ *rads/yr*) with τ in years. The short dash line (bottom) is the usual EBE (H = 1), the top line with long dashes is the classical heat forcing model and the solid line is the (H = 1/2) HEBE.